

# Simulation Based Composite Likelihood

Lorenzo Rimella\*

Department of Mathematics and Statistics, Lancaster University, UK

Chris Jewell

Department of Mathematics and Statistics, Lancaster University, UK

Paul Fearnhead

Department of Mathematics and Statistics, Lancaster University, UK

16th October 2023

## Abstract

Inference for high-dimensional hidden Markov models is challenging due to the exponential-in-dimension computational cost of the forward algorithm. To address this issue, we introduce an innovative composite likelihood approach called “Simulation Based Composite Likelihood” (SimBa-CL). With SimBa-CL, we approximate the likelihood by the product of its marginals, which we estimate using Monte Carlo sampling. In a similar vein to approximate Bayesian computation (ABC), SimBa-CL requires multiple simulations from the model, but, in contrast to ABC, it provides a likelihood approximation that guides the optimization of the parameters. Leveraging automatic differentiation libraries, it is simple to calculate gradients and Hessians to not only speed-up optimization, but also to build approximate confidence sets. We conclude with an extensive experimental section, where we empirically validate our theoretical results, conduct a comparative analysis with SMC, and apply SimBa-CL to real-world Aptomavirus data.

*Keywords:* Hidden Markov model; Composite likelihood; Monte Carlo approximation.

## 1 Introduction

Discrete-state hidden Markov models (HMMs) are common in many applications, such as epidemics [Allen, 2008, Britton, 2010], systems biology [Wilkinson, 2018] and ecology [Glennie et al., 2023]. Increasingly there is interest in individual-based models [e.g. Keeling and Eames, 2005, Rimella et al., 2023a], in which the HMM explicitly describes the state of

---

\*[l.rimella@lancaster.ac.uk](mailto:l.rimella@lancaster.ac.uk)

each individual agent in a population. For example, an individual-based epidemic model may characterise each person in a population as having a latent state, being either susceptible, infected or recovered. This state is typically observed noisily, with a sample of individuals being detected as infected with a possibly imperfect diagnostic test [e.g. [Cocker et al., 2023b](#)]. Thus, whilst there may be only a small number of states for each individual, this corresponds to a latent state-space that grows exponentially with the number of individuals.

In theory, likelihood calculations for such discrete-state HMMs is tractable using the forward-backward recursions [[Scott, 2002](#)]. However the computational cost of these recursions is at least linear in the size of the state-space of the HMM: this means that they are infeasible for individual-based models with moderate or larger population sizes. This has led to a range of approximate inference methods. These include Monte Carlo methods such as MCMC and sequential Monte Carlo. Whilst such methods can work well, often they scale poorly with the population size – which may lead to poor mixing of MCMC algorithms or large Monte Carlo variance of the weights in sequential Monte Carlo. An alternative approach is approximate Bayesian computation (ABC), where one simulates from the model for different parameter values, and then approximates the posterior for the parameter based on how similar each simulated data set is to the true data. Such a method needs informative, low-dimensional, summary statistics to be available so that one can accurately measure how close a simulated data set is to the true data. Furthermore ABC can struggle with complex models with many parameters, as the number of summary statistics needs to increase with the number of parameters [[Fearnhead and Prangle, 2012](#)].

In this paper we consider individual-based HMMs where we have individual level observations. We present a computationally efficient method for inference that is based on the simple observation: if we fix the state of all members of the population except one, then we can analytically calculate the conditional likelihood of that one individual using forward-backward recursions. This idea has been used before within MCMC algorithms that update the state of each individual in turn conditional on the states of the other individuals [[Touloupou et al., 2020](#)]. Here we use it in a different way. By simulating multiple realisations of the states of the other individuals we can average the conditional likelihood to obtain a Monte Carlo estimate of the likelihood of the data for a given individual. We then sum the log of these estimated likelihoods over individuals to obtain a composite log-likelihood [[Varin, 2008](#)] that can be maximised using, for example, stochastic gradient descent, to estimate the parameters.

We introduce the general class of models we consider in [Section 2](#). We then show how to obtain a Monte Carlo estimate of the likelihood for the observations associated with a single individual, which can be used as the basis of a composite likelihood for our model. The calculation of the likelihood for each individual involves accounting for feedback between the state of the individual in question, and the probability distribution of future states of the rest of the population. A computationally more efficient method can be obtained by ignoring this feedback – and we present theory that bounds the error of this approach, and show that it can decay to zero as the population size tends to infinity. Then in [Section 4](#) we show how we can get confidence regions around estimators based on maximising our composite

likelihood. We then demonstrate the efficiency for individual-based epidemic models both on simulated data and on data from the 2001 UK foot and mouth outbreak.

## 2 Model

### 2.1 Notation

Given the integer  $t \in \mathbb{N}$ , we denote the set of integers from 1 to  $t$  as  $[t]$ , and we use  $[0 : t]$  if we want to include 0. Additionally, we use  $[t]$  as shorthand for indexing, for instance  $x_{[t]}$  denotes the collection  $x_1, \dots, x_t$ . Given an index  $n \in [N]$ , we use  $x^n$  to denote the  $n$ th component of  $x$  and  $x^{\setminus n}$  to denote the  $(N - 1)$ -dimensional vector obtained by removing the  $n$ th component from  $x$ . If required, we augment the superscript notation and use  $x^{(i)}$  to refer to the vector  $x^{(i)}$  with components  $x^{(i),n}$ . For a finite and discrete set  $\mathcal{S}$ , we represent the cardinality of  $\mathcal{S}$  as  $\mathbf{card}(\mathcal{S})$ , and we use the shorthand  $\sum_x$  to express the sum over all elements of  $\mathcal{S}$ .

We use bold font to denote random variables and regular font for deterministic quantities. For the underlying probability measure, we commonly use  $p$  and, for the sake of clarity, we focus on its functional form, for instance we use  $p(x_t|x_{t-1}, \theta)$  for the probability of  $\mathbf{x}_t = x_t$  given  $\mathbf{x}_{t-1} = x_{t-1}$  and the parameters  $\theta$ .

### 2.2 Hidden Markov models and likelihood computation

A hidden Markov model (HMM)  $(\mathbf{x}_0, (\mathbf{x}_t, \mathbf{y}_t)_{t \geq 1})$  is a stochastic process where the unobserved process  $(\mathbf{x}_t)_{t \geq 0}$  is a Markov chain, and the observed process  $(\mathbf{y}_t)_{t \geq 1}$  is such that, for any  $t \geq 1$ ,  $\mathbf{y}_t$  is conditionally independent of all the other variables given  $\mathbf{x}_t$ . See [Chopin and Papaspiliopoulos \[2020\]](#) for a comprehensive review of HMMs.

Within this study, we focus on the specific scenario of HMMs on finite dimensional state-spaces. Precisely, we consider  $(\mathbf{x}_t)_{t \geq 0}$  to take values on the state-space  $\mathcal{X}^N$ , which satisfies a product form,  $\mathcal{X}^N = \times_{n \in [N]} \mathcal{X}$ , where  $\mathcal{X}$  is finite and discrete. We also consider  $(\mathbf{y}_t)_{t \geq 1}$  to be on the space  $\mathcal{Y}^N$ , which also satisfies a product form,  $\mathcal{Y}^N = \times_{n \in [N]} \mathcal{Y}$ , but here  $\mathcal{Y}$  can be of any form.

Given a collection of parameters  $\theta$ , an HMM is fully defined through its components: the initial distribution  $p(x_0|\theta)$ , which is the distribution of  $\mathbf{x}_0$ ; the transition kernel  $p(x_t|x_{t-1}, \theta)$ , which is the distribution of  $\mathbf{x}_t$  given  $\mathbf{x}_{t-1}$ ; and the emission distribution  $p(y_t|x_t, \theta)$ , which is the distribution of  $\mathbf{y}_t$  given  $\mathbf{x}_t$ . Given the assumption that  $\mathcal{X}$  is finite and discrete, the probability distribution  $p(x_0|\theta)$  takes the form of a probability vector with  $\mathbf{card}(\mathcal{X})^N$  elements, while  $p(x_t|x_{t-1}, \theta)$  corresponds to a  $\mathbf{card}(\mathcal{X})^N \times \mathbf{card}(\mathcal{X})^N$  stochastic matrix.

For a given time horizon  $T \in \mathbb{N}$ , we may assume that the data sequence  $y_1, \dots, y_T$  is generated from the aforementioned hidden Markov model with parameters  $\theta^*$ . Our primary interest is in inferring the parameter  $\theta^*$  responsible for generating the data or, in cases where the model is not fully identifiable, a set of parameters that are equally likely. The computation of the likelihood for HMMs with discrete state-space is relatively straightforward and

involves marginalization over the entire state-space:

$$p(y_{[T]}|\theta) = \sum_{x_{[0:T]}} p(x_0|\theta) \prod_{t \in [T]} p(x_t|x_{t-1}, \theta) p(y_t|x_t, \theta). \quad (1)$$

In practice, to avoid marginalizing on an exponential-in-time state-space, the likelihood is recursively computed using the Forward algorithm, which recursively compute the filtering distribution  $p(x_t|y_t, \theta)$  and the likelihood increments  $p(y_t|y_{[t-1]}, \theta)$ . The  $t + 1$  step of Forward algorithm comprises of two operations, namely, prediction:

$$\left\{ \begin{array}{l} p(x_{t+1}|x_t, \theta) \\ p(x_t|y_{[t]}, \theta) \end{array} \right\} \xrightarrow{\text{prediction}} \left\{ \begin{array}{l} p(x_{t+1}|y_{[t]}, \theta) = \sum_{x_t} p(x_{t+1}|x_t, \theta) p(x_t|y_{[t]}, \theta) \\ p(x_t|y_{[t]}, \theta) \end{array} \right\},$$

where the transition kernel is applied to the previous filtering distribution, and correction:

$$\left\{ \begin{array}{l} p(y_{t+1}|x_{t+1}, \theta) \\ p(x_{t+1}|y_{[t]}, \theta) \end{array} \right\} \xrightarrow{\text{correction}} \left\{ \begin{array}{l} p(x_{t+1}|y_{[t+1]}, \theta) = \frac{p(y_{t+1}|x_{t+1}, \theta)p(x_{t+1}|y_{[t]}, \theta)}{p(y_{t+1}|y_{[t]}, \theta)} \\ p(y_{t+1}|y_{[t]}, \theta) = \sum_{x_{t+1}} p(y_{t+1}|x_{t+1}, \theta)p(x_{t+1}|y_{[t]}, \theta) \end{array} \right\},$$

from which the likelihood increments  $p(y_t|y_{[t-1]}, \theta)$ , with  $p(y_1|y_{[0]}, \theta) := p(y_1|\theta)$ , are then combined to compute the likelihood:

$$p(y_{[T]}|\theta) = \prod_{t \in [T]} p(y_t|y_{[t-1]}, \theta).$$

Despite its simplicity, the Forward algorithm necessitates a marginalization on the full state-space, incurring a computational cost that is, at worst, quadratic in the cardinality of the state-space. For the considered scenario, this translates in a complexity of  $\mathcal{O}(\text{card}(\mathcal{X})^{2N})$ , making the Forward algorithm unfeasible for large values of  $N$ .

Obviously, more sophisticated techniques are available to perform inference in HMMs. Notable among these are techniques such as Approximate Bayesian Computation [Beaumont, 2019], Sequential Monte Carlo [Doucet et al., 2001], and Variational Inference [Blei et al., 2017]. While a complete overview of alternative methods is out of the scope of this work, it is noteworthy that even for these approaches, tackling the challenges of scaling up to high-dimensional HMMs, large values of  $N$ , remains a significant obstacle, comparable to the challenges faced by the Forward algorithm.

### 2.3 Factorial structure

Research has demonstrated that introducing certain factorization structures into the underlying model could yield to approximate algorithms with interesting theoretical and computational properties [Rebeschini and Van Handel, 2015, Rimella and Whiteley, 2022]. Moreover, the prospect of inference in high-dimensional HMMs without any assumptions about the

model structure appears implausible. Therefore, we restrict our study to the HMMs with initial distribution, transition kernel, and emission distribution that satisfy the following factorizations:

$$\begin{aligned}
 p(x_0|\theta) &= \prod_{n \in [N]} p(x_0^n|\theta), & p(x_t|x_{t-1}, \theta) &= \prod_{n \in [N]} p(x_t^n|x_{t-1}^n, \theta), \\
 p(y_t|x_t, \theta) &= \prod_{n \in [N]} p(y_t^n|x_t^n, \theta),
 \end{aligned} \tag{2}$$

which essentially says that we can decompose the initial distribution in  $N$  probability vectors of size  $\text{card}(\mathcal{X})$ , the transition kernel in  $N$  stochastic matrices that are  $\text{card}(\mathcal{X}) \times \text{card}(\mathcal{X})$ , whose elements also depend on  $x_{t-1}$ , and the observation  $n$  is conditionally independent from all the other variables given  $\mathbf{x}_t^n$ .

It is important to mention that the introduced factorisation does not resolve our problems; rather, it serves as an essential foundation upon which we construct our approximation. Furthermore, the factorization given by (2) is common in several real world applications, among which: epidemics [Rimella et al., 2023b,a], traffic modelling [Silva et al., 2015], sociology [Bianchi and Squazzoni, 2015] and finance [Samanidou et al., 2007].

### 3 Simulation based composite likelihood: SimBa-CL

From model structure shown in Section 2.3, we can notice that by fixing the state of all but one component of the latent process,  $x_{[T]}^{\setminus n}$  say, we can leverage the factorisation and calculate probabilities related to the time-trajectory of the remaining state,  $x_{[T]}^n$ , with a computational cost that is  $\mathcal{O}(\text{card}(\mathcal{X}))$ . This idea has been used within Gibbs-style MCMC updates for epidemics see Touloupou et al. [2020]. We show how to use this idea, together with using Monte Carlo to average over  $x_{[T]}^{\setminus n}$ , to calculate the marginal likelihoods  $p(y_{[T]}^n|\theta)$ . We can then use the produce of these marginal likelihoods,  $\prod_{n \in [N]} p(y_{[T]}^n|\theta)$ , as an approximate likelihood that can be maximised to estimate  $\theta$ . This idea is related to some approximations in discrete state-space HMMs and sequential Monte Carlo [Boyen and Koller, 1999, 2013, Rebeschini and Van Handel, 2015, Rimella and Whiteley, 2022], and corresponds to the framework of composite marginal likelihood [Varin, 2008, Varin et al., 2011]. We return to this latter point in Section 4.

Using  $p(y_{[T]}|\theta) \approx \prod_{n \in [N]} p(y_{[T]}^n|\theta)$  still falls short, as the computation of  $p(y_{[T]}^n|\theta)$  continues to require a recursive marginalization on  $\mathcal{X}^N$ . Yet, we can express the marginal likelihood  $p(y_{[T]}^n|\theta)$  as:

$$p(y_{[T]}^n|\theta) = \sum_{x_{[0:T-1]}^{\setminus n}} p(x_{[0:T-1]}^{\setminus n}|\theta) p(y_{[T]}^n|x_{[0:T-1]}^{\setminus n}, \theta), \tag{3}$$

where:

$$p\left(y_{[T]}^n | x_{[0:T-1]}^{\setminus n}, \theta\right) = \sum_{x_{[0:T]}^n} p(x_T^n | x_{T-1}, \theta) p\left(x_{[0:T-1]}^n | x_{[0:T-1]}^{\setminus n}, \theta\right) \prod_{t \in [T]} p(y_t^n | x_t^n, \theta).$$

We have two necessary ingredients for calculating  $p\left(y_{[T]}^n | \theta\right)$ : firstly,  $p\left(y_{[T]}^n | x_{[0:T-1]}^{\setminus n}, \theta\right)$ , which demands  $T$  recursive marginalizations on  $\mathcal{X}$  given  $x_{[0:T-1]}^{\setminus n}$ ; secondly, a marginalization on  $\mathcal{X}^{N-1}$  through  $p\left(x_{[0:T-1]}^{\setminus n} | \theta\right)$ , see (3). On a superficial glance, Equation (3) might appear to involve circular reasoning, given that marginalizing over  $\mathcal{X}^{N-1}$  remains computationally unfeasible. However, when sampling from the process is both inexpensive and straightforward, we can resort to estimating (3) using Monte Carlo sampling.

We refer to this procedure as ‘‘Simulation Based Composite Likelihood’’, or ‘‘SimBa-CL’’ in short. In the following sections, we give an in-depth discussion on SimBa-CL, and show how we can target the true marginals of the likelihood and build a likelihood approximation in  $\mathcal{O}(N^2)$ , see Section 3.1, how to approximate the marginals of the likelihood and build an approximation of the likelihood in  $\mathcal{O}(N)$ , see Section 3.2, and how to generalise SimBa-CL, see Section 3.4. For the sake of presentation, we remove the dependence on the parameter  $\theta$ , and focus on the filtering aspects of the algorithms for a fixed  $\theta$ .

### 3.1 SimBa-CL with feedback

Given efficient sampling from  $p(x_{[0:T-1]}^{\setminus n})$  and low-cost evaluation of  $p(y_{[T]}^n | x_{[0:T-1]}^{\setminus n})$  for a given  $x_{[0:T-1]}^{\setminus n}$ , we can readily deduce a Monte Carlo estimate of the marginal likelihood from (3):

$$p\left(y_{[T]}^n\right) \approx \frac{1}{P} \sum_{i \in [P]} p\left(y_{[T]}^n | x_{[0:T-1]}^{(i), \setminus n}\right), \quad (4)$$

where  $P \in \mathbb{N}$  is the number of Monte Carlo samples and  $x_{[0:T-1]}^{(i), \setminus n} \sim p\left(x_{[0:T-1]}^{\setminus n}\right)$ . Repeating (4) for all  $n \in [N]$  and computing the product across  $n$  of these Monte Carlo estimates represents then a reasonable strategy for approximating the likelihood of the model.

Two ingredients are pivotal in the computation of (4): (i) sampling from the model and (ii) calculating  $p(y_{[T]}^n | x_{[0:T-1]}^{\setminus n})$ . Sampling from  $p(x_{[0:T-1]}^{\setminus n})$  can be achieved by sampling  $x_{[0:T-1]}$  from  $p(x_{[0:T-1]})$  and then selecting the subset  $x_{[0:T-1]}^{\setminus n}$ . It is worth noting that sampling from the entire process is generally straightforward and commonly employed in simulation based algorithm like approximate Bayesian computation (ABC) [Beaumont, 2019] and sequential Monte Carlo (SMC) [Doucet et al., 2001]. However, calculating  $p(y_{[T]}^n | x_{[0:T-1]}^{\setminus n})$  is intricate and demands a meticulous derivation of an alternative Forward algorithm, which takes into account the simulation outcome  $x_{[0:T-1]}^{\setminus n}$ .

For the computation of  $p(y_{[T]}^n | x_{[0:T-1]}^{\setminus n})$ , it is important to recognise that  $p(x_{[0:T-1]}^{\setminus n} | x_{[0:T-1]}^{\setminus n})$  can be reformulated as a product between the transition dynamics and the probability of

observing a certain simulation outcome:

$$p\left(x_{[0:T-1]}^n | x_{[0:T-1]}^{\setminus n}\right) = p(x_0^n) \prod_{t \in [T-1]} p(x_t^n | x_{t-1}) f\left(x_{t-1}^n, x_{[0:t]}^{\setminus n}\right), \quad (5)$$

where we refer to  $f(x_{t-1}^n, x_{[0:t]}^{\setminus n}) := p(x_t^n | x_{t-1}^n, x_{[0:t-1]}^{\setminus n})$  as the simulation feedback, and so:

$$f\left(x_{t-1}^n, x_{[0:t]}^{\setminus n}\right) = \frac{\prod_{\bar{n} \in [N] \setminus n} p(x_{\bar{n}}^{\bar{n}} | x_{t-1})}{\sum_{\bar{x}_{t-1}^{\bar{n}}} \prod_{\bar{n} \in [N] \setminus n} p\left(x_{\bar{n}}^{\bar{n}} | \bar{x}_{t-1}^{\bar{n}}, x_{[0:t-1]}^{\setminus n}\right) p\left(\bar{x}_{t-1}^{\bar{n}} | x_{[0:t-1]}^{\setminus n}\right)}, \quad (6)$$

where  $p\left(x_0^n | x_{[0:0]}^{\setminus n}\right) = p(x_0^n)$  for the factorisation of the initial distribution. More details on the factorisation (5) and the derivation of the simulation feedback (6) are available in the supplementary material.

By reformulating  $p\left(x_{[0:T-1]}^n | x_{[0:T-1]}^{\setminus n}\right)$  as depicted in (5), we arrive at the following expression:

$$p\left(y_{[T]}^n | x_{[0:T-1]}^{\setminus n}\right) = \sum_{x_{[0:T]}^n} p(x_0^n) \prod_{t \in [T-1]} f\left(x_{t-1}^n, x_{[0:t]}^{\setminus n}\right) \prod_{t \in [T]} p(x_t^n | x_{t-1}) p(y_t^n | x_t^n), \quad (7)$$

which resembles the likelihood of an HMM, see (1). Specifically, it comprises the usual transition dynamic term  $p(x_t^n | x_{t-1})$  accompanied by two likelihood terms: one originating from the simulation outcome  $f\left(x_{t-1}^n, x_{[0:t]}^{\setminus n}\right)$ , and another concerning the observation  $p(y_t^n | x_t^n)$ . We can then establish a Forward algorithm involving two corrections, one that is correcting according to the emission distribution:

$$\left\{ \begin{array}{l} p(y_t^n | x_t^n) \\ p(x_t^n | y_{[t-1]}^n, x_{[0:t]}^{\setminus n}) \end{array} \right\} \xrightarrow{\text{observation correction}} \left\{ \begin{array}{l} p(x_t^n | y_{[t]}^n, x_{[0:t]}^{\setminus n}) = \frac{p(y_t^n | x_t^n) p(x_t^n | y_{[t-1]}^n, x_{[0:t]}^{\setminus n})}{p(y_t^n | y_{[t-1]}^n, x_{[0:t]}^{\setminus n})} \\ p(y_t^n | y_{[t-1]}^n, x_{[0:t]}^{\setminus n}) = \sum_{x_t^n} p(y_t^n | x_t^n) p(x_t^n | y_{[t-1]}^n, x_{[0:t]}^{\setminus n}) \end{array} \right\}, \quad (8)$$

and the other that is correcting according to the simulation feedback:

$$\left\{ \begin{array}{l} f\left(x_t^n, x_{[0:t+1]}^{\setminus n}\right) \\ p(x_t^n | y_{[t]}^n, x_{[0:t]}^{\setminus n}) \end{array} \right\} \xrightarrow{\text{feedback correction}} \left\{ \begin{array}{l} p(x_t^n | y_{[t]}^n, x_{[0:t+1]}^{\setminus n}) = \frac{f\left(x_t^n, x_{[0:t+1]}^{\setminus n}\right) p(x_t^n | y_{[t]}^n, x_{[0:t]}^{\setminus n})}{p\left(x_{t+1}^{\setminus n} | y_{[t]}^n, x_{[0:t]}^{\setminus n}\right)} \\ p\left(x_{t+1}^{\setminus n} | y_{[t]}^n, x_{[0:t]}^{\setminus n}\right) = \sum_{x_t^n} f\left(x_t^n, x_{[0:t+1]}^{\setminus n}\right) p\left(x_t^n | y_{[t]}^n, x_{[0:t]}^{\setminus n}\right) \end{array} \right\}. \quad (9)$$

The prediction follows as is in the basic HMM scenario with  $p(x_t^n | x_{t-1})$  as transition kernel and  $p\left(x_{t-1}^n | y_{[t-1]}^n, x_{[0:t]}^{\setminus n}\right)$  for the distribution to update:

$$\left\{ \begin{array}{l} p(x_t^n | x_{t-1}) \\ p\left(x_{t-1}^n | y_{[t-1]}^n, x_{[0:t]}^{\setminus n}\right) \end{array} \right\} \xrightarrow{\text{feedback correction}} \left\{ \begin{array}{l} p\left(x_t^n | y_{[t-1]}^n, x_{[0:t]}^{\setminus n}\right) = \sum_{x_{t-1}^n} p(x_t^n | x_{t-1}) p\left(x_{t-1}^n | y_{[t-1]}^n, x_{[0:t]}^{\setminus n}\right) \end{array} \right\}. \quad (10)$$



Remark that the order of these operations depends on the model structure, in our specific case we have: feedback correction, prediction, observation correction.

It is important to note that the computation of the simulation feedback  $f\left(x_{t-1}^n, x_{[0:t-1]}^n\right)$  relies on  $p\left(x_{t-1}^n|x_{[0:t-1]}^n\right)$ . In this particular context, the HMMs theory still proves to be handy as  $p\left(x_{t-1}^n|x_{[0:t-1]}^n\right)$  is the posterior distribution on  $x_{t-1}^n$  given the simulation output as observations. Consequently, this interpretation enables the employment of another Forward algorithm to compute recursively these intermediate quantities, where the correction step is given by:

$$\left\{ \begin{array}{l} \prod_{\bar{n} \in [N] \setminus n} p(x_{t-1}^{\bar{n}} | x_{t-1}^n) \\ p(x_{t-1}^n | x_{[0:t-1]}^n) \end{array} \right\} \xrightarrow{\text{correction}} \left\{ \begin{array}{l} p(x_{t-1}^n | x_{[0:t]}^n) = \frac{\prod_{\bar{n} \in [N] \setminus n} p(x_{t-1}^{\bar{n}} | x_{t-1}^n) p(x_{t-1}^n | x_{[0:t-1]}^n)}{p(x_{t-1}^n | x_{[0:t-1]}^n)} \\ p(x_t^n | x_{[0:t-1]}^n) = \sum_{x_{t-1}^n} \prod_{\bar{n} \in [N] \setminus n} p(x_t^{\bar{n}} | x_{t-1}^{\bar{n}}) p(x_{t-1}^{\bar{n}} | x_{[0:t-1]}^n) \end{array} \right\}, \quad (11)$$

and the prediction follows:

$$\left\{ \begin{array}{l} p(x_t^n | x_{t-1}^n) \\ p(x_{t-1}^n | x_{[0:t]}^n) \end{array} \right\} \xrightarrow{\text{prediction}} \left\{ p(x_t^n | x_{[0:t]}^n) = \sum_{x_{t-1}^n} p(x_t^n | x_{t-1}^n) p(x_{t-1}^n | x_{[0:t]}^n) \right\}. \quad (12)$$

An iterative application of the aforementioned steps provides a collection of likelihood increments on both the simulation output and the observations, enabling the computation of  $p\left(y_{[T]}^n | x_{[0:T-1]}^n\right)$  as follows:

$$p\left(y_{[T]}^n | x_{[0:T-1]}^n\right) = p\left(y_T^n | y_{[T-1]}^n, x_{[0:T-1]}^n\right) \prod_{t \in [T-1]} p\left(y_t^n | y_{[t-1]}^n, x_{[0:t]}^n\right) p\left(x_t^n | y_{[t-1]}^n, x_{[0:t-1]}^n\right), \quad (13)$$

where  $p\left(y_1^n | y_{[0]}^n, x_{[0:0]}^n\right) := p\left(y_1^n | x_0^n\right)$  and  $p\left(x_1^n | y_{[0]}^n, x_{[0]}^n\right) := p\left(x_1^n | x_{[0]}^n, \theta\right)$ .

The final algorithm, named ‘‘SimBa-CL with feedback’’, is presented in Algorithm 1, and the key steps are: simulation from the model, application of the Forward step With Feedback and application of the Forward step For Feedback. The computational complexity of running Algorithm 1 is  $\mathcal{O}\left(PTN^2 \mathbf{card}(\mathcal{X})^2\right)$ , wherein  $P$ ,  $T$ ,  $N$  come from looping over number of simulations, time steps and dimensions,  $\mathbf{card}(\mathcal{X})^2$  comes from marginalizing over the state-space  $\mathcal{X}$ , and the extra  $N$  terms refers to the simulation feedback computation. It is noteworthy that this cost can potentially be reduced to  $\mathcal{O}\left(PTN \max_n \{\mathbf{card}(\mathbf{Neig}(n))\} \mathbf{card}(\mathcal{X})^2\right)$  if the transition kernel  $p\left(x_t^n | x_{t-1}^n, \theta\right)$  presents some local structure. Precisely, if  $p\left(x_t^n | x_{t-1}^n, \theta\right) = p\left(x_t^n | \bar{x}_{t-1}^n, \theta\right)$  for any  $x_{t-1}^{\mathbf{Neig}(n)} = \bar{x}_{t-1}^{\mathbf{Neig}(n)}$ , where  $\mathbf{Neig}$  represents a function mapping any  $n \in [N]$  onto a set in the power set of  $[N]$ . In practical terms, this indicates that computing the simulation feedback can be computationally cheaper if the inter-dimension interactions are sparse. Also it is important to notice that the algorithm can be run in parallel on both the dimension and the simulation, making the dependence on  $P$  and the first dependence on  $N$  less heavy.



---

**Algorithm 1** SimBa-CL with feedback

---

**Require:**  $p(x_0)$ ,  $p(x_t|x_{t-1})$ ,  $p(y_t|x_t)$  and their factorisations

**for each**  $i \in [P]$  **do**

$x_0^{(i)} \sim p(x_0)$

**for**  $t \in [T]$  **do**

$x_t^{(i)} \sim p(x_t|x_{t-1}^{(i)})$  and compute  $f(x_{t-1}^n, x_{[0:t]}^{(i), \setminus n})$

**for each**  $n \in [N]$  **do**

if  $t \neq T$ , run the feedback correction (9) and get:  $\left\{ \begin{array}{l} p(x_{t-1}^n | y_{[t-1]}^n, x_{[0:t]}^{(i), \setminus n}) \\ p(x_t^{(i), \setminus n} | y_{[t-1]}^n, x_{[0:t-1]}^{(i), \setminus n}) \end{array} \right\}$

Run the prediction (10) and get:  $\left\{ p(x_t^n | y_{[t-1]}^n, x_{[0:t]}^{(i), \setminus n}) \right\}$

Run the observation correction (8) and get:  $\left\{ \begin{array}{l} p(x_t^n | y_t^n, x_{[0:t]}^{(i), \setminus n}) \\ p(y_t^n | y_{[t-1]}^n, x_{[0:t]}^{(i), \setminus n}) \end{array} \right\}$

Run the correction (11) and get:  $\left\{ \begin{array}{l} p(x_{t-1}^n | x_{[0:t]}^{(i), \setminus n}) \\ p(x_t^{(i), \setminus n} | x_{[0:t-1]}^{(i), \setminus n}) \end{array} \right\}$

Run the prediction (12) and get:  $\left\{ p(x_t^n | x_{[0:t]}^{(i), \setminus n}) \right\}$

**end for**

**end for**

Compute  $p(y_{[T]}^n | x_{[0:T-1]}^{(i), \setminus n})$  as in (13)

**end for**

Return  $\frac{1}{P} \sum_{i \in [P]} p(y_{[T]}^n | x_{[0:T-1]}^{(i), \setminus n})$

---

### 3.2 SimBa-CL without feedback

An important aspect of SimBa-CL with feedback is that it targets the true marginals of the likelihood, trading off with a computational cost that, in the worst case scenario, scales quadratically with the dimension  $N$ . However, one could contemplate a strategy involving the removal of the simulation feedback and design a SimBa-CL that is more computationally efficient, while being “close” to SimBa-CL with feedback.

Looking back at (7), omitting the simulation feedback yields to:

$$p(y_{[T]}^n | x_{[0:T-1]}^{\setminus n}) \approx \sum_{x_{[0:T]}^n} p(x_0^n) \prod_{t \in [T]} p(x_t^n | x_{t-1}^n) p(y_t^n | x_t^n) =: \tilde{p}(y_{[T]}^n | x_{[0:T-1]}^{\setminus n}), \quad (14)$$

from which we have the following marginal likelihood approximation:

$$p(y_{[T]}^n) \approx \sum_{x_{[0:T-1]}^{\setminus n}} p(x_{[0:T-1]}^{\setminus n}) \tilde{p}(y_{[T]}^n | x_{[0:T-1]}^{\setminus n}) =: \tilde{p}(y_{[T]}^n),$$

where we emphasised that we are relying on an approximation by using the notation  $\tilde{p}$ . It can be seen that  $\tilde{p}\left(y_{[T]}^n\right)$  is still a proper marginal likelihood, as it sums to one when marginalizing on  $\mathcal{Y}$ , but it is not the true marginal likelihood, as the latter has to consider the simulation feedback.

Upon scrutinizing (14), we can recognise the same likelihood structure as (1). This time, we are isolating our calculation to a single component  $n$  and fixing the others through simulation from model. This suggests that a simple Forward algorithm can be run in isolation on each dimension, by fixing the others to the simulation outcome, and so provide some approximate likelihood increments  $\tilde{p}\left(y_t^n|y_{[t-1]}, x_{[0:t-1]}^n\right)$ . Concretely, the corresponding Forward algorithm will require a prediction step:

$$\left\{ \begin{array}{l} p\left(x_{t+1}^n|x_t\right) \\ \tilde{p}\left(x_t^n|y_{[t]}^n, x_{[0:t-1]}^n\right) \end{array} \right\} \xrightarrow{\text{prediction}} \left\{ \begin{array}{l} \tilde{p}\left(x_{t+1}^n|y_{[t]}^n, x_{[0:t]}^n\right) = \sum_{x_t^n} p\left(x_{t+1}^n|x_t\right) \tilde{p}\left(x_t^n|y_{[t]}^n, x_{[0:t-1]}^n\right) \\ \end{array} \right\}, \quad (15)$$

and a correction step:

$$\left\{ \begin{array}{l} p\left(y_{t+1}^n|x_{t+1}^n\right) \\ \tilde{p}\left(x_{t+1}^n|y_{[t]}^n, x_{[0:t]}^n\right) \end{array} \right\} \xrightarrow{\text{correction}} \left\{ \begin{array}{l} \tilde{p}\left(x_{t+1}^n|y_{[t+1]}^n, x_{[0:t]}^n\right) = \frac{p\left(y_{t+1}^n|x_{t+1}^n\right)\tilde{p}\left(x_{t+1}^n|y_{[t]}^n, x_{[0:t]}^n\right)}{\tilde{p}\left(y_{t+1}^n|y_{[t]}^n, x_{[0:t]}^n\right)} \\ \tilde{p}\left(y_{t+1}^n|y_{[t]}^n, x_{[0:t]}^n\right) = \sum_{x_{t+1}^n} p\left(y_{t+1}^n|x_{t+1}^n\right) \tilde{p}\left(x_{t+1}^n|y_{[t]}^n, x_{[0:t]}^n\right) \end{array} \right\}, \quad (16)$$

where the dependence on  $x_t^{\setminus n}$  is introduced during prediction without any feedback. Treating  $x_t^{\setminus n}$  in this way is essentially considering a functional dependence rather than a probabilistic one, in the sense that we fix the other  $N - 1$  components just to compute the transition kernel  $p(x_{t+1}^n|x_t)$  on component  $n$ .

Recursively applying (15) and (16) provides a sequence of approximate marginal likelihood increments which can be then used to approximate the marginal likelihood for a fixed simulation in the usual way:

$$\tilde{p}\left(y_{[T]}^n|x_{[0:T-1]}^n\right) = \prod_{t \in [T]} \tilde{p}\left(y_t^n|y_{[t-1]}^n, x_{[0:t-1]}^n\right),$$

where  $\tilde{p}\left(y_1^n|y_{[0]}^n, x_{[0:0]}^n\right) := \tilde{p}\left(y_1^n|x_{[0]}^n\right)$ . The marginal likelihood approximation is then obtained as the mean of the Monte Carlo approximations, and we named this final algorithm SimBa-CL without feedback, see Algorithm 2.

When comparing Algorithm 2 with Algorithm 1, the simplicity of the latter becomes evident. The computational cost is reduced from  $\mathcal{O}\left(PTN^2\text{card}(\mathcal{X})^2\right)$  to  $\mathcal{O}\left(PTN\text{card}(\mathcal{X})^2\right)$ . Also, as with Algorithm 1, our new SimBa-CL procedure is parallelisable on both  $N$  and  $P$ .

---

**Algorithm 2** Simulation likelihood without feedback

---

**Require:**  $p(x_0)$ ,  $p(x_t|x_{t-1})$ ,  $p(y_t|x_t)$  and their factorisation

**for each**  $i \in [P]$  **do**

$x_0^{(i)} \sim p(x_0)$

**for**  $t \in [T]$  **do**

$x_t^{(i)} \sim p(x_t|x_{t-1}^{(i)})$

**for each**  $n \in [N]$  **do**

Run the prediction (15) and get:  $\left\{ \tilde{p} \left( x_t^n | y_{[t-1]}^n, x_{[0:t-1]}^{(i), \setminus n} \right) \right\}$

Run the correction (16) and get:  $\left\{ \begin{array}{l} \tilde{p} \left( x_t^n | y_t^n, x_{[0:t-1]}^{(i), \setminus n} \right) \\ \tilde{p} \left( y_t^n | y_{[t-1]}^n, x_{[0:t-1]}^{(i), \setminus n} \right) \end{array} \right\}$

**end for**

**end for**

**end for**

Return  $\frac{1}{P} \sum_{i \in [P]} \tilde{p} \left( y_{[T]}^n | x_{[0:T-1]}^{i, \setminus n}, \theta \right)$

---

### 3.3 KL-bound for SimBa-CL with and without feedback

To evaluate the impact of excluding the simulation feedback from SimBa-CL, a natural approach is to compare the two estimates of the marginal likelihood:

$$p(y_{[T]}^n) = \sum_{x_{[0:T]}^n} p(x_{[0:T]}^n) \sum_{x_{[0:T]}^n} p(x_{[0:T]}^n | x_{[0:T]}^n) \prod_{t \in [T]} p(y_t^n | x_t^n),$$
$$\tilde{p}(y_{[T]}^n) = \sum_{x_{[0:T]}^n} p(x_{[0:T]}^n) \sum_{x_{[0:T]}^n} p(x_0^n) \prod_{t \in [T]} p(x_t^n | x_{t-1}^n) p(y_t^n | x_t^n).$$

As both  $p(y_{[T]}^n)$  and  $\tilde{p}(y_{[T]}^n)$  are probability distributions on  $\mathcal{Y}^T$ , a simple way of comparing them is the Kullback-Leibler divergence, which we denote with  $\mathbf{KL}[p(\mathbf{x}) || q(\mathbf{x})]$  for  $p, q$  probability distributions on a general discrete space and  $q(x) = 0$  implying  $p(x) = 0$  (absolute continuity).

The objective of this section is then to establish an upper bound for  $\mathbf{KL} \left[ p \left( \mathbf{y}_{[T]}^n \right) || \tilde{p} \left( \mathbf{y}_{[T]}^n \right) \right]$ , which will also demonstrate that, under certain conditions, our “without feedback” approximation consistently improves. Naturally, for theoretical results, we must rely on technical assumptions, which we will strive to explain from an intuitive perspective as much as possible.

**Assumption 1.** For any  $n, \bar{n} \in [N]$  and for any  $x_t^{\bar{n}} \in \mathcal{X}$ , if  $x_{t-1}, \bar{x}_{t-1} \in \mathcal{X}^N$  are such that  $x_{t-1}^{\setminus n} = \bar{x}_{t-1}^{\setminus n}$  then:

$$|p(x_t^{\bar{n}} | x_{t-1}) - p(x_t^{\bar{n}} | \bar{x}_{t-1})| \leq \frac{s_{\bar{n}}}{N} |d_{n, \bar{n}}(x_{t-1}^n) - d_{n, \bar{n}}(\bar{x}_{t-1}^n)|,$$

where  $d_{n,\bar{n}} : \mathcal{X} \rightarrow \mathbb{R}_+$  and  $s_{\bar{n}}$  is a positive constant.

Assumption 1 ensures the boundness of the transition dynamic when altering the states of only  $n \in [N]$  at time  $t - 1$ . This essentially asserts that changing the state of a single component at time  $t - 1$  minimally impact the dynamics of the other components. In essence, the impact is measured in terms of the function  $d_{n,\bar{n}}$ , which shows how changes in  $n$  affect any other dimension  $\bar{n}$ . This concept is similar in flavour to the decay of correlation property explained in [Rebeschini and Van Handel \[2015\]](#) and [Rimella and Whiteley \[2022\]](#), which ensures a weak sensitivity of the conditional distributions on any  $n$  given a perturbation on any other dimension. Compare to [Rebeschini and Van Handel \[2015\]](#) and [Rimella and Whiteley \[2022\]](#) our assumption is way less intricate and it simply requires some form of linear decay in the overall dimension  $N$ . In simple terms, in large systems with interconnected dimensions minor changes have diminishing effects, which is also intuitively true in many real world application, like individual-based models for epidemiology [[Shamil et al., 2021](#), [Rimella et al., 2023a](#), [Cocker et al., 2023a](#)].

**Assumption 2.** For any  $n, \bar{n} \in [N]$ , if  $x_{t-1}, \bar{x}_{t-1} \in \mathcal{X}^N$  are such that  $x_{t-1}^{\setminus \bar{n}} = \bar{x}_{t-1}^{\setminus \bar{n}}$  then there exists  $0 < \epsilon < 1$  such that:

$$\sum_{x_t^n} p(x_t^n | x_{t-1}) \frac{1}{p(x_t^n | \bar{x}_{t-1})^2} \leq \frac{1}{\epsilon^2}, \quad \text{and} \quad \sum_{x_t^n} p(x_t^n | x_{t-1}) \frac{1}{p(x_t^n | \bar{x}_{t-1})^3} \leq \frac{1}{\epsilon^3}.$$

Assumption 2 imposes bounds on the expectations of the square and the cube of the reciprocal of the transition kernel. It is worth noting that this assumption is not excluding the case  $p(x_t^n | x_{t-1}, \theta) = 0$ , but rather ensures that the non-zero elements of the transition kernel are always non-zero.

Under assumptions 1-2 and the additional assumption that the effect of an interaction on a single dimension does not exceed  $N$ , we can state the following theorem.

**Theorem 1.** If  $|d_{n,\bar{n}}(x^n) - d_{n,\bar{n}}(\bar{x}^n)| < N$  for any  $x^n, \bar{x}^n \in \mathcal{X}$  and assumptions 1-2 hold, then for any  $n \in [N]$ :

$$\text{KL} [p(\mathbf{y}_{[T]}^n) || \tilde{p}(\mathbf{y}_{[T]}^n)] \leq \frac{a(\epsilon)}{N} \sum_{t \in [T]} \mathbb{E} \left\{ \frac{1}{N} \sum_{\bar{n} \in [N], \bar{n} \neq n} s_{\bar{n}}^{MAX} \text{Var} \left[ d_{n,\bar{n}}(\mathbf{x}_{t-1}^n) \mid \mathbf{x}_{[0:t-1]}^{\setminus n} \right] \right\},$$

where  $a(\epsilon) := 2 \left[ \frac{1}{2\epsilon^2} + \frac{1}{3\epsilon^3} \right]$  and  $s_n^{MAX} := \max\{s_n^2, s_n^3\}$ .

*Proof.* The proof requires the Data Processing inequality, a Taylor expansion of the function  $f(z) = \log(1+z)$  and Jensen's inequality. The full proof is available in the supplementary material.  $\square$

From Theorem 1 we can observe that the approximation improves when: (i)  $N$  increases; and (ii) the expected variance of the interaction term across dimensions decreases. Hence, our SimBa-CL without feedback will be more or less the same as the SimBa-CL with feedback whenever we are considering a sufficiently large  $N$  and not too noisy scenario.

### 3.4 SimBa-CL on general partitions

Up until now, we have implicitly assumed that approximating  $p(y_{[T]})$  involves a product of marginals across all dimensions. However, it is worth considering that a complete factorization across  $[N]$  might not be the optimal choice, and potentially disregarding interdependencies among dimensions.

It is hence not too difficult to imagine the existence of a more suitable factorization that better captures interdimensional interactions. Specifically, we consider a partition  $\mathcal{K}$  on  $[N]$  and reformulate our likelihood approximation as follows:

$$p(y_{[T]}) \approx \prod_{K \in \mathcal{K}} p(y_{[T]}^K), \quad \text{or} \quad p(y_{[T]}) \approx \prod_{K \in \mathcal{K}} \tilde{p}_{\mathcal{K}}(y_{[T]}^K), \quad (17)$$

where on the left we have the actual product of the true marginals and on the right  $\tilde{p}_{\mathcal{K}}$  denotes the generalization of  $\tilde{p}$ . As for SimBa-CL with and without feedback we can reformulate our marginals and approximate marginals as a simulation from the model followed by an HMM likelihood:

$$p(y_{[T]}^K) := \sum_{x_{[0:T]}^{\setminus K}} p(x_{[0:T]}^{\setminus K}) \sum_{x_{[0:T]}^K} p(x_{[0:T]}^K | x_{[0:T]}^{\setminus K}) \prod_{t \in [T]} \prod_{n \in K} p(y_t^n | x_t^n); \quad (18)$$

$$\tilde{p}_{\mathcal{K}}(y_{[T]}^K) := \sum_{x_{[0:T]}^{\setminus K}} p(x_{[0:T]}^{\setminus K}) \sum_{x_{[0:T]}^K} \prod_{n \in K} p(x_0^n) \prod_{t \in [T]} p(x_t^n | x_{t-1}^n) p(y_t^n | x_t^n). \quad (19)$$

As it can be extrapolated from (17), the likelihood approximations are now including all the interaction inside  $K$ , while still enforcing some form of factorisation.

As seen in Section 3.1 and in Section 3.2, (18) aims to approximate the true marginals over  $K \in \mathcal{K}$ , while (19) only offers approximations. Once again, akin to SimBa-CL with feedback, if we want to approximate the true marginals of the likelihood we need some form of simulation feedback. This time, the simulation feedback will be from  $x_{[0:t]}^{\setminus K}$  onto  $x_{t-1}^K$ , as we are considering probability distributions on  $K$ .

We can then easily adapt Algorithm 1 and Algorithm 2, transitioning from a full factorisation to a factorisation on the partition  $\mathcal{K}$ . Note that, the algorithm requires operations on the space  $\mathcal{X}^K$  and so a computational cost that is exponential in the maximum number of components contained in  $K$ :  $\mathcal{O}(PT \text{card}(\mathcal{K}) \text{card}(\mathcal{X})^{2 \max_{K \in \mathcal{K}} \text{card}(K)})$ . More details and theoretical results are available in the supplementary material.

## 4 Confidence sets for SimBa-CL

Composite likelihoods are generally obtained as product of likelihoods components, whose structure dependent on the considered model, see [Varin et al. \[2011\]](#) for a review on composite likelihood methods. There are two classes of composite likelihoods: composite conditional likelihoods and composite marginal likelihoods. Composite conditional likelihoods combine

conditional distributions obtained from the main likelihood [Besag, 1974, 1975, Vecchia, 1988, Mardia et al., 2008], while composite marginal likelihoods work on the marginal distributions [Cox and Reid, 2004, Chandler and Bate, 2007, Varin and Vidoni, 2008]. Considering that both SimBa-CL with and without feedback are represented as a product of the marginals of the likelihood, one can easily draw parallels with the composite marginal likelihoods literature and exploit the asymptotic theory to build confidence sets.

The first step is to find the maximum composite likelihood estimator  $\hat{\theta}_{CL}$  by maximising the composite likelihood  $\mathcal{L}_{CL}(\theta; y_{[T]}) = \prod_{K \in \mathcal{K}} \mathcal{L}_{CL}^K(\theta; y_{[T]}^K)$  or, equivalently, the composite log-likelihood  $\ell_{CL}(\theta; y_{[T]}) = \sum_{K \in \mathcal{K}} \ell_{CL}^K(\theta; y_{[T]}^K)$ , where  $\mathcal{L}_{CL}^K(\theta; y_{[T]}^K)$  and  $\ell_{CL}^K(\theta; y_{[T]}^K)$  depends on the considered SimBa-CL. As SimBa-CL does not require any resampling, the resulting procedure is suited to automatic differentiation, which allows us to optimise the parameters via any gradient descent technique [Hinton et al., 2012, Zeiler, 2012, Kingma and Ba, 2014].

The second step is to notice that in the composite likelihood literature, we have some form of asymptotic normality for  $\hat{\theta}_{CL}$  [Lindsay, 1988, Varin, 2008]:

$$\hat{\theta}_{CL} \stackrel{d}{\approx} \mathcal{N}(\theta, G(\theta)^{-1}),$$

where  $G(\theta)$  is the Godambe information matrix [Godambe, 1960]. It then follows that, upon estimation Godambe information matrix, we can build confidence sets for  $\hat{\theta}_{CL}$  as multidimensional ellipsoids.

The final step is to estimate the Godambe information matrix, which is given by  $G(\theta) = S(\theta)V(\theta)^{-1}S(\theta)$ , and so decomposed in the sensitivity matrix and the variability matrix:

$$S(\theta) = \mathbb{E}_{\theta} \left\{ -\text{Hess}_{\theta} [\ell_{CL}(\theta; \mathbf{y}_{[T]})] \right\} \quad \text{and} \quad V(\theta) = \text{Var}_{\theta} \left\{ \nabla_{\theta} [\ell_{CL}(\theta; \mathbf{y}_{[T]})] \right\},$$

where  $\text{Hess}_{\theta}$  and  $\nabla_{\theta}$  are the Hessian and the gradient with respect to  $\theta$ , and can be computed via automatic differentiation given  $\theta$  and a realisation of  $\mathbf{y}_{[T]}$ . Given that we can compute Hessian and the gradient given  $\theta, y_{[T]}$ , we can also estimate expectation and the variance via simulations from the model (expected information). Approximating  $S(\theta)$  and  $V(\theta)$  with the actual observations (observed information) is slightly discussed in the supplementary material along with some experiments.

## 4.1 Bartlett identities

The computation of the Hessian can be resource-intensive, especially when using automatic differentiation, and variance estimation might be noisy. We can then simplify the form of sensitivity and variability matrix by invoking the first and second Bartlett identities. Note that, when considering SimBa-CL with feedback the identities hold asymptotically in the number of Monte Carlo samples  $P$ , while for SimBa-CL without feedback they hold only

approximately. The sensitivity matrix and variability matrix can be then reformulated as:

$$S(\theta) = \sum_{K \in \mathcal{K}} \mathbb{E}_\theta \left\{ \nabla_\theta [\ell_{CL}^K(\theta; y_{[T]}^K)] \nabla_\theta [\ell_{CL}^K(\theta; y_{[T]}^K)]^\top \right\},$$

$$V(\theta) = \sum_{K, \tilde{K} \in \mathcal{K}} \mathbb{E}_\theta \left\{ \nabla_\theta [\ell_{CL}^K(\theta; y_{[T]}^K)] \nabla_\theta [\ell_{CL}^{\tilde{K}}(\theta; y_{[T]}^{\tilde{K}})]^\top \right\},$$

where  $=$  becomes  $\approx$  if we do not include the feedback, and where both matrices can be once again estimated via simulation. More details are available in the supplementary material.

## 5 Experiments

The experiments center on the field of epidemiological modelling, and specifically they focus on individual-based models (IBMs). Individual-based models arise when we want to describe an epidemic from an individual perspective. The complexity of IBMs lies in their high-dimensional state-space, making close-form likelihood computationally unfeasible. However, these models satisfy the factorisation outlined in (2), making them the perfect candidates for our SimBa-CL.

SimBa-CL is implemented in Python using the library TensorFlow and available at the GitHub repository: <https://github.com/epiforensics/simba-cl>, and all the experiments were run on a 32gb Tesla V100 GPU.

More experiments and more details on the presented experiments are available in the supplementary material.

### 5.1 The effect of feedback and partition's choice on SimBa-CL

In this section we perform a cross-comparison on a susceptible-infected-susceptible (SIS) individuals based model on SimBa-CL with feedback on  $\mathcal{K} = \{\{1\}, \dots, \{N\}\}$  (“fully factorised SimBa-CL with feedback”), SimBa-CL without feedback on  $\mathcal{K} = \{\{1\}, \dots, \{N\}\}$  (“fully factorised SimBa-CL without feedback”), and SimBa-CL without feedback on  $\mathcal{K} = \{\{1, 2\}, \dots, \{N-1, N\}\}$  (“coupled SimBa-CL without feedback”), where  $N$  is assumed to be even.

#### 5.1.1 Model

Building upon the framework introduced by [Ju et al. \[2021\]](#) and [Rimella et al. \[2023b\]](#), where  $n$  represent an individual and  $w_n$  is a vector of covariates. We consider a  $p(x_0^n | \theta)$  with an initial probability of infection of  $\frac{1}{1 + \exp(-\beta_0^\top w_n)}$  and a transition kernel  $p(x_t^n | x_{t-1}, \theta)$  with a probability of transitioning from S to I of  $1 - \exp\left[-\lambda_n \left(\frac{\sum_{n \in [N]} \mathbb{1}(x_{t-1}^n = 2)}{N} + \iota\right)\right]$  and a probability of transitioning from I to S of  $1 - \exp(-\gamma_n)$ , where  $\lambda_n = 1/(1 + \exp(-\beta_\lambda^\top w_n))$  and  $\gamma_n = 1/(1 + \exp(-\beta_\gamma^\top w_n))$  and with  $w_n, \beta_0, \beta_\lambda, \beta_\gamma \in \mathbb{R}^2$ . Moreover we consider  $p(y_t^n | x_t^n, \theta) =$



$q^{x_t^n} \mathbb{I}(y_t^n \neq 0) + (1 - q^{x_t^n}) \mathbb{I}(y_t^n = 0)$ , with  $q \in [0, 1]^2$ . Unless specify otherwise, our baseline model employs  $N = 1000$ ,  $T = 100$ ,  $w_n$  to be such that  $w_n^1 = 1$  and  $w_n^2 \sim \mathbf{Normal}(0, 1)$ , and the data generating parameters  $\beta_0 = [-\log((1/0.01) - 1), 0]^\top$ ,  $\beta_\lambda = [-1, 2]^\top$ ,  $\beta_\gamma = [-1, -1]^\top$ ,  $q = [0.6, 0.4]^\top$  and  $\iota = 0.001$ . It is also important to mention that the considered SIS satisfies Assumption 1 and Assumption 2.

### 5.1.2 Empirical evaluation of the Kullback-Leibler divergence

We start by comparing our SimBa-CL methods in terms of empirical Kullback-Leibler divergence (KL) on a set of simulated data. Different settings are considered: an increasing population size  $N = [10, 100, 1000]$ ; either “high”  $\beta_0 = [-6.9, 0]^\top$  or “base”  $\beta_0 = [-4.60, 0]^\top$  or “low”  $\beta_0 = [-2.20, 0]^\top$ , i.e. around either 0.1% or 1% or 10% of initial infected; and “base” and “low”  $\iota = [0.001, 0.01]$ . Note that different  $\beta_0$  and  $\iota$  control the variance of the process, as having more infected at the beginning of the epidemic or including more environmental effect result in an epidemic that is closer to the equilibrium.

$N$	1000	100	100	100	100	10
$\beta_0$	base	high	low	base	base	base
$\iota$	base	base	base	base	low	base
<b>KL</b> on feedback	0.3 (0.2)	7.5 (3.2)	0.8 (0.4)	5.9 (2.9)	1.4 (1)	49.6 (17.2)
<b>KL</b> on partition	1.4 (0.3)	36.1 (6.6)	3 (0.9)	35.1 (7)	5.6 (2)	177.3 (36.5)

Table 1: Comparing empirical KL between SimBa-CL and under different scenarios. All the numerical values have been multiply by  $10^9$  to improve visualisation.

Table 1 reports mean and standard deviations of the empirical KL per each scenario. Focusing on the fourth column, which contrasts the fully factorised SimBa-CL with and without feedback, we can notice that: increasing  $N$  decreases the KL and decreasing the variance decreases the KL. Similar conclusions can be drawn for the fifth column, which compares the fully factorise SimBa-CL without feedback with the coupled SimBa-CL without feedback. These comments suggests less and less differences across the methods when increasing  $N$  and decreasing the variance, which is in line with our theoretical results.

### 5.1.3 Comparing likelihood surfaces

We proceed to undertake a comparison of profile likelihood surfaces for the baseline IBM SIS model using the following protocol: (i) choose one among  $\beta_0$ ,  $\beta_\lambda$ ,  $\beta_\gamma$  and  $q$ ; (ii) simulate using the baseline model, and ensure at least 10 infected in the epidemic realisation; (iii) create a bi-dimensional grid on the chosen parameter; (iv) per each element of the grid compute our SimBa-CL methods by fixing the other parameters to their real values.

The outcomes of this experiment are illustrated in Figure 1. Interestingly, all the considered SimBa-CL exhibit a consistent shape, meaning that, in the SIS scenario, including the feedback or choosing a coarser partition has a limited impact on the overall likelihood. Furthermore, it becomes evident that all these methods effectively recover the data-generating

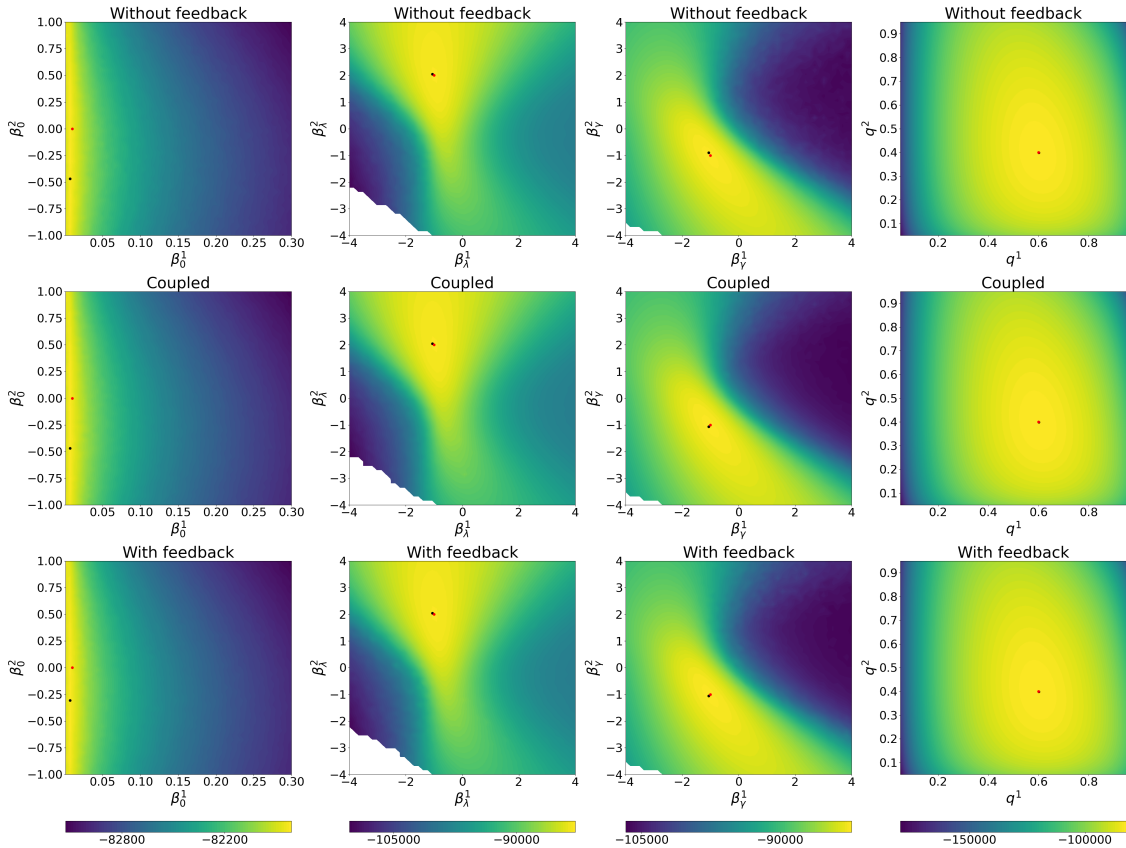


Figure 1: Profile log-likelihood surfaces for  $\beta_0, \beta_\lambda, \beta_\gamma, q$ . From top to bottom, fully factorised SimBa-CL without feedback, coupled SimBa-CL without feedback, and fully factorised SimBa-CL with feedback. Red dots locate the data generating parameter, while black dots are used for the maximum on the grid.

parameter, except for  $\beta_0$ . Note that there is an obvious identifiability issue with  $\beta_0$  as  $\beta_0^2 = 0$  implies covariate  $w_n^2$  to not be used. However, given that  $w_n^2$  is random, we could have more initial infected associated to  $w_n^2 < 0$ , which gives an higher likelihood to models where  $\beta_0^2 < 0$ . A similar reasoning can be replicated for  $w_n^2 > 0$ , which explains the symmetry of the likelihood surface of  $\beta_0$  on the vertical axis.

## 5.2 Asymptotic properties of SimBa-CL

We can now turn to the problem of computing the maximum composite likelihood estimator and the corresponding confidence sets. As proven in theorems 1, for a sufficiently “regular” model and a sufficiently large  $N$ , including the simulation feedback and using a coarser partition bears marginal significance for SimBa-CL. We hence narrow our studies to the asymptotic properties of the fully factorised SimBa-CL without feedback. As a toy model, we consider again the IBM SIS described in Section 5.1.1.

### 5.2.1 Maximum SimBa-CL convergence and coverage in two dimensions

We start our exploration by looking at the bi-dimensional parameter  $\beta_\lambda$ , given all the other parameters fixed to their baseline values. The hope is that  $\beta_\lambda$  is easily identifiable as it highly influence the evolution of the epidemics, and so we can test the asymptotic properties on a well-behaved parameter.

To explore the asymptotics of SimBa-CL we investigate four scenarios with an increasing amount of data: (i)  $N = 100, T = 100$ ; (ii)  $N = 100, T = 300$ ; (iii)  $N = 1000, T = 100$ ; (iv)  $N = 1000, T = 300$ . Per each scenario, we simulate 100 epidemics and per each dataset we optimize  $\beta_\lambda$  through Adam optimization [Kingma and Ba, 2014], aiming to minimize the negative log-likelihood. After optimization, we have a sample of 100 bi-dimensional parameters per each scenario, which can be turned into box-plots as shown in Figure 2. Here, as both  $T$  and  $N$  increases, we can observe an evident shrinkage towards the true parameter, suggesting consistency of the maximum SimBa-CL estimator when  $N$  and  $T$  increases.

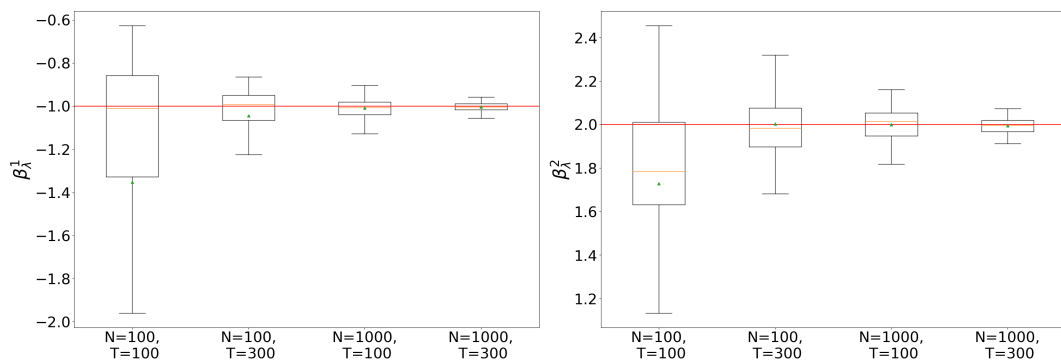


Figure 2: Box-plots on the optimized  $\beta_\lambda$ . On the left,  $\beta_\lambda^1$ , on the right,  $\beta_\lambda^2$ . Horizontal solid orange lines show the medians and green triangles are used for the means. Horizontal red solid lines show the true parameters.

Taking the investigation a step further, we analyse the empirical coverage of confidence sets built as explained in Section 4. We consider  $N = 1000, T = 300$  and the optimized parameters from the previous experiment. We start by calculating the Godambe information matrix without using the approximate Bartlett identities, and we build 95% 2-dimensional confidence sets for our parameter  $\beta_\lambda$ . The procedure results in a coverage of 1 and so an overestimation of uncertainty. However, when repeating the same procedure using the approximate Bartlett identities, the coverage now aligns with the theoretical coverage of 0.95. This favorable outcome can be attributed to less noisy estimates, as we are exploiting the factorisation in the model and so computing expectations on lower dimensional spaces.

## 5.2.2 Maximum Simba-CL convergence and coverage in nine dimensions

Transitioning to a substantially more intricate scenario, we set our sights on the estimation of all model parameters  $\theta = (\beta_0, \beta_\lambda, \beta_\gamma, q, \iota)$ . Analogous to the 2-dimensional case, we simulate from the model 100 times and per each simulation we optimize the parameters using Adam optimizer. The outcomes are reported in Figure 3.

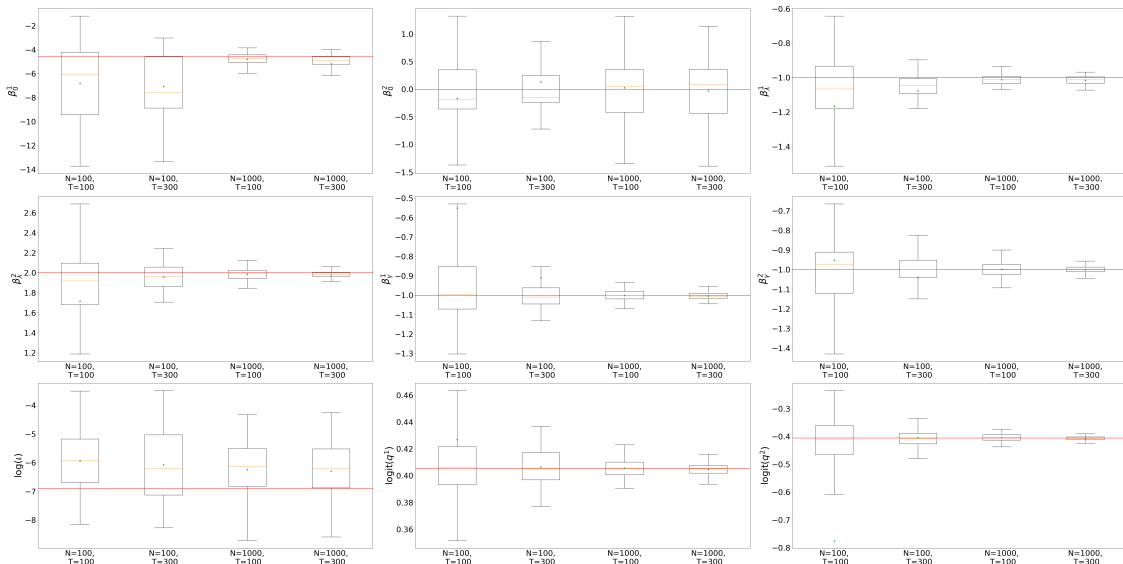


Figure 3: Box-plots on the optimized  $\theta = (\beta_0, \beta_\lambda, \beta_\gamma, q, \iota)$ . Parameters labels are reported on the y-axes. Horizontal orange solid lines show the medians and green triangles are used for the means. Horizontal red solid lines show the true parameters.

Foremost, it becomes apparent that increasing the value of  $T$  does not influence  $\beta_0$ . This arises due to the fact that observations in the later time periods carry scarce information on the initial condition. Moreover, recall that  $w_n^2 \sim \mathbf{Normal}(0, 1)$  and  $\beta_0^2 = 0$ . This makes the parameter not identifiable, as commented in Section 5.1. This ill-posed model definition implies that increasing  $N$  will not improve the uncertainty around our estimate as  $\beta_0^2 < 0$  and  $\beta_0^2 > 0$  can be equally likely, while the unbiasedness is preserved due to the symmetry of the set of equally likely parameters. At the same time, the parameter  $\iota$  and  $\beta_\lambda$  are also hard to identify as smaller (or bigger) estimates of  $\beta_\lambda$  will lead to bigger (or smaller) estimates of  $\iota$ . Indeed,  $\beta_\lambda$  governs the infection rates from the community, while  $\iota$  represents the environmental effect. It is then clear that generating an epidemic from  $\beta_\lambda, \iota$  is equivalent to generating one by decreasing  $\beta_\lambda$  and increasing accordingly  $\iota$ . This correlation is especially vivid in Figure 3, as an over-estimation of  $\iota$  (log-scale) lead to an underestimation of  $\beta_\lambda$ .

Clearly, in a 9-dimensional scenario, the process of recovering empirically the theoretical coverage is substantially more complicated. Jointly, we find 0 coverage of the 9-dimensional 95% confidence sets, irrespective of whether the Bartlett identities are employed or not. We then compute the confidence intervals on single parameters by marginalising the 9-

dimensional Gaussian distribution. Marginally, we find that using the approximate Bartlett identities improve the coverages, see Table 2 for numerical values.

Parameter	$\beta_0$	$\beta_\lambda$	$\beta_\gamma$	$q$	$\iota$
Without Bartlett	0.17 and 0.05	0.61 and 0.87	0.8 and 1.	0.87 and 0.5	0.02
With Bartlett	0.98 and 0.89	0.99 and 0.75	0.97 and 0.97	1. and 0.98	0.92

Table 2: Empirical coverage per each parameter when computing the Godambe information matrix with and without the approximate Bartlett identities. Whenever the parameter is bi-dimensional the coverage per each component is reported in the same cell separated by “and”.

### 5.3 Comparing SimBa-CL with sequential Monte Carlo

As SimBa-CL methods provide biased estimates of the likelihood, the objective of this section is to compare SimBa-CL methods with both sequential Monte Carlo (SMC) and block sequential Monte Carlo (BSMC) algorithms. While SMC provides unbiased particles estimate of the likelihood [Chopin and Papaspiliopoulos, 2020], this quantity can suffer high variance in high-dimensional scenarios. On the other hand, BSMC deals with the curse of dimensionality by providing a factorised, albeit biased, particles estimate of the likelihood [Rebeschini and Van Handel, 2015], aligning with SimBa-CL.

Building upon the insights of the previous sections, we compare SMC and BSMC with fully factorised SimBa-CL without feedback. Regarding the SMC comparison, we consider two approaches: the auxiliary particle filter (APF) and the SMC with proposal distribution given by the approximate optimal proposal distribution developed by Rimella et al. [2023b]. Due to the curse of dimensionality we expect poor performances of the APF, hence we include the Block APF in our analysis. The block APF works as the Block particle filter [Rebeschini and Van Handel, 2015], a BSMC algorithm, but it propose particles according to the transition kernel informed by the current observation.

#### 5.3.1 Model

In the subsequent sections we work again on the IBM SIS model from Section 5.1.1. However, we also analyse an individual-based susceptible-exposed-infected-removed (SEIR) model. Specifically, we still have some bi-dimensional covariates  $w_n$ , while  $p(x_0^n|\theta)$  is now 4-dimensional with the second and the fourth components being zero and the first and the third components being as in IBM SIS. Similarly, the transition kernel  $p(x_t^n|x_{t-1}, \theta)$  is a 4 by 4 matrix with the same dynamics of IBM SIS when considering transitions from S to E and from I to R, with the addition of a transition E to I with probability  $1 - e^{-\rho}$ . Unless specified otherwise, we consider as the baseline model the one with:  $N = 1000$ ,  $T = 100$  and the data generating parameters set to  $\beta_0 = [-\log((1/0.01) - 1), 0]^\top$ ,  $\beta_\lambda = [-1, 2]^\top$ ,  $\rho = 0.2$ ,  $\beta_\gamma = [-1, -1]^\top$ ,  $q = [0, 0, 0.6, 0.4]^\top$ .

### 5.3.2 SimBa-CL and SMC for an individual-based SIS model

We consider the baseline SIS model with  $N = 1000$ , and precisely: we generate the data; we run SimBa-CL and the baselines algorithms 100 times on the given data using the data generating parameters; and we estimate the mean and standard deviation of the log-likelihood. The results are reported in Table 3.

P	512	1024	2048	Time (sec)
APF	-81103.37 (46.04)	-81046.57 (49.65)	-80976.34 (36.08)	1.05s
h=5	-79551.92 (1.79)	-79552.24 (1.6)	-79552.81 (1.57)	3.78s
h=10	-79551.9 (1.81)	-79552.22 (1.47)	-79553.01 (1.56)	5.61s
Block APF	-79565.69 (5.84)	-79558.44 (3.95)	Out of memory	2.97s
SimBa-CL	-79612.74 (3.4)	-79612.31 (2.37)	-79612.34 (1.55)	1.03s

Table 3: Log-likelihood means and log-likelihood standard deviations for the baseline SIS model with  $N = 1000$ .  $h$  is the number of future observations included in Rimella et al. [2023b] ( $h = 0$  correspond to APF).

Notably, the method proposed by Rimella et al. [2023b] emerges as the best method in terms of log-likelihood mean and variance, as it yields to unbiased estimates of the likelihood and it reduces the variance. Our SimBa-CL exhibits superior computational efficiency, with a running time that is also almost three times faster than vanilla Block APF.

As the bias from our SimBa-CL seems significant compared to the one from Block APF, we run a paired comparison on the profile likelihood surfaces as in Section 5.1, and report them in Figure 4. It can be noticed that both SimBa-CL and Block APF generate similar likelihood surfaces whose maxima are close to the data generating parameter. Unfortunately, we could not include in our studies the SMC from Rimella et al. [2023b] for computational reasons.

### 5.3.3 SimBa-CL and SMC for an individual-based SEIR model

The section concludes with a comparison on the baseline IBM SEIR. As for the SIS model we simulate synthetic data, we run our SimBa-CL along with the baselines algorithms using the data generating parameter, and we estimate the mean and variance of the resulting log-likelihood computations. The outcomes are reported in Table 4.

It is important to note that the SEIR scenario is considerably more complex than the SIS scenario. In the SEIR case, observing only infected and removed makes difficult for the SMC algorithms to prevent particle failure, without the use of a very informative proposal distributions.

Table 4 clearly shows that, in order to avoid failure of the SMC, we need a smart proposal distribution as the one proposed by Rimella and Whiteley [2022], and also a large  $h$  to reach a reasonable log-likelihood variance. On the other hand, our SimBa-CL is able to reach almost comparable log-likelihood variance almost ten times faster than the SMC.



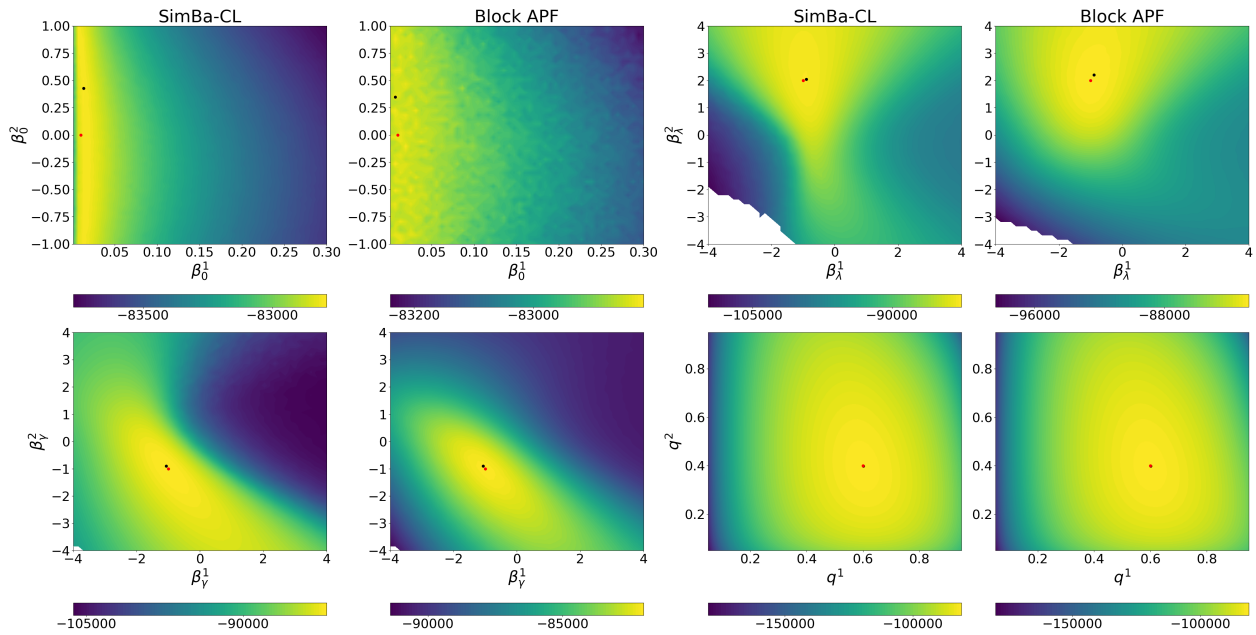


Figure 4: Profile log-likelihood surfaces for  $\beta_0, \beta_\lambda, \beta_\gamma, q$  from fully factorised SimBa-CL without feedback (first and third column) and Block APF (second and the fourth columns). Red dots are used for the data generating parameter, while black dots locate the maximum on the grid.

P	512	1024	2048	Time (sec)
APF	Failed	Failed	Failed	1.2s
h=5	-43447.56 (52.04)	-43419.52 (51.08)	-43391.0 (52.41)	4.44s
h=20	-43004.55 (5.38)	-43001.9 (4.65)	-42999.76 (3.7)	11.08s
h=50	-42999.93 (3.44)	-42998.13 (2.72)	-42996.74 (2.39)	20.88s
Block APF	Failed	Failed	Failed	2.09s
SimBa	-43683.85 (9.54)	-43683.67 (7.35)	-43683.76 (5.16)	1.25s

Table 4: Log-likelihood means and log-likelihood standard deviations for the baseline SEIR model with  $N = 1000$ .  $h$  is the number of future observations included in [Rimella et al. \[2023b\]](#) ( $h = 0$  correspond to APF).

## 5.4 2001 UK Foot and mouth disease outbreak

In the year 2001, the United Kingdom experienced an outbreak of foot and mouth disease, a highly contagious virus affecting cloven-hoofed animals. Over an 8 month period, 2026 farms out of 188361 in the UK were infected, concentrated in the North and South West of England, and costing an estimated £8 billion to public and private sectors [[UK National Audit Office](#)]. The publicly available dataset (<http://www.defra.gov.uk>) has been extensively studied, and we choose as an example an analysis of the 8791 farms in the Cumbria region to compare to a previous similar MCMC-based analysis in [Jewell et al. \[2009\]](#).



### 5.4.1 Model

Similar to previous models, we consider an individual-based model with farms as the individual. We assume farms exist in Susceptible, Infected, Notified (i.e. quarantined on detection), and Removed states (the SINR model). Transitions from S to I and I to N follow a discrete-time stochastic process, with infected farms immediately quarantined, and N to R (farm culling) occurs deterministically after 1 day.

We consider an initial probability of infection for farm  $n$  of  $1 - \exp\left\{-\tau \frac{\sum_{\tilde{n} \in [N]} \lambda_{\tilde{n},n}}{N}\right\}$ , with parameter  $\tau > 0$ . We assume transition probabilities  $Pr(x_{t+1}^n = N | x_t^n = I) = 1 - \exp\{-\gamma\}$ ,  $\gamma > 0$ , and  $Pr(x_{t+1}^n = N | x_t^n = I) = 1$ . We assume individual infection probabilities  $Pr(x_{t+1}^n = I | x_t^n = S, x_t) = 1 - \exp\left\{-\frac{\sum_{\tilde{n} \in [N]} \lambda_{\tilde{n},n} \mathbb{I}(x_{t-1}^{\tilde{n}}=2)}{N}\right\}$ , where  $\lambda_{\tilde{n},n}$  is the infection pressure exerted by an infected farm  $\tilde{n}$  to a susceptible farm  $n$  and formulated as:

$$\lambda_{\tilde{n},n} = \frac{\delta}{N} [\zeta (w_{\tilde{n}}^c)^\chi + (w_{\tilde{n}}^s)^\chi] [\xi (w_n^c)^\chi + (w_n^s)^\chi] \frac{\psi}{E_{\tilde{n},n}^2 + \psi^2},$$

with  $\delta, \xi, \zeta, \chi, \psi$  positive parameters,  $w_n^c$  number of cattle in the  $n$ -th farm,  $w_n^s$  number of sheep in the  $n$ -th farm and  $E_{\tilde{n},n}$  the Euclidean distance in kilometres between farm  $\tilde{n}$  and farm  $n$ . This SINR model is an example of heterogeneous mixing individual-based model as the infectious contacts are not homogeneous in space. The emission distribution follows the usual formulation  $p(y_t^n | x_t^n, \theta) = q^{x_t^n} \mathbb{I}(y_t^n \neq 0) + (1 - q^{x_t^n}) \mathbb{I}(y_t^n = 0)$ , with  $q = [0, 0, 1, 0]^\top$  as we observe perfectly the notified.

### 5.4.2 Inference

We run 100 optimization using Adam on our fully factorised SimBa-CL without feedback and select the “best” simulation according to its final SimBa-CL score. We then estimate the Godambe information matrix using the approximate Bartlett identities. As we learned the parameters in a log-scale, we need to use log-Normal’s when plotting the parameters distributions, see Figure 5.

The parameter  $\tau$  can be intuitively understood as the time interval between the first infection and the first notified infections, marking the onset of the notification process. In Figure 5 we can recognise an optimal  $\tau$  of about 40, suggesting a relatively slow start in notifying farms. Furthermore we can observe a mean time before notification of about 2.5 days, leading to an estimate of 3.5 days for the mean infection period, encompassing the period from farm infection to culling. This implies a relatively fast intervention once the notification process is implemented. Also, from the last row of Figure 5, we can notice a decrease of over 60% of the infectivity after just 2 km, which could be used to define containment zones around infected farms.

Parameters  $\zeta, \chi, \xi$  are more difficult to interpret as they regulate the susceptibility and infectivity of farms according to the number of animals. To help visualising their effect we produce Table 5, which shows average susceptibility and infectivity of: a medium-size farm

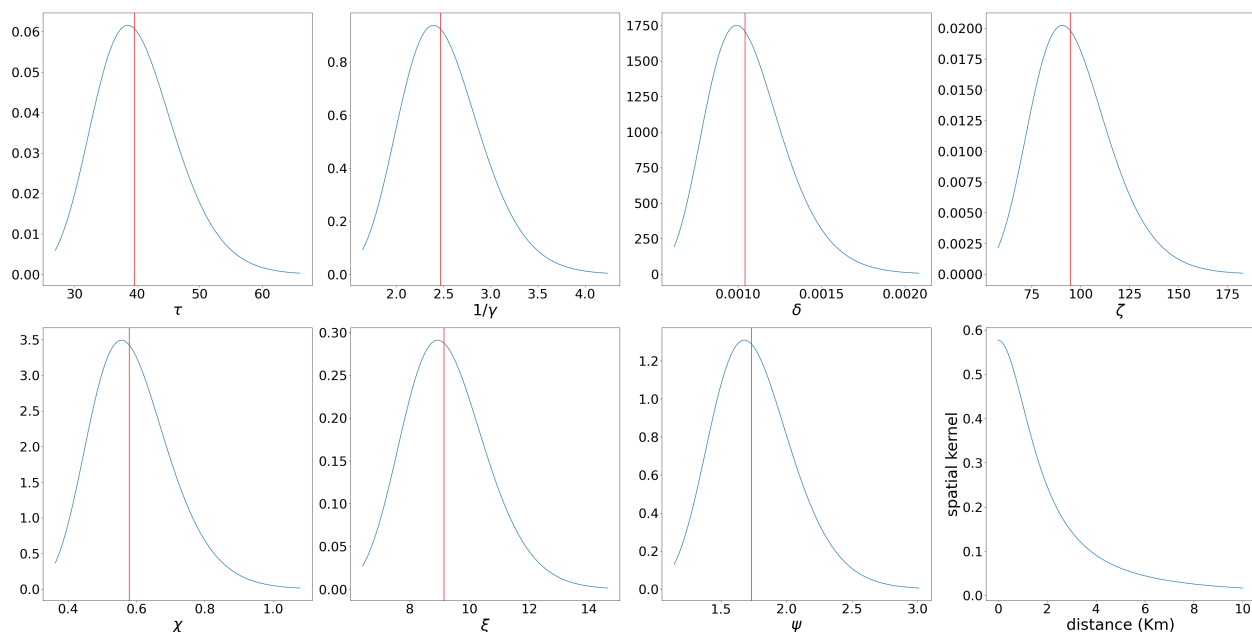


Figure 5: FMD parameters' distributions and spatial kernel decay. Parameters' labels are reported on the x-axes. Red solid lines represent the maximum SimBa-CL estimator. The last plot of the second row shows the spatial decay of infectivity in Km.

Nr. cattle	Nr. sheep	Mean susceptibility	Mean infectivity
100	0	131.83	1364.99
0	1000	54.69	54.69
50	500	124.84	950.17
2	6	16.49	144.37

Table 5: Mean susceptibility and mean infectivity for four farms conformations.

with only cattle, a medium-size farm with only sheep, a large-size farm and a small-size farm. From Table 5 we can deduce that the effect of owing cattle is significantly higher than the one of owing sheep for both infectivity and susceptibility, and that even small farms can affect the epidemic spread. This agrees with the study from [Jewell et al., 2013] and also with the Directive of the Council of the European Union.

## Funding

This work is supported by EPSRC grants EP/R018561/1 (Bayes4Health) and EP/R034710/1 (CoSInES).

## References

- L. J. Allen. An introduction to stochastic epidemic models. In *Mathematical epidemiology*, pages 81–130. Springer, 2008.
- M. A. Beaumont. Approximate bayesian computation. *Annual review of statistics and its application*, 6:379–403, 2019.
- J. Besag. Spatial interaction and the statistical analysis of lattice systems. *Journal of the Royal Statistical Society: Series B (Methodological)*, 36(2):192–225, 1974.
- J. Besag. Statistical analysis of non-lattice data. *Journal of the Royal Statistical Society: Series D (The Statistician)*, 24(3):179–195, 1975.
- F. Bianchi and F. Squazzoni. Agent-based models in sociology. *Wiley Interdisciplinary Reviews: Computational Statistics*, 7(4):284–306, 2015.
- D. M. Blei, A. Kucukelbir, and J. D. McAuliffe. Variational inference: A review for statisticians. *Journal of the American statistical Association*, 112(518):859–877, 2017.
- X. Boyen and D. Koller. Exploiting the architecture of dynamic systems. In *AAAI/IAAI*, pages 313–320, 1999.
- X. Boyen and D. Koller. Tractable inference for complex stochastic processes. *arXiv preprint arXiv:1301.7362*, 2013.
- T. Britton. Stochastic epidemic models: a survey. *Mathematical biosciences*, 225(1):24–35, 2010.
- R. E. Chandler and S. Bate. Inference for clustered data using the independence loglikelihood. *Biometrika*, 94(1):167–183, 2007.
- N. Chopin and O. Papaspiliopoulos. *Introduction to Sequential Monte Carlo*. Springer International Publishing, 2020.
- D. Cocker, K. Chidziwisano, M. Mphasa, T. Mwapasa, J. M. Lewis, B. Rowlingson, M. Sammarro, W. Bakali, C. Salifu, A. Zuza, et al. Investigating one health risks for human colonisation with extended spectrum beta-lactamase producing e. coli and k. pneumoniae in malawian households: a longitudinal cohort study. *The Lancet Microbe*, 2023a.
- D. Cocker, M. Sammarro, K. Chidziwisano, N. Elviss, S. Jacob, H. Kajumbula, L. Mugisha, D. Musoke, P. Musicha, A. Roberts, B. Rowlingson, A. Singer, R. Byrne, T. Edwards, R. Lester, C. Wilson, B. Hollihead, N. Thomson, C. Jewell, T. Morse, and N. Feasey. Drivers of Resistance in Uganda and Malawi (DRUM): a protocol for the evaluation of One-Health drivers of Extended Spectrum Beta Lactamase (ESBL) resistance in Low-Middle Income Countries (LMICs) [version 2; peer review: 1 approved, 1 approved with

- reservations]. *Wellcome Open Res*, 7:55, 2023b. doi: [\url{https://doi.org/10.12688/wellcomeopenres.17581.2}](https://doi.org/10.12688/wellcomeopenres.17581.2).
- D. R. Cox and N. Reid. A note on pseudolikelihood constructed from marginal densities. *Biometrika*, 91(3):729–737, 2004.
- Directive of the Council of the European Union, 2003. COUNCIL DIRECTIVE 2003/85/EC of 29 September 2003 on Community measures for the control of foot-and-mouth disease repealing Directive 85/111/EEC and Decisions 89/531/EEC and 91/665/EEC and amending Directive 92/46/EEC, Official Journal of the European Union.
- A. Doucet, N. De Freitas, and N. Gordon. An introduction to sequential monte carlo methods. *Sequential Monte Carlo methods in practice*, pages 3–14, 2001.
- P. Fearnhead and D. Prangle. Constructing summary statistics for approximate Bayesian computation: semi-automatic approximate Bayesian computation. *Journal of the Royal Statistical Society Series B: Statistical Methodology*, 74(3):419–474, 2012.
- R. Glennie, T. Adam, V. Leos-Barajas, T. Michelot, T. Photopoulou, and B. T. McClintock. Hidden Markov models: Pitfalls and opportunities in ecology. *Methods in Ecology and Evolution*, 14(1):43–56, 2023.
- V. P. Godambe. An optimum property of regular maximum likelihood estimation. *The Annals of Mathematical Statistics*, 31(4):1208–1211, 1960.
- G. Hinton, N. Srivastava, and K. Swersky. Neural networks for machine learning: Lecture 6a, overview of mini-batch gradient descent. <http://www.cs.toronto.edu/~hinton/coursera/lecture6/lec6.pdf>, 2012.
- C. Jewell, J. Brown, M. Keeling, L. Green, G. Roberts, et al. Bayesian epidemic risk prediction-knowledge transfer and usability at all levels. In *Society for Veterinary Epidemiology and Preventive Medicine. Proceedings of a meeting held in Madrid, Spain, 20-22 March 2013*, pages 127–142. Society for Veterinary Epidemiology and Preventive Medicine, 2013.
- C. P. Jewell, T. Kypraios, P. Neal, and G. O. Roberts. Bayesian analysis for emerging infectious diseases. *Bayesian Analysis*, 4:465–496, 2009.
- N. Ju, J. Heng, and P. E. Jacob. Sequential monte carlo algorithms for agent-based models of disease transmission. *arXiv preprint arXiv:2101.12156*, 2021.
- M. J. Keeling and K. T. Eames. Networks and epidemic models. *Journal of the Royal Society Interface*, 2(4):295–307, 2005.
- D. P. Kingma and J. Ba. Adam: A method for stochastic optimization. *arXiv preprint arXiv:1412.6980*, 2014.

- B. G. Lindsay. Composite likelihood methods. *Comtemporary Mathematics*, 80(1):221–239, 1988.
- K. V. Mardia, G. Hughes, C. C. Taylor, and H. Singh. A multivariate von mises distribution with applications to bioinformatics. *Canadian Journal of Statistics*, 36(1):99–109, 2008.
- P. Rebeschini and R. Van Handel. Can local particle filters beat the curse of dimensionality? *The Annals of Applied Probability*, 25:2809–2866, 2015.
- L. Rimella and N. Whiteley. Exploiting locality in high-dimensional factorial hidden markov models. *The Journal of Machine Learning Research*, 23(1):134–167, 2022.
- L. Rimella, S. Alderton, M. Sammarro, B. Rowlingson, D. Cocker, N. Feasey, P. Fearnhead, and C. Jewell. Inference on extended-spectrum beta-lactamase Escherichia coli and Klebsiella pneumoniae data through SMC2. *Journal of the Royal Statistical Society Series C: Applied Statistics*, page qlad055, 07 2023a. ISSN 0035-9254. doi: 10.1093/jrsssc/qlad055. URL <https://doi.org/10.1093/jrsssc/qlad055>.
- L. Rimella, C. Jewell, and P. Fearnhead. Approximating Optimal SMC Proposal Distributions in Individual-Based Epidemic Models. *Statistica Sinica*, pages SS–2022–0198, 05 2023b. ISSN 1017-0405. doi: 10.5705/ss.202022.0198.
- E. Samanidou, E. Zschischang, D. Stauffer, and T. Lux. Agent-based models of financial markets. *Reports on Progress in Physics*, 70(3):409, 2007.
- S. L. Scott. Bayesian methods for hidden Markov models: Recursive computing in the 21st century. *Journal of the American statistical Association*, 97(457):337–351, 2002.
- M. S. Shamil, F. Farheen, N. Ibtehaz, I. M. Khan, and M. S. Rahman. An agent-based modeling of covid-19: validation, analysis, and recommendations. *Cognitive computation*, pages 1–12, 2021.
- R. Silva, S. M. Kang, and E. M. Airoldi. Predicting traffic volumes and estimating the effects of shocks in massive transportation systems. *Proceedings of the National Academy of Sciences*, 112(18):5643–5648, 2015.
- P. Touloupou, B. Finkenstädt, and S. E. Spencer. Scalable Bayesian inference for coupled hidden Markov and semi-Markov models. *Journal of Computational and Graphical Statistics*, 29(2):238–249, 2020.
- UK National Audit Office, 2022. URL <https://www.nao.org.uk/reports/the-2001-outbreak-of-foot-and-mouth-disease>. Report by the Comptroller and auditor general: "The 2001 outbreak of foot and mouth disease."
- C. Varin. On composite marginal likelihoods. *Asta advances in statistical analysis*, 92(1): 1–28, 2008.

- C. Varin and P. Vidoni. Pairwise likelihood inference for general state space models. *Econometric Reviews*, 28(1-3):170–185, 2008.
- C. Varin, N. Reid, and D. Firth. An overview of composite likelihood methods. *Statistica Sinica*, pages 5–42, 2011.
- A. V. Vecchia. Estimation and model identification for continuous spatial processes. *Journal of the Royal Statistical Society: Series B (Methodological)*, 50(2):297–312, 1988.
- D. J. Wilkinson. *Stochastic modelling for systems biology*. CRC press, 2018.
- M. D. Zeiler. Adadelta: an adaptive learning rate method. *arXiv preprint arXiv:1212.5701*, 2012.

## A Simulation based composite likelihood: assumptions and proofs

In this section we provide the details about the theoretical results from the main paper. Apart from giving full proofs of the results, we will also discuss the validity of the assumptions.

### A.1 Discussion on the assumptions and the simulation feedback

Here we show that our assumptions from the main paper are valid for a specific class of models. Specifically, we consider an SIS individual-based model as from the experimental section, and so:

$$\begin{aligned}
 p(x_0^n) &= \left[ \frac{1 - \frac{1}{1 + \exp(-\beta_0^\top w_n)}}{\frac{1}{1 + \exp(-\beta_0^\top w_n)}} \right]; \\
 p(x_t^n | x_{t-1}^n) &= \left[ \begin{array}{c} e^{-\lambda_n \left( \frac{\sum_{\bar{n} \in [N]} \mathbb{I}(x_{t-1}^{\bar{n}}=2)}{N} + \iota \right)} \\ 1 - e^{-\gamma_n} \end{array} \quad \begin{array}{c} 1 - e^{-\lambda_n \left( \frac{\sum_{\bar{n} \in [N]} \mathbb{I}(x_{t-1}^{\bar{n}}=2)}{N} + \iota \right)} \\ e^{-\gamma_n} \end{array} \right]; \\
 p(y_t^n | x_t^n) &= q^{x_t^n} \mathbb{I}(y_t^n \neq 0) + (1 - q^{x_t^n}) \mathbb{I}(y_t^n = 0),
 \end{aligned}$$

where  $\lambda_n, \gamma_n$  are positive and  $q \in [0, 1]^2$ .

The first assumption we consider is reported below.

**Assumption 3.** For any  $n, \bar{n} \in [N]$  and for any  $x_t^{\bar{n}} \in \mathcal{X}$ , if  $x_{t-1}, \bar{x}_{t-1} \in \mathcal{X}^N$  are such that  $x_{t-1}^{\setminus n} = \bar{x}_{t-1}^{\setminus n}$  then:

$$|p(x_t^{\bar{n}} | x_{t-1}) - p(x_t^{\bar{n}} | \bar{x}_{t-1})| \leq \frac{s_{\bar{n}}}{N} |d_{n, \bar{n}}(x_{t-1}^n) - d_{n, \bar{n}}(\bar{x}_{t-1}^n)|,$$

where  $d_{n, \bar{n}} : \mathcal{X} \rightarrow \mathbb{R}_+$  and  $s_{\bar{n}}$  is a positive constant.

This is one of the key assumptions to prove our first result on SimBa-CL and precisely provide bounds on the Kullback-Leibler divergence between the fully factorised SimBa-CL with and without feedback.

To prove the validity of the bound we simply consider the difference between  $p(x_t^{\bar{n}}|x_{t-1})$  and  $p(x_t^{\bar{n}}|\bar{x}_{t-1})$  when  $x_{t-1}, \bar{x}_{t-1} \in \mathcal{X}^N$  are such that  $x_{t-1}^{\setminus n} = \bar{x}_{t-1}^{\setminus n}$ .

$$\begin{aligned}
& p(x_t^{\bar{n}}|x_{t-1}) - p(x_t^{\bar{n}}|\bar{x}_{t-1}) \\
&= \begin{cases} e^{-\lambda_{\bar{n}}\left(\frac{\sum_{m \in [N]} \mathbb{I}(x_{t-1}^m=2)}{N} + \iota\right)} - e^{-\lambda_n\left(\frac{\sum_{m \in [N]} \mathbb{I}(\bar{x}_{t-1}^m=2)}{N} + \iota\right)} & \text{if } x_{t-1}^{\bar{n}} = 1, x_t^{\bar{n}} = 1 \\ -e^{-\lambda_{\bar{n}}\left(\frac{\sum_{m \in [N]} \mathbb{I}(x_{t-1}^m=2)}{N} + \iota\right)} + e^{-\lambda_n\left(\frac{\sum_{m \in [N]} \mathbb{I}(\bar{x}_{t-1}^m=2)}{N} + \iota\right)} & \text{if } x_{t-1}^{\bar{n}} = 1, x_t^{\bar{n}} = 2 \\ 0 & \text{if } x_{t-1}^{\bar{n}} = 2, x_t^{\bar{n}} = 1 \\ 0 & \text{if } x_{t-1}^{\bar{n}} = 2, x_t^{\bar{n}} = 2 \end{cases}
\end{aligned}$$

hence:

$$|p(x_t^{\bar{n}}|x_{t-1}) - p(x_t^{\bar{n}}|\bar{x}_{t-1})| \leq \left| e^{-\lambda_{\bar{n}}\left(\frac{\sum_{m \in [N]} \mathbb{I}(x_{t-1}^m=2)}{N} + \iota\right)} - e^{-\lambda_n\left(\frac{\sum_{m \in [N]} \mathbb{I}(\bar{x}_{t-1}^m=2)}{N} + \iota\right)} \right|.$$

Consider the function  $e^{-x}$ , from the mean value theorem we have that:

$$e^{-a} - e^{-b} = (-e^{-c})(a - b),$$

with  $c \in [a, b]$  provide  $a < b$ . Then we can apply the mean value theorem on the domain  $[0, +\infty]$  and get:

$$\begin{aligned}
& |p(x_t^{\bar{n}}|x_{t-1}) - p(x_t^{\bar{n}}|\bar{x}_{t-1})| \leq \left| e^{-\lambda_{\bar{n}}\left(\frac{\sum_{m \in [N]} \mathbb{I}(x_{t-1}^m=2)}{N} + \iota\right)} - e^{-\lambda_n\left(\frac{\sum_{m \in [N]} \mathbb{I}(\bar{x}_{t-1}^m=2)}{N} + \iota\right)} \right| \\
&= |e^{-c}| \left| \lambda_{\bar{n}} \left( \frac{\sum_{m \in [N]} \mathbb{I}(x_{t-1}^m=2)}{N} + \iota \right) - \lambda_n \left( \frac{\sum_{m \in [N]} \mathbb{I}(\bar{x}_{t-1}^m=2)}{N} + \iota \right) \right| \\
&\leq \lambda_{\bar{n}} \left| \left( \frac{\sum_{m \in [N]} \mathbb{I}(x_{t-1}^m=2)}{N} + \iota \right) - \left( \frac{\sum_{m \in [N]} \mathbb{I}(\bar{x}_{t-1}^m=2)}{N} + \iota \right) \right|,
\end{aligned}$$

where the last step follows from  $c$  and  $\lambda_{\bar{n}}$  being positive. Now remark that  $x_{t-1}^{\setminus n} = \bar{x}_{t-1}^{\setminus n}$ ,



hence:

$$\begin{aligned}
|p(x_t^{\bar{n}}|x_{t-1}) - p(x_t^{\bar{n}}|\bar{x}_{t-1})| &\leq \lambda_{\bar{n}} \left| \left( \frac{\sum_{m \in [N]} \mathbb{I}(x_{t-1}^m = 2)}{N} + \iota \right) - \left( \frac{\sum_{m \in [N]} \mathbb{I}(\bar{x}_{t-1}^m = 2)}{N} + \iota \right) \right| \\
&\leq \lambda_{\bar{n}} \left| \frac{\sum_{m \in [N]} \mathbb{I}(x_{t-1}^m = 2)}{N} - \frac{\sum_{m \in [N]} \mathbb{I}(\bar{x}_{t-1}^m = 2)}{N} \right| \\
&\leq \frac{\lambda_{\bar{n}}}{N} |\mathbb{I}(x_{t-1}^n = 2) - \mathbb{I}(\bar{x}_{t-1}^n = 2)|,
\end{aligned}$$

and so our assumption is satisfied for  $s_{\bar{n}} = \lambda_{\bar{n}}$  and  $d_{n,\bar{n}}(x) = \mathbb{I}(x = 2)$ . Note that the proof is straightforward to generalise for transition kernels that include infectivity and spatial kernels. Indeed, instead of  $\lambda_{\bar{n}} \sum_{m \in [N]} \mathbb{I}(x_{t-1}^m = 2)$  we could have  $\lambda_{\bar{n}} \sum_{m \in [N]} \xi_m \psi_{\bar{n},m} \mathbb{I}(x_{t-1}^m = 2)$  where  $\xi_m$  is the infectivity and  $\psi_{\bar{n},m}$  is the spatial kernel telling how individuals  $\bar{n}$  and  $m$  are connected. This alternative transition kernel will similarly satisfy our assumption with for  $s_{\bar{n}} = \lambda_{\bar{n}}$  and  $d_{n,\bar{n}}(x) = \xi_n \psi_{n,\bar{n}} \mathbb{I}(x = 2)$ .

We now conclude by proving the validity of the second assumption, reported for completeness below.

**Assumption 4.** For any  $n, \bar{n} \in [N]$ , if  $x_{t-1}, \bar{x}_{t-1} \in \mathcal{X}^N$  are such that  $x_{t-1}^{\bar{n}} = \bar{x}_{t-1}^{\bar{n}}$  then there exists  $0 < \epsilon < 1$  such that:

$$\sum_{x_t^n} p(x_t^n | x_{t-1}) \frac{1}{p(x_t^n | \bar{x}_{t-1})^2} \leq \frac{1}{\epsilon^2}, \quad \text{and} \quad \sum_{x_t^n} p(x_t^n | x_{t-1}) \frac{1}{p(x_t^n | \bar{x}_{t-1})^3} \leq \frac{1}{\epsilon^3}.$$

Again if we consider our SIS individuals-based model we can notice that 4 is simply requiring that the matrix obtained by doing the ratio element by element of the transition kernel computed in  $x_{t-1}$  with the square /cube of itself computed in  $\bar{x}_{t-1}$  has the sum of the rows bounded. This is straightforward to prove by noting that:

$$\begin{aligned}
p(x_t^n | x_{t-1}) &= \begin{bmatrix} e^{-\lambda_n \left( \frac{\sum_{\bar{n} \in [N]} \mathbb{I}(x_{t-1}^{\bar{n}} = 2)}{N} + \iota \right)} & 1 - e^{-\lambda_n \left( \frac{\sum_{\bar{n} \in [N]} \mathbb{I}(x_{t-1}^{\bar{n}} = 2)}{N} + \iota \right)} \\ 1 - e^{-\gamma_n} & e^{-\gamma_n} \end{bmatrix} \\
&\geq \begin{bmatrix} e^{-\lambda_n(1+\iota)} & 1 - e^{-\lambda_n \iota} \\ 1 - e^{-\gamma_n} & e^{-\gamma_n} \end{bmatrix},
\end{aligned}$$

hence if we choose  $\epsilon = \max_{n \in [N]} \max\{e^{-\lambda_n(1+\iota)}, 1 - e^{-\lambda_n \iota}, 1 - e^{-\gamma_n}, e^{-\gamma_n}\}$ , the validity of the assumption follows trivially.

There is still an additional assumption that used for the proof of theorem, and precisely:  $|d_{n,\bar{n}}(x^n) - d_{n,\bar{n}}(\bar{x}^n)| < N$ . Again for the specific case of SIS we have  $d_{n,\bar{n}}(x) = \mathbb{I}(x = 2)$  and so  $|\mathbb{I}(x = 2) - \mathbb{I}(\bar{x} = 2)|$  which is obviously less or equal to 1 and so way smaller than  $N$ .

As explained in the main paper, our assumptions are not limited to assumptions 3-4, and we need some adjusted versions of them when working with SimBa-CL for general partitions, which are again reported below for completeness.

**Assumption 5.** For any  $K \in \mathcal{K}$  and for any  $x_t^{\bar{n}} \in \mathcal{X}$  with  $\bar{n} \notin K$ , if  $x_{t-1}, \bar{x}_{t-1} \in \mathcal{X}^N$  are such that  $x_{t-1}^{\setminus K} = \bar{x}_{t-1}^{\setminus K}$  then:

$$|p(x_t^{\bar{n}}|x_{t-1}) - p(x_t^{\bar{n}}|\bar{x}_{t-1})| \leq \frac{s_{\bar{n}}}{N} |d_{K,\bar{n}}(x_{t-1}^n) - d_{K,\bar{n}}(\bar{x}_{t-1}^n)|.$$

where  $d_{K,\bar{n}} : \mathcal{X}^K \rightarrow \mathbb{R}_+$  and  $s_{\bar{n}}$  is a positive constant.

**Assumption 6.** For any  $K, \bar{K} \in \mathcal{K}$ , if  $x_{t-1}, \bar{x}_{t-1} \in \mathcal{X}^N$  are such that  $x_{t-1}^{\setminus \bar{K}} = \bar{x}_{t-1}^{\setminus \bar{K}}$  then there exists  $0 < \epsilon < 1$  such that:

$$\sum_{x_t^n} p(x_t^n|x_{t-1}) \frac{1}{p(x_t^n|\bar{x}_{t-1})^2} \leq \frac{1}{\epsilon^2}, \quad \text{and} \quad \sum_{x_t^n} p(x_t^n|x_{t-1}) \frac{1}{p(x_t^n|\bar{x}_{t-1})^3} \leq \frac{1}{\epsilon^3}.$$

Again both assumptions are valid for the SIS case. Indeed, Assumption 5 can be proven to be valid for SIS by following the same steps and by observing that:

$$|p(x_t^{\bar{n}}|x_{t-1}) - p(x_t^{\bar{n}}|\bar{x}_{t-1})| \leq \frac{\lambda_{\bar{n}}}{N} \left| \sum_{n \in K} \mathbb{I}(x_{t-1}^n = 2) - \mathbb{I}(\bar{x}_{t-1}^n = 2) \right|,$$

and so our  $d_{K,\bar{n}}(x^K) = \sum_{n \in K} \mathbb{I}(x^n = 2)$ , from which we can also notice  $|d_{K,\bar{n}}(x^K) - d_{K,\bar{n}}(\bar{x}^K)| < N$ . At the same time, the proof of Assumption 6 does not change.

We now discuss the simulation feedback. Note that we have a recursive formula for  $p(x_{[0:T]}^n|x_{[0:T]}^{\setminus n})$ :

$$\begin{aligned} p(x_{[0:T]}^n|x_{[0:T]}^{\setminus n}) &= p(x_T|x_{[0:T-1]}) \frac{p(x_{[0:T-1]}^n|x_{[0:T-1]}^{\setminus n})}{p(x_{[T]}^{\setminus n}|x_{[0:T-1]}^{\setminus n})} \\ &= p(x_T^n|x_{T-1}) \frac{p(x_T^{\setminus n}|x_{T-1})}{p(x_{[T]}^{\setminus n}|x_{[0:T-1]}^{\setminus n})} p(x_{[0:T-1]}^n|x_{[0:T-1]}^{\setminus n}) \\ &= p(x_T^n|x_{T-1}) \\ &= \frac{\prod_{\bar{n} \in [N], \bar{n} \neq n} p(x_T^{\bar{n}}|x_{T-1})}{\sum_{\bar{x}_{T-1}^n} \prod_{\bar{n} \in [N], \bar{n} \neq n} p(x_T^{\bar{n}}|\bar{x}_{T-1}^{\bar{n}}, x_{[T-1]}^{\setminus n}) p(\bar{x}_{t-1}^n|x_{[0:T-1]}^{\setminus n})} \\ &\quad p(x_{[0:T-1]}^n|x_{[0:T-1]}^{\setminus n}), \end{aligned}$$

and so if we follow the same step down to  $t = 1$  we obtain:

$$\begin{aligned}
p(x_{[0:T]}^n | x_{[0:T]}^{\setminus n}) &= \prod_{t \in [T]} p(x_t^n | x_{t-1}) \\
&\prod_{t \in [T]} \frac{\prod_{\bar{n} \in [N], \bar{n} \neq n} p(x_t^{\bar{n}} | x_{t-1})}{\sum_{\bar{x}_{t-1}^n} \prod_{\bar{n} \in [N], \bar{n} \neq n} p(x_t^{\bar{n}} | \bar{x}_{t-1}^n, x_{[t-1]}^{\setminus n}) p(\bar{x}_{t-1}^n | x_{[0:T-1]}^{\setminus n})} \\
&p(x_0^n | x_0^{\setminus n}) \\
&= p(x_0^n) \prod_{t \in [T]} p(x_t^n | x_{t-1}) \\
&\prod_{t \in [T]} \frac{\prod_{\bar{n} \in [N], \bar{n} \neq n} p(x_t^{\bar{n}} | x_{t-1})}{\sum_{\bar{x}_{t-1}^n} \prod_{\bar{n} \in [N], \bar{n} \neq n} p(x_t^{\bar{n}} | \bar{x}_{t-1}^n, x_{[t-1]}^{\setminus n}) p(\bar{x}_{t-1}^n | x_{[0:T-1]}^{\setminus n})}.
\end{aligned} \tag{20}$$

Here we recognise our simulation feedback indeed in the main paper we have:

$$f(x_{t-1}^n, x_{[0:t]}^{\setminus n}) = \frac{\prod_{\bar{n} \in [N] \setminus n} p(x_t^{\bar{n}} | x_{t-1}, )}{\sum_{\bar{x}_{t-1}^n} \prod_{\bar{n} \in [N] \setminus n} p(x_t^{\bar{n}} | \bar{x}_{t-1}^n, x_{[t-1]}^{\setminus n}, ) p(\bar{x}_{t-1}^n | x_{[0:t-1]}^{\setminus n}, )}.$$

We can then notice that removing the simulation feedback is like assuming some form of independence on the future as it is like we are recursively removing terms of the form  $p(x_t^{\setminus n} | x_{t-1}) / p(x_{[t]}^{\setminus n} | x_{[0:t-1]}^{\setminus n})$ .

## A.2 KL bounds for fully factorised SimBa-CL

To prove Theorem 1 we require a series of intermediate results.

We start by showing the Data processing inequality, which allows to bound the KL between the marginals with the KL between the joints.

**Lemma 2. (Data processing inequality)** *Consider two joint distributions  $p(x, y)$  and  $q(x, y)$  and let  $p_y(y)$  and  $q_y(y)$  be their marginals over  $y$ , then:*

$$\mathbf{KL}(p_y(y) || q_y(y)) \leq \mathbf{KL}(p(x, y) || q(x, y)) \tag{21}$$

*provided that  $q$  is absolutely continuous with respect to  $p$ .*

*Proof.* It can be easily proved that if  $q$  is absolutely continuous with respect to  $p$  then  $q_y$  is absolutely continuous with respect to  $p_y$  and so also the left hand side of the statement is well-defined.

To prove (21) we can simply use the chain rule:

$$\begin{aligned}
\mathbf{KL}(p(x, y)||q(x, y)) &= \sum_{x, y} p(x, y) \log \left( \frac{p(x, y)}{q(x, y)} \right) = \sum_{x, y} p_{x|y}(x|y)p_y(y) \log \left( \frac{p_{x|y}(x|y)p_y(y)}{q_{x|y}(x|y)q_y(y)} \right) \\
&= \sum_{x, y} p_{x|y}(x|y)p_y(y) \left[ \log \left( \frac{p_{x|y}(x|y)}{q_{x|y}(x|y)} \right) + \log \left( \frac{p_y(y)}{q_y(y)} \right) \right] \\
&= \sum_{x, y} p_{x|y}(x|y)p_y(y) \log \left( \frac{p_{x|y}(x|y)}{q_{x|y}(x|y)} \right) + \sum_{x, y} p_{x|y}(x|y)p_y(y) \log \left( \frac{p_y(y)}{q_y(y)} \right) \\
&= \mathbb{E}_{p_y(\mathbf{y})} \left[ \sum_x p_{x|y}(x|\mathbf{y}) \log \left( \frac{p_{x|y}(x|\mathbf{y})}{q_{x|y}(x|\mathbf{y})} \right) \right] + \sum_y p_y(y) \log \left( \frac{p_y(y)}{q_y(y)} \right) \\
&= \mathbb{E}_{p_y(\mathbf{y})} [\mathbf{KL}(p_{x|y}(x|\mathbf{y})||q_{x|y}(x|\mathbf{y}))] + \mathbf{KL}(p_y(y)||q_y(y)) \\
&\geq \mathbf{KL}(p_y(y)||q_y(y)),
\end{aligned}$$

where the last step follows from the positivity of the KL divergence.  $\square$

The next proposition gives us a bound for the log of a ratio, which will be use in the proof of the main theorem to bound the KL.

**Proposition 3.** *Consider the function  $f(x, y) = \log(x/y)$  with  $x, y \in (0, 1]$  then:*

$$f(x, y) \leq \begin{cases} -\frac{y-x}{x} + \frac{(y-x)^2}{2x^2} & y \geq x \\ -\frac{y-x}{x} + \frac{(y-x)^2}{2x^2} + \frac{(x-y)^3}{3x^2y} & y < x \end{cases}.$$

*Proof.* Note that:

$$f(x, y) = \log \left( \frac{x}{y} \right) = -\log \left( \frac{y}{x} \right) = -\log \left( 1 + \frac{y-x}{x} \right)$$

and given that  $y/x > 0$  also  $1 + \frac{y-x}{x} > 0$ , meaning that  $\frac{y-x}{x} > -1$ . We can then provide bounds for  $h(z) = -\log(1+z)$  with  $z \in (-1, +\infty)$ . To do so we analyse  $z \in (-1, 0)$  and  $z \in [0, +\infty)$ .

Let start with the case  $z \in [0, +\infty)$ , notice that  $\tilde{h}(z) = h(z) + z - \frac{z^2}{2}$  is such that:

- $\tilde{h}(0) = h(0) = 0$ ;
- $\tilde{h}'(z) = h'(z) + 1 - z = \frac{-1+1-z^2}{1+z} = \frac{-z^2}{1+z} < 0$  for all  $z \in [0, +\infty)$ ;

from which we conclude  $\tilde{h}(z) \leq 0$  for all  $z \in [0, +\infty)$ , given that  $\tilde{h}(0) = 0$  and the function is strictly decreasing on the domain. This implies  $h(z) \leq -z + \frac{z^2}{2}$  on  $z \in [0, +\infty)$ .

Let us now analyse the case  $z \in (-1, 0)$ , notice that  $\tilde{h}(z)$  is also decreasing on  $z \in (-1, 0)$  and given that  $\tilde{h}(0) = 0$ , we can only prove  $\tilde{h}(0) > 0$ . To find an upper bound for  $h(z)$  we use its Taylor expansion, and the fact that  $-z \in (0, 1)$ :

$$\begin{aligned}
h(z) &= \sum_{i=0}^{\infty} \frac{h^{(i)}(0)z^i}{i!} = \sum_{i=1}^{\infty} \frac{(-1)^i z^i}{i} \leq -z + \frac{z^2}{2} + \frac{1}{3} \sum_{i=3}^{\infty} (-z)^i \\
&= -z + \frac{z^2}{2} + \frac{1}{3} \left( \frac{1}{1+z} - 1 + z - z^2 \right) \\
&= -z + \frac{z^2}{2} + \frac{1}{3} \left( \frac{1 - 1 + z^2 - z^2 - z^3}{1+z} \right) \\
&= -z + \frac{z^2}{2} - \frac{1}{3} \left( \frac{z^3}{1+z} \right),
\end{aligned}$$

which prove the upper bound for  $z \in (-1, 0)$ .

We can put everything together and complete the proof, consider  $z = \frac{y-x}{x}$  we have then:

$$\begin{aligned}
f(x, y) &= -\log \left( 1 + \frac{y-x}{x} \right) \\
&\leq \begin{cases} -\frac{y-x}{x} + \frac{\left(\frac{y-x}{x}\right)^2}{2} & \frac{y-x}{x} \in [0, +\infty) \\ -\frac{y-x}{x} + \frac{\left(\frac{y-x}{x}\right)^2}{2} - \frac{1}{3} \left( \frac{\left(\frac{y-x}{x}\right)^3}{1+\left(\frac{y-x}{x}\right)} \right) & \frac{y-x}{x} \in (-1, 0) \end{cases} \\
&= \begin{cases} -\frac{y-x}{x} + \frac{\left(\frac{y-x}{x}\right)^2}{2} & \frac{y-x}{x} \geq 0 \\ -\frac{y-x}{x} + \frac{\left(\frac{y-x}{x}\right)^2}{2} - \frac{1}{3} \left( \frac{\left(\frac{y-x}{x}\right)^3}{x^3 \left(1+\left(\frac{y-x}{x}\right)\right)} \right) & \frac{y-x}{x} < 0 \end{cases} \\
&= \begin{cases} -\frac{y-x}{x} + \frac{(y-x)^2}{2x^2} & y \geq x \\ -\frac{y-x}{x} + \frac{(y-x)^2}{2x^2} + \frac{(x-y)^3}{3x^2y} & y < x \end{cases}.
\end{aligned}$$

□

The following corollary applies the above proposition to bound the KL between to distributions.

**Corollary 4.** *Consider two probability distribution  $p, \tilde{p}$  on a finite state space, with  $p$  absolutely continuous with respect to  $\tilde{p}$ , then:*

$$\begin{aligned}
\mathbf{KL}(p(x)||\tilde{p}(x)) &\leq \frac{1}{2} \sum_x p(x) \frac{1}{p(x)^2} (\tilde{p}(x) - p(x))^2 \\
&\quad + \frac{1}{3} \sum_x p(x) \frac{1}{\tilde{p}(x)^3} |p(x) - \tilde{p}(x)|^3
\end{aligned}$$

*Proof.* The proof follows from Proposition 3 with the convention  $0 \log(0) = 0$  and  $0 \log(0/0) = 0$ . Notice that whenever  $p(x) = 0$  we have  $0 \log(0)$  and whenever  $\tilde{p}(x) = 0$  we have  $0 \log(0/0)$  from absolute continuity, hence following the convention we can safely remove those  $x$ 's from the sum and apply our proposition (apply Proposition 3 with  $x = p(x)$  and  $y = \tilde{p}(x) \in (0, 1]$ ). The bound follows from:

$$\begin{aligned}
\mathbf{KL}(p(x)||\tilde{p}(x)) &= \sum_x p(x) \log \left( \frac{p(x)}{\tilde{p}(x)} \right) \\
&\leq \sum_x p(x) \left[ -\frac{\tilde{p}(x) - p(x)}{p(x)} + \frac{(\tilde{p}(x) - p(x))^2}{2p(x)^2} \right] \\
&\quad + \sum_x \mathbb{I}(\tilde{p}(x) < p(x)) p(x) \frac{(p(x) - \tilde{p}(x))^3}{3p(x)^2 \tilde{p}(x)} \\
&= -\sum_x p(x) \left[ \frac{\tilde{p}(x) - p(x)}{p(x)} \right] + \sum_x p(x) \left[ \frac{(\tilde{p}(x) - p(x))^2}{2p(x)^2} \right] \\
&\quad + \sum_x \mathbb{I}(\tilde{p}(x) < p(x)) p(x) \frac{(p(x) - \tilde{p}(x))^3}{3p(x)^2 \tilde{p}(x)} \\
&= \sum_x p(x) \left[ \frac{(\tilde{p}(x) - p(x))^2}{2p(x)^2} \right] \\
&\quad + \sum_x \mathbb{I}(\tilde{p}(x) < p(x)) p(x) \frac{(p(x) - \tilde{p}(x))^3}{3p(x)^2 \tilde{p}(x)} \\
&= \frac{1}{2} \sum_x p(x) \frac{1}{p(x)^2} (\tilde{p}(x) - p(x))^2 \\
&\quad + \frac{1}{3} \sum_x \mathbb{I}(\tilde{p}(x) < p(x)) p(x) \frac{1}{p(x)^2 \tilde{p}(x)} (p(x) - \tilde{p}(x))^3 \\
&\leq \frac{1}{2} \sum_x p(x) \frac{1}{p(x)^2} (\tilde{p}(x) - p(x))^2 \\
&\quad + \frac{1}{3} \sum_x \mathbb{I}(\tilde{p}(x) < p(x)) p(x) \frac{1}{\tilde{p}(x)^3} (p(x) - \tilde{p}(x))^3 \\
&\leq \frac{1}{2} \sum_x p(x) \frac{1}{p(x)^2} (\tilde{p}(x) - p(x))^2 \\
&\quad + \frac{1}{3} \sum_x p(x) \frac{1}{\tilde{p}(x)^3} |p(x) - \tilde{p}(x)|^3
\end{aligned}$$

□

We now provide the full proof of Theorem 1. We start by proving absolute continuity and so the validity of the KL computation. We then move to the Data processing inequality

which we use to switch from a KL between  $p(y_{[T]}^n)$  and  $\tilde{p}(y_{[T]}^n)$  to a KL between  $p(x_{[0:T]}, y_{[T]}^n)$  and  $\tilde{p}(x_{[0:T]}, y_{[T]}^n)$ . After some reformulation of the quantities we are able to apply Jensen inequality and Corollary 4 which gives us a bound in term of transition kernel difference and ratios. The final step is then the application of the assumptions along with recognising the definitio of the variance.

*proof of Theorem 1.* Remark that we want to compute the KL-divergence between:

- $p(y_{[T]}^n) = \sum_{x_{[0:T]}} p(x_{[0:T]}^{\setminus n}) p(x_{[0:T]}^n | x_{[0:T]}^{\setminus n}) \prod_{t \in [T]} p(y_t^n | x_t^n)$ ;
- $\tilde{p}(y_{[T]}^n) = \sum_{x_{[0:T]}} p(x_{[0:T]}^{\setminus n}) p(x_0^n | \theta) \prod_{t \in [T]} p(x_t^n | x_{t-1}) p(y_t^n | x_t^n)$ ;

hence the first step is to prove that  $p(y_{[T]}^n)$  is absolutely continuous with respect to  $\tilde{p}(y_{[T]}^n)$ , and so for a fixed  $y_{[T]}^n$  we have  $\tilde{p}(y_{[T]}^n) = 0$  implies  $p(y_{[T]}^n) = 0$ , this is necessary to ensure that the KL divergence is well-defined. Note that we have  $\tilde{p}(y_{[T]}^n) = 0$  if and only if for any  $x_{[0:T]}$ :

1.  $p(x_{[0:T]}^{\setminus n}) = 0$  or /and,
2.  $p(x_0^n | \theta) \prod_{t \in [T]} p(x_t^n | x_{t-1}) = 0$  or /and,
3.  $\prod_{t \in [T]} p(y_t^n | x_t^n) = 0$ .

We can observe that conditions 1. and 3. implies also  $p(y_{[T]}^n) = 0$ , so it is enough to prove that 2. implies  $p(y_{[T]}^n) = 0$  to ensure absolute continuity. Consider  $p(x_{[0:T]}^n | x_{[0:T]}^{\setminus n}, \theta)$ , given that from (20) we have:

$$p(x_{[0:T]}^n | x_{[0:T]}^{\setminus n}, \theta) = p(x_0^n) \prod_{t \in [T]} p(x_t^n | x_{t-1}, \theta) f(x_{t-1}^n, x_{[0:t]}^{\setminus n}),$$

we can conclude that 2. implies  $p(x_{[0:T]}^n | x_{[0:T]}^{\setminus n}, \theta) = 0$ . Note that the proof of absolute continuity relies on the joint  $p(x_{[0:T]}, y_{[T]}^n)$  being absolutely continuous with respect to  $\tilde{p}(x_{[0:T]}, y_{[T]}^n)$ . Given that the KL is well-defined we can now proceed with the proof.

Start by applying Lemma 2 and get:

$$\begin{aligned} \mathbf{KL}(p(\mathbf{y}_{[T]}^n) || \tilde{p}(\mathbf{y}_{[T]}^n)) &\leq \mathbf{KL}(p(x_{[0:T]}, y_{[T]}^n) || \tilde{p}(x_{[0:T]}, y_{[T]}^n)) \\ &= \sum_{y_{[T]}^n} \sum_{x_{[0:T]}} p(x_{[0:T]}, y_{[T]}^n) \log \left( \frac{p(x_{[0:T]}, y_{[T]}^n)}{\tilde{p}(x_{[0:T]}, y_{[T]}^n)} \right). \end{aligned}$$



Use now the definition of  $\tilde{p}(x_{[0:T]}, y_{[T]}^n)$ :

$$\begin{aligned}
\mathbf{KL}(p(\mathbf{y}_{[T]}^n) || \tilde{p}(\mathbf{y}_{[T]}^n)) &\leq \sum_{y_{[T]}^n} \sum_{x_{[0:T]}} p(x_{[0:T]}, y_{[T]}^n) \log \left( \frac{p(x_{[0:T]}, y_{[T]}^n)}{\tilde{p}(x_{[0:T]}, y_{[T]}^n)} \right) \\
&= \sum_{y_{[T]}^n} \sum_{x_{[0:T]}} p(x_{[0:T]}^{\setminus n}) p(x_{[0:T]}^n | x_{[0:T]}^{\setminus n}) \prod_{t \in [T]} p(y_t^n | x_t^n) \\
&\quad \log \left( \frac{p(x_{[0:T]}^{\setminus n}) p(x_{[0:T]}^n | x_{[0:T]}^{\setminus n}) \prod_{t \in [T]} p(y_t^n | x_t^n)}{p(x_{[0:T]}^{\setminus n}) p(x_0^n) \prod_{t \in [T]} p(x_t^n | x_{t-1}^n)} \right) \\
&= \sum_{x_{[0:T]}} p(x_{[0:T]}^{\setminus n}) p(x_{[0:T]}^n | x_{[0:T]}^{\setminus n}) \sum_{y_{[T]}^n} \prod_{t \in [T]} p(y_t^n | x_t^n) \log \left( \frac{p(x_{[0:T]}^{\setminus n}) p(x_{[0:T]}^n | x_{[0:T]}^{\setminus n})}{p(x_{[0:T]}^{\setminus n}) p(x_0^n) \prod_{t \in [T]} p(x_t^n | x_{t-1}^n)} \right)
\end{aligned}$$

from which we can also simplify  $p(x_{[0:T]}^{\setminus n})$  and given that  $\sum_{y_{[T]}^n} \prod_{t \in [T]} p(y_t^n | x_t^n) = 1$  we conclude:

$$\begin{aligned}
\mathbf{KL}(p(\mathbf{y}_{[T]}^n) || \tilde{p}(\mathbf{y}_{[T]}^n)) &\leq \sum_{x_{[0:T]}} p(x_{[0:T]}^{\setminus n}) p(x_{[0:T]}^n | x_{[0:T]}^{\setminus n}) \sum_{y_{[T]}^n} \prod_{t \in [T]} p(y_t^n | x_t^n) \log \left( \frac{p(x_{[0:T]}^{\setminus n}) p(x_{[0:T]}^n | x_{[0:T]}^{\setminus n})}{p(x_{[0:T]}^{\setminus n}) p(x_0^n) \prod_{t \in [T]} p(x_t^n | x_{t-1}^n)} \right) \\
&= \sum_{x_{[0:T]}} p(x_{[0:T]}^{\setminus n}) p(x_{[0:T]}^n | x_{[0:T]}^{\setminus n}) \log \left( \frac{p(x_{[0:T]}^n | x_{[0:T]}^{\setminus n})}{p(x_0^n) \prod_{t \in [T]} p(x_t^n | x_{t-1}^n)} \right).
\end{aligned}$$

Now we can use the recursive definition of  $p(x_{[0:T]}^n | x_{[0:T]}^{\setminus n})$  in (20):

$$\begin{aligned}
\mathbf{KL}(p(\mathbf{y}_{[T]}^n) || \tilde{p}(\mathbf{y}_{[T]}^n)) &\leq \sum_{x_{[0:T]}} p(x_{[0:T]}^{\setminus n}) p(x_{[0:T]}^n | x_{[0:T]}^{\setminus n}) \log \left( \frac{p(x_{[0:T]}^n | x_{[0:T]}^{\setminus n})}{p(x_0^n) \prod_{t \in [T]} p(x_t^n | x_{t-1}^n)} \right) \\
&= \sum_{x_{[0:T]}} p(x_{[0:T]}) \log \left( \frac{p(x_{[0:T]}^n | x_{[0:T]}^{\setminus n})}{p(x_0^n) \prod_{t \in [T]} p(x_t^n | x_{t-1}^n)} \right) \\
&= \sum_{x_{[0:T]}} p(x_{[0:T]}) \log \left( \frac{p(x_0^n) \prod_{t \in [T]} p(x_t^n | x_{t-1}^n) f(x_{t-1}^n, x_{[0:t]}^n)}{p(x_0^n) \prod_{t \in [T]} p(x_t^n | x_{t-1}^n)} \right) \\
&= \sum_{x_{[0:T]}} p(x_{[0:T]}) \log \left( \prod_{t \in [T]} f(x_{t-1}^n, x_{[0:t]}^n) \right) = \sum_{x_{[0:T]}} p(x_{[0:T]}) \sum_{t \in [T]} \log \left( f(x_{t-1}^n, x_{[0:t]}^n) \right).
\end{aligned}$$

Note now that we can move the sum over time steps in front and, given that the argument

of the logarithm depends only on  $x_{[0:t-1]}, x_t^{\setminus n}$  we can also simplify  $p(x_{[0:T]})$ :

$$\begin{aligned}
\mathbf{KL}(p(\mathbf{y}_{[T]}^n) || \tilde{p}(\mathbf{y}_{[T]}^n)) &\leq \sum_{x_{[0:T]}} p(x_{[0:T]}) \sum_{t \in [T]} \log \left( f \left( x_{t-1}^n, x_{[0:t]}^{\setminus n} \right) \right) \\
&= \sum_{t \in [T]} \sum_{x_{[0:t-1]}, x_t^{\setminus n}} p(x_{[0:t-1]}) \prod_{\bar{n} \in [N], \bar{n} \neq n} p(x_t^{\bar{n}} | x_{t-1}) \\
&\quad \log \left( \frac{\prod_{\bar{n} \in [N], \bar{n} \neq n} p(x_t^{\bar{n}} | x_{t-1})}{\sum_{\bar{x}_{t-1}^n} \prod_{\bar{n} \in [N], \bar{n} \neq n} p(x_t^{\bar{n}} | \bar{x}_{t-1}) p(\bar{x}_{t-1}^n | x_{[0:t-1]}^{\setminus n})} \right), \tag{22}
\end{aligned}$$

where  $\bar{x}_{t-1}$  is such that  $\bar{x}_{t-1}^{\setminus n} = x_{t-1}^{\setminus n}$  and  $\bar{x}_{t-1}^n \neq x_{t-1}^n$ .

Given that  $-\log(x)$  is a convex function and the denominator of our logarithm is an expectation we can apply Jensen inequality:

$$\begin{aligned}
&\log \left( \frac{\prod_{\bar{n} \in [N], \bar{n} \neq n} p(x_t^{\bar{n}} | x_{t-1})}{\sum_{\bar{x}_{t-1}^n} \prod_{\bar{n} \in [N], \bar{n} \neq n} p(x_t^{\bar{n}} | \bar{x}_{t-1}) p(\bar{x}_{t-1}^n | x_{[0:t-1]}^{\setminus n})} \right) \\
&= -\log \left( \sum_{\bar{x}_{t-1}^n} p(\bar{x}_{t-1}^n | x_{[0:t-1]}^{\setminus n}) \frac{\prod_{\bar{n} \in [N], \bar{n} \neq n} p(x_t^{\bar{n}} | \bar{x}_{t-1})}{\prod_{\bar{n} \in [N], \bar{n} \neq n} p(x_t^{\bar{n}} | x_{t-1})} \right) \\
&\leq -\sum_{\bar{x}_{t-1}^n} p(\bar{x}_{t-1}^n | x_{[0:t-1]}^{\setminus n}) \log \left( \prod_{\bar{n} \in [N], \bar{n} \neq n} \frac{p(x_t^{\bar{n}} | \bar{x}_{t-1})}{p(x_t^{\bar{n}} | x_{t-1})} \right) \\
&= \sum_{\bar{x}_{t-1}^n} p(\bar{x}_{t-1}^n | x_{[0:t-1]}^{\setminus n}) \log \left( \prod_{\bar{n} \in [N], \bar{n} \neq n} \frac{p(x_t^{\bar{n}} | x_{t-1})}{p(x_t^{\bar{n}} | \bar{x}_{t-1})} \right).
\end{aligned}$$

Joining (22) with the above yields to:

$$\begin{aligned}
\mathbf{KL}(p(\mathbf{y}_{[T]}^n) || \tilde{p}(\mathbf{y}_{[T]}^n)) &\leq \sum_{t \in [T]} \sum_{x_{[0:t-1]}, x_t^{\setminus n}} p(x_{[0:t-1]}, x_t^{\setminus n}) \left[ \sum_{\bar{x}_{t-1}^n} p(\bar{x}_{t-1}^n | x_{[0:t-1]}^{\setminus n}) \right. \\
&\quad \left. \log \left( \prod_{\bar{n} \in [N], \bar{n} \neq n} \frac{p(x_t^{\bar{n}} | x_{t-1})}{p(x_t^{\bar{n}} | \bar{x}_{t-1})} \right) \right] \\
&= \sum_{t \in [T]} \sum_{x_{[0:t-1]}, x_t^{\setminus n}} p(x_{[0:t-1]}, x_t^{\setminus n}) \left[ \sum_{\bar{x}_{t-1}^n} p(\bar{x}_{t-1}^n | x_{[0:t-1]}^{\setminus n}) \sum_{\bar{n} \in [N], \bar{n} \neq n} \log \left( \frac{p(x_t^{\bar{n}} | x_{t-1})}{p(x_t^{\bar{n}} | \bar{x}_{t-1})} \right) \right].
\end{aligned}$$

Similarly to what we did with the time steps sum, we can move the sum over the dimensions  $\bar{n}$  and exchange the order with  $\sum_{x_t^{\setminus n}}$ , this will allow us to have a dependence on  $\bar{n}$  and so

simplify  $p(x_t^{\setminus n}|x_{t-1})$  to  $p(x_t^{\bar{n}}|x_{t-1})$ :

$$\begin{aligned}
& \mathbf{KL}(p(\mathbf{y}_{[T]}^n) || \tilde{p}(\mathbf{y}_{[T]}^n)) \\
& \leq \sum_{t \in [T]} \sum_{x_{[0:t-1]}, x_t^{\setminus n}} p(x_{[0:t-1]}, x_t^{\setminus n}) \left[ \sum_{\bar{x}_{t-1}^n} p(\bar{x}_{t-1}^n | x_{[0:t-1]}^{\setminus n}) \sum_{\bar{n} \in [N], \bar{n} \neq n} \log \left( \frac{p(x_t^{\bar{n}} | x_{t-1})}{p(x_t^{\bar{n}} | \bar{x}_{t-1})} \right) \right] \\
& = \sum_{t \in [T]} \sum_{x_{[0:t-1]}, x_t^{\setminus n}} p(x_{[0:t-1]}) p(x_t^{\setminus n} | x_{t-1}) \left[ \sum_{\bar{x}_{t-1}^n} p(\bar{x}_{t-1}^n | x_{[0:t-1]}^{\setminus n}) \sum_{\bar{n} \in [N], \bar{n} \neq n} \log \left( \frac{p(x_t^{\bar{n}} | x_{t-1})}{p(x_t^{\bar{n}} | \bar{x}_{t-1})} \right) \right] \\
& = \sum_{t \in [T]} \sum_{x_{[0:t-1]}} \sum_{\bar{x}_{t-1}^n} p(\bar{x}_{t-1}^n | x_{[0:t-1]}^{\setminus n}) p(x_{[0:t-1]}) \left[ \sum_{x_t^{\setminus n}} p(x_t^{\setminus n} | x_{t-1}) \sum_{\bar{n} \in [N], \bar{n} \neq n} \log \left( \frac{p(x_t^{\bar{n}} | x_{t-1})}{p(x_t^{\bar{n}} | \bar{x}_{t-1})} \right) \right] \\
& = \sum_{t \in [T]} \sum_{x_{[0:t-1]}} \sum_{\bar{x}_{t-1}^n} p(\bar{x}_{t-1}^n | x_{[0:t-1]}^{\setminus n}) p(x_{[0:t-1]}) \sum_{\bar{n} \in [N], \bar{n} \neq n} \left[ \sum_{x_t^{\bar{n}}} p(x_t^{\bar{n}} | x_{t-1}) \log \left( \frac{p(x_t^{\bar{n}} | x_{t-1})}{p(x_t^{\bar{n}} | \bar{x}_{t-1})} \right) \right] \\
& = \sum_{t \in [T]} \sum_{x_{[0:t-1]}} \sum_{\bar{x}_{t-1}^n} p(\bar{x}_{t-1}^n | x_{[0:t-1]}^{\setminus n}) p(x_{[0:t-1]}) \sum_{\bar{n} \in [N], \bar{n} \neq n} \mathbf{KL}(p(\mathbf{x}_t^{\bar{n}} | \mathbf{x}_{t-1}) || p(\mathbf{x}_t^{\bar{n}} | \bar{\mathbf{x}}_{t-1})).
\end{aligned}$$

We can now use Corollary 4 and get:

$$\begin{aligned}
& \mathbf{KL}(p(\mathbf{y}_{[T]}^n) || \tilde{p}(\mathbf{y}_{[T]}^n)) \\
& \leq \sum_{t \in [T]} \sum_{x_{[0:t-1]}} \sum_{\bar{x}_{t-1}^n} p(\bar{x}_{t-1}^n | x_{[0:t-1]}^{\setminus n}) p(x_{[0:t-1]}) \sum_{\bar{n} \in [N], \bar{n} \neq n} \mathbf{KL}(p(\mathbf{x}_t^{\bar{n}} | \mathbf{x}_{t-1}) || p(\mathbf{x}_t^{\bar{n}} | \bar{\mathbf{x}}_{t-1})) \\
& \leq \sum_{t \in [T]} \sum_{x_{[0:t-1]}} \sum_{\bar{x}_{t-1}^n} p(\bar{x}_{t-1}^n | x_{[0:t-1]}^{\setminus n}) p(x_{[0:t-1]}) \\
& \quad \sum_{\bar{n} \in [N], \bar{n} \neq n} \frac{1}{2} \left[ \sum_{x_t^{\bar{n}}} p(x_t^{\bar{n}} | x_{t-1}) \frac{1}{p(x_t^{\bar{n}} | x_{t-1})^2} (p(x_t^{\bar{n}} | x_{t-1}) - p(x_t^{\bar{n}} | \bar{x}_{t-1}))^2 \right] \\
& \quad + \frac{1}{3} \left[ \sum_{x_t^{\bar{n}}} p(x_t^{\bar{n}} | x_{t-1}) \frac{1}{p(x_t^{\bar{n}} | \bar{x}_{t-1})^3} |p(x_t^{\bar{n}} | x_{t-1}) - p(x_t^{\bar{n}} | \bar{x}_{t-1})|^3 \right].
\end{aligned}$$

We can then bound the differences between the kernels with our Assumption 3:

$$\begin{aligned}
& \mathbf{KL}(p(\mathbf{y}_{[T]}^n) \parallel \tilde{p}(\mathbf{y}_{[T]}^n)) \\
& \leq \sum_{t \in [T]} \sum_{x_{[0:t-1]}} \sum_{\bar{x}_{t-1}^n} p(\bar{x}_{t-1}^n | x_{[0:t-1]}^n) p(x_{[0:t-1]}) \\
& \quad \sum_{\bar{n} \in [N], \bar{n} \neq n} \frac{1}{2} \left[ \sum_{x_t^{\bar{n}}} p(x_t^{\bar{n}} | x_{t-1}) \frac{1}{p(x_t^{\bar{n}} | x_{t-1})^2} (p(x_t^{\bar{n}} | x_{t-1}) - p(x_t^{\bar{n}} | \bar{x}_{t-1}))^2 \right] \\
& \quad + \frac{1}{3} \left[ \sum_{x_t^{\bar{n}}} p(x_t^{\bar{n}} | x_{t-1}) \frac{1}{p(x_t^{\bar{n}} | \bar{x}_{t-1})^3} |p(x_t^{\bar{n}} | x_{t-1}) - p(x_t^{\bar{n}} | \bar{x}_{t-1})|^3 \right] \\
& \leq \sum_{t \in [T]} \sum_{x_{[0:t-1]}} \sum_{\bar{x}_{t-1}^n} p(\bar{x}_{t-1}^n | x_{[0:t-1]}^n) p(x_{[0:t-1]}) \\
& \quad \sum_{\bar{n} \in [N], \bar{n} \neq n} \frac{1}{2} \left[ \sum_{x_t^{\bar{n}}} p(x_t^{\bar{n}} | x_{t-1}) \frac{1}{p(x_t^{\bar{n}} | x_{t-1})^2} \frac{s_{\bar{n}}^2}{N^2} |d_{n, \bar{n}}(x_{t-1}^n) - d_{n, \bar{n}}(\bar{x}_{t-1}^n)|^2 \right] \\
& \quad + \frac{1}{3} \left[ \sum_{x_t^{\bar{n}}} p(x_t^{\bar{n}} | x_{t-1}) \frac{1}{p(x_t^{\bar{n}} | \bar{x}_{t-1})^3} \frac{s_{\bar{n}}^3}{N^3} |d_{n, \bar{n}}(x_{t-1}^n) - d_{n, \bar{n}}(\bar{x}_{t-1}^n)|^3 \right],
\end{aligned}$$

and Assumption 4:

$$\begin{aligned}
& \mathbf{KL}(p(\mathbf{y}_{[T]}^n) \parallel \tilde{p}(\mathbf{y}_{[T]}^n)) \\
& \leq \sum_{t \in [T]} \sum_{x_{[0:t-1]}} \sum_{\bar{x}_{t-1}^n} p(\bar{x}_{t-1}^n | x_{[0:t-1]}^n) p(x_{[0:t-1]}) \\
& \quad \sum_{\bar{n} \in [N], \bar{n} \neq n} \frac{1}{2} \frac{s_{\bar{n}}^2}{N^2} |d_{n, \bar{n}}(x_{t-1}^n) - d_{n, \bar{n}}(\bar{x}_{t-1}^n)|^2 \left[ \sum_{x_t^{\bar{n}}} p(x_t^{\bar{n}} | x_{t-1}) \frac{1}{p(x_t^{\bar{n}} | x_{t-1})^2} \right] \\
& \quad + \frac{1}{3} \frac{s_{\bar{n}}^3}{N^3} |d_{n, \bar{n}}(x_{t-1}^n) - d_{n, \bar{n}}(\bar{x}_{t-1}^n)|^3 \left[ \sum_{x_t^{\bar{n}}} p(x_t^{\bar{n}} | x_{t-1}) \frac{1}{p(x_t^{\bar{n}} | \bar{x}_{t-1})^3} \right] \\
& \leq \sum_{t \in [T]} \sum_{x_{[0:t-1]}} \sum_{\bar{x}_{t-1}^n} p(\bar{x}_{t-1}^n | x_{[0:t-1]}^n) p(x_{[0:t-1]}) \\
& \quad \sum_{\bar{n} \in [N], \bar{n} \neq n} \frac{1}{2} \frac{s_{\bar{n}}^2}{\epsilon^2 N^2} |d_{n, \bar{n}}(x_{t-1}^n) - d_{n, \bar{n}}(\bar{x}_{t-1}^n)|^2 + \frac{1}{3} \frac{s_{\bar{n}}^3}{\epsilon^3 N^3} |d_{n, \bar{n}}(x_{t-1}^n) - d_{n, \bar{n}}(\bar{x}_{t-1}^n)|^3 \\
& \leq \sum_{t \in [T]} \sum_{x_{[0:t-1]}} \sum_{\bar{x}_{t-1}^n} p(\bar{x}_{t-1}^n | x_{[0:t-1]}^n) p(x_{[0:t-1]}) \\
& \quad \sum_{\bar{n} \in [N], \bar{n} \neq n} \left[ \frac{1}{2} \frac{s_{\bar{n}}^2}{\epsilon^2 N} + \frac{1}{3} \frac{s_{\bar{n}}^3}{\epsilon^3 N} \right] \frac{1}{N} |d_{n, \bar{n}}(x_{t-1}^n) - d_{n, \bar{n}}(\bar{x}_{t-1}^n)|^2
\end{aligned}$$

where in the last step we used  $|d_{n,\bar{n}}(x_{t-1}^n) - d_{n,\bar{n}}(\bar{x}_{t-1}^n)| < N$ . We can use  $s_n^{MAX} := \max\{s_n^2, s_n^3\}$  and reformulate:

$$\begin{aligned}
& \mathbf{KL}(p(\mathbf{y}_{[T]}^n) || \tilde{p}(\mathbf{y}_{[T]}^n)) \\
& \leq \sum_{t \in [T]} \sum_{x_{[0:t-1]}} \sum_{\bar{x}_{t-1}^n} p(\bar{x}_{t-1}^n | x_{[0:t-1]}^n) p(x_{[0:t-1]}) \\
& \quad \sum_{\bar{n} \in [N], \bar{n} \neq n} \left[ \frac{1}{2} \frac{s_{\bar{n}}^2}{\epsilon^2 N} + \frac{1}{3} \frac{s_{\bar{n}}^3}{\epsilon^3 N} \right] \frac{1}{N} |d_{n,\bar{n}}(x_{t-1}^n) - d_{n,\bar{n}}(\bar{x}_{t-1}^n)|^2 \\
& \leq \left[ \frac{1}{2} \frac{1}{\epsilon^2 N} + \frac{1}{3} \frac{1}{\epsilon^3 N} \right] \sum_{t \in [T]} \sum_{\bar{n} \in [N], \bar{n} \neq n} \frac{s_n^{MAX}}{N} \\
& \quad \sum_{x_{[0:t-1]}} \sum_{\bar{x}_{t-1}^n} p(\bar{x}_{t-1}^n | x_{[0:t-1]}^n) p(x_{[0:t-1]}) |d_{n,\bar{n}}(x_{t-1}^n) - d_{n,\bar{n}}(\bar{x}_{t-1}^n)|^2.
\end{aligned}$$

Now we need to work on:

$$\sum_{x_{[0:t-1]}} \sum_{\bar{x}_{t-1}^n} p(\bar{x}_{t-1}^n | x_{[0:t-1]}^n) p(x_{[0:t-1]}) |d_{n,\bar{n}}(x_{t-1}^n) - d_{n,\bar{n}}(\bar{x}_{t-1}^n)|^2,$$

which can be reformulated by expanding the square:

$$\sum_{x_{[0:t-1]}} \sum_{\bar{x}_{t-1}^n} p(\bar{x}_{t-1}^n | x_{[0:t-1]}^n) p(x_{[0:t-1]}) \left( d_{n,\bar{n}}(x_{t-1}^n)^2 - 2d_{n,\bar{n}}(x_{t-1}^n) d_{n,\bar{n}}(\bar{x}_{t-1}^n) + d_{n,\bar{n}}(\bar{x}_{t-1}^n)^2 \right),$$

and we can work on three terms inside the parenthesis separately. Firstly, we have:

$$\begin{aligned}
\sum_{x_{[0:t-1]}} \sum_{\bar{x}_{t-1}^n} p(\bar{x}_{t-1}^n | x_{[0:t-1]}^n) p(x_{[0:t-1]}) d_{n,\bar{n}}(x_{t-1}^n)^2 &= \mathbb{E} \left[ d_{n,\bar{n}}(\mathbf{x}_{t-1}^n)^2 \right] \\
&= \mathbb{E} \left\{ \mathbb{E} \left[ d_{n,\bar{n}}(\mathbf{x}_{t-1}^n)^2 \mid \mathbf{x}_{[0:t-1]}^n \right] \right\},
\end{aligned}$$

as we have no dependence on  $\bar{x}_{t-1}^n$  and where the last step follows from the law of total expectations. Now we look at the other squared term:

$$\begin{aligned}
& \sum_{x_{[0:t-1]}} \sum_{\bar{x}_{t-1}^n} p(\bar{x}_{t-1}^n | x_{[0:t-1]}^n) p(x_{[0:t-1]}) d_{n,\bar{n}}(\bar{x}_{t-1}^n)^2 \\
&= \sum_{x_{[0:t-1]}^n} \sum_{\bar{x}_{t-1}^n} p(\bar{x}_{t-1}^n | x_{[0:t-1]}^n) p(x_{[0:t-1]}^n) d_{n,\bar{n}}(\bar{x}_{t-1}^n)^2 = \mathbb{E} \left\{ \mathbb{E} \left[ d_{n,\bar{n}}(\mathbf{x}_{t-1}^n)^2 \mid \mathbf{x}_{[0:t-1]}^n \right] \right\},
\end{aligned}$$

as again we have no dependence on  $x_{[0:t-1]}^n$  and so we can marginalise them out from  $p(x_{[0:t-1]})$ .

There is only the cross term left, and try to reformulate it as an expectation:

$$\begin{aligned}
& \sum_{x_{[0:t-1]}} \sum_{\bar{x}_{t-1}^n} p(\bar{x}_{t-1}^n | x_{[0:t-1]}^{\setminus n}) p(x_{[0:t-1]}) d_{n,\bar{n}}(x_{t-1}^n) d_{n,\bar{n}}(\bar{x}_{t-1}^n) \\
&= \sum_{x_{[0:t-2]}} \sum_{x_{t-1}^{\setminus n}} \sum_{x_{t-1}^n} \sum_{\bar{x}_{t-1}^n} p(x_{[0:t-1]}) p(\bar{x}_{t-1}^n | x_{[0:t-1]}^{\setminus n}) d_{n,\bar{n}}(x_{t-1}^n) d_{n,\bar{n}}(\bar{x}_{t-1}^n) \\
&= \sum_{x_{[0:t-2]}^{\setminus n}} \sum_{x_{t-1}^{\setminus n}} \sum_{x_{t-1}^n} \sum_{\bar{x}_{t-1}^n} p(x_{[0:t-2]}^{\setminus n}, x_{t-1}) p(\bar{x}_{t-1}^n | x_{[0:t-1]}^{\setminus n}) d_{n,\bar{n}}(x_{t-1}^n) d_{n,\bar{n}}(\bar{x}_{t-1}^n) \\
&= \sum_{x_{[0:t-1]}^{\setminus n}} p(x_{[0:t-1]}^{\setminus n}) \sum_{x_{t-1}^n} \sum_{\bar{x}_{t-1}^n} p(x_{t-1}^n | x_{[0:t-1]}^{\setminus n}) p(\bar{x}_{t-1}^n | x_{[0:t-1]}^{\setminus n}) d_{n,\bar{n}}(x_{t-1}^n) d_{n,\bar{n}}(\bar{x}_{t-1}^n) \\
&= \sum_{x_{[0:t-1]}^{\setminus n}} p(x_{[0:t-1]}^{\setminus n}) \left[ \sum_{x_{t-1}^n} p(x_{t-1}^n | x_{[0:t-1]}^{\setminus n}) d_{n,\bar{n}}(x_{t-1}^n) \right] \left[ \sum_{\bar{x}_{t-1}^n} p(\bar{x}_{t-1}^n | x_{[0:t-1]}^{\setminus n}) d_{n,\bar{n}}(\bar{x}_{t-1}^n) \right] \\
&= \sum_{x_{[0:t-1]}^{\setminus n}} p(x_{[0:t-1]}^{\setminus n}) \mathbb{E} \left[ d_{n,\bar{n}}(\mathbf{x}_{t-1}^n) \mid \mathbf{x}_{[0:t-1]}^{\setminus n} \right]^2 = \mathbb{E} \left\{ \mathbb{E} \left[ d_{n,\bar{n}}(\mathbf{x}_{t-1}^n) \mid \mathbf{x}_{[0:t-1]}^{\setminus n} \right]^2 \right\}.
\end{aligned}$$

From the three reformulations above it follows that:

$$\begin{aligned}
& \mathbf{KL}(p(\mathbf{y}_{[T]}^n) \parallel \tilde{p}(\mathbf{y}_{[T]}^n)) \\
&\leq \left[ \frac{1}{2\epsilon^2 N} + \frac{1}{3\epsilon^3 N} \right] \\
&\quad \sum_{t \in [T]} \sum_{\bar{n} \in [N], \bar{n} \neq n} \frac{s_{\bar{n}}^{MAX}}{N} \sum_{x_{[0:t-1]}} \sum_{\bar{x}_{t-1}^n} p(\bar{x}_{t-1}^n | x_{[0:t-1]}^{\setminus n}) p(x_{[0:t-1]}) |d_{n,\bar{n}}(x_{t-1}^n) - d_{n,\bar{n}}(\bar{x}_{t-1}^n)|^2 \\
&\leq \left[ \frac{1}{2\epsilon^2 N} + \frac{1}{3\epsilon^3 N} \right] \\
&\quad \sum_{t \in [T]} \sum_{\bar{n} \in [N], \bar{n} \neq n} \frac{s_{\bar{n}}^{MAX}}{N} \left[ 2\mathbb{E} \left\{ \mathbb{E} \left[ d_{n,\bar{n}}(\mathbf{x}_{t-1}^n)^2 \mid \mathbf{x}_{[0:t-1]}^{\setminus n} \right] \right\} - 2\mathbb{E} \left\{ \mathbb{E} \left[ d_{n,\bar{n}}(\mathbf{x}_{t-1}^n) \mid \mathbf{x}_{[0:t-1]}^{\setminus n} \right]^2 \right\} \right] \\
&\leq 2 \left[ \frac{1}{2\epsilon^2 N} + \frac{1}{3\epsilon^3 N} \right] \sum_{\bar{n} \in [N], \bar{n} \neq n} \frac{s_{\bar{n}}^{MAX}}{N} \left[ \sum_{t \in [T]} \mathbb{E} \left\{ \text{Var} \left[ d_{n,\bar{n}}(\mathbf{x}_{t-1}^n) \mid \mathbf{x}_{[0:t-1]}^{\setminus n} \right] \right\} \right] \\
&\leq 2 \left[ \frac{1}{2\epsilon^2 N} + \frac{1}{3\epsilon^3 N} \right] \sum_{t \in [T]} \mathbb{E} \left\{ \frac{1}{N} \sum_{\bar{n} \in [N], \bar{n} \neq n} s_{\bar{n}}^{MAX} \text{Var} \left[ d_{n,\bar{n}}(\mathbf{x}_{t-1}^n) \mid \mathbf{x}_{[0:t-1]}^{\setminus n} \right] \right\},
\end{aligned}$$

which completes the proof. □

### A.3 KL bounds for SimBa-CL for general partitions

As explained in the main paper we can generalise SimBa-CL with and without feedback to work on different factorisations of the dimensions. Precisely, if we have a general partition  $\mathcal{K}$  of  $[N]$ , then we can define for each  $K \in \mathcal{K}$ :

$$p(y_{[T]}^K) := \sum_{x_{[0:T]}} p(x_{[0:T]}^{\setminus K}) p(x_{[0:T]}^K | x_{[0:T]}^{\setminus K}) \prod_{t \in [T]} \prod_{n \in K} p(y_t^n | x_t^n);$$

$$\tilde{p}_{\mathcal{K}}(y_{[T]}^K) := \sum_{x_{[0:T]}} p(x_{[0:T]}^{\setminus K}) \prod_{n \in K} p(x_0^n) \prod_{t \in [T]} p(x_t^n | x_{t-1}^n) p(y_t^n | x_t^n),$$

and then combine them as  $p_{\mathcal{K}}(y_{[T]}) := \prod_{K \in \mathcal{K}} p(y_{[T]}^K)$  and as  $\tilde{p}_{\mathcal{K}}(y_{[T]}) := \prod_{K \in \mathcal{K}} \tilde{p}_{\mathcal{K}}(y_{[T]}^K)$  to provide an approximation of our likelihood  $p(y_{[T]})$ . In this case we are computing the marginals on subsets of the state-space, which can be particularly suited when we expect strong dependence inside the elements of the partition, e.g. an agent-based model with individuals partitioned in households.

Again  $p_{\mathcal{K}}(y_{[T]})$  can be seen as a SimBa-CL with feedback, where the likelihood is approximated with the product of the true marginals, and  $\tilde{p}_{\mathcal{K}}(y_{[T]})$  can be seen as a SimBa-CL without feedback. As for the fully factorise case, we have a recursive formula for  $p(x_{[0:T]}^K | x_{[0:T]}^{\setminus K})$  given by:

$$p(x_{[0:T]}^K | x_{[0:T]}^{\setminus K}) = \prod_{n \in K} p(x_0^n) \prod_{t \in [T]} p(x_t^n | x_{t-1}^n) f_K(x_{t-1}^K, x_{[0:t]}^{\setminus K}),$$

where the simulation feedback is now:

$$f_K(x_{t-1}^K, x_{[0:t]}^{\setminus K}) := \frac{\prod_{\bar{n} \in [N] \setminus K} p(x_t^{\bar{n}} | x_{t-1}^{\bar{n}})}{\sum_{\bar{x}_{t-1}^K} \prod_{\bar{n} \in [N] \setminus K} p(x_t^{\bar{n}} | \bar{x}_{t-1}^{\bar{n}}, x_{[t-1]}^{\setminus K}) p(\bar{x}_{t-1}^K | x_0^{\setminus K}, x_{[t-1]}^{\setminus K})},$$

As for SimBa-CL with and without feedback, with these general terms referring to the the fully factorise case, we can assess the degradation of approximation quality when excluding the feedback from the procedure. Naturally, we need a more general version of Assumption 1 and Assumption 2, given that we are now dealing with changes across multiple dimensions.

**Assumption 7.** For any  $K \in \mathcal{K}$  and for any  $x_t^{\bar{n}} \in \mathcal{X}$  with  $\bar{n} \notin K$ , if  $x_{t-1}, \bar{x}_{t-1} \in \mathcal{X}^N$  are such that  $x_{t-1}^{\setminus K} = \bar{x}_{t-1}^{\setminus K}$  then:

$$|p(x_t^{\bar{n}} | x_{t-1}) - p(x_t^{\bar{n}} | \bar{x}_{t-1})| \leq \frac{s_{\bar{n}}}{N} |d_{K, \bar{n}}(x_{t-1}^n) - d_{K, \bar{n}}(\bar{x}_{t-1}^n)|.$$

where  $d_{K, \bar{n}} : \mathcal{X}^K \rightarrow \mathbb{R}_+$  and  $s_{\bar{n}}$  is a positive constant.

**Assumption 8.** For any  $K, \bar{K} \in \mathcal{K}$ , if  $x_{t-1}, \bar{x}_{t-1} \in \mathcal{X}^N$  are such that  $x_{t-1}^{\setminus \bar{K}} = \bar{x}_{t-1}^{\setminus \bar{K}}$  then there exists  $0 < \epsilon < 1$  such that:

$$\sum_{x_t^n} p(x_t^n | x_{t-1}) \frac{1}{p(x_t^n | \bar{x}_{t-1})^2} \leq \frac{1}{\epsilon^2}, \quad \text{and} \quad \sum_{x_t^n} p(x_t^n | x_{t-1}) \frac{1}{p(x_t^n | \bar{x}_{t-1})^3} \leq \frac{1}{\epsilon^3}.$$

Assumption 7 and Assumption 8 provides the required generalisations. Assumption 7 is measuring the interactions on  $K \in \mathcal{K}$  and ensuring that changes on  $K$  have a limited impact on the dynamic of the process. Meanwhile, Assumption 8 formulates a stronger ergodicity.

As for the fully factorise case, given the assumptions, we can bound the **KL**-divergence between our SimBa-CL with and without feedback on general partitions. As it can be noticed from the statement of Theorem 5, there are a couple of deviations from the fully factorise case.

**Theorem 5.** *If  $|d_{K,\bar{n}}(x^K) - d_{K,\bar{n}}(\bar{x}^K)| < N$  for any  $x^K, \bar{x}^K \in \mathcal{X}^K$  and for any  $K \in \mathcal{K}$ , and assumptions 2-7 hold, then for any  $K \in \mathcal{K}$ :*

$$\mathbf{KL} [p(\mathbf{y}_{[T]}^K) || \tilde{p}_{\mathcal{K}}(\mathbf{y}_{[T]}^K)] \leq \frac{a(\epsilon)}{N} \sum_{t \in [T]} \mathbb{E} \left\{ \frac{1}{N} \sum_{\bar{n} \in [N] \setminus K} s_{\bar{n}}^{MAX} \text{Var} \left[ d_{K,\bar{n}}(\mathbf{x}_{t-1}^K) \mid \mathbf{x}_{[0:t-1]}^{\setminus K} \right] \right\},$$

where  $a(\epsilon) := 2 \left[ \frac{1}{2\epsilon^2} + \frac{1}{3\epsilon^3} \right]$  and  $s_n^{MAX} := \max\{s_n^2, s_n^3\}$ .

Once more, we can interpret the bound as the one from Theorem 1, suggesting to exclude the feedback whenever the dimension  $N$  is large and when the process noise is contained.

Given assumptions 5-6 we can prove bounds on the KL-divergence between the with feedback case and the without feedback case.

*proof of Theorem 5.* The proof of Theorem 2 follows the same steps as the proof of Theorem 1, with  $K$  instead of  $n$ . However, the last steps are slightly different due to a different assumption to apply. We report them here for completeness.

Precisely after proving that our KL is well-defined, applying the data processing inequality, exploiting the factorisations in the model and applying Jensen we reach the point of using Corollary 4 and get:

$$\begin{aligned} & \mathbf{KL}(p(\mathbf{y}_{[T]}^K) || \tilde{p}(\mathbf{y}_{[T]}^K)) \\ & \leq \sum_{t \in [T]} \sum_{x_{[0:t-1]}} \sum_{\bar{x}_{t-1}^K} p(\bar{x}_{t-1}^K | x_{[0:t-1]}^{\setminus K}) p(x_{[0:t-1]}) \sum_{\bar{n} \in [N] \setminus K} \mathbf{KL}(p(\mathbf{x}_t^{\bar{n}} | \mathbf{x}_{t-1}) || p(\mathbf{x}_t^{\bar{n}} | \bar{\mathbf{x}}_{t-1})) \\ & \leq \sum_{t \in [T]} \sum_{x_{[0:t-1]}} \sum_{\bar{x}_{t-1}^K} p(\bar{x}_{t-1}^K | x_{[0:t-1]}^{\setminus K}) p(x_{[0:t-1]}) \\ & \quad \sum_{\bar{n} \in [N] \setminus K} \frac{1}{2} \left[ \sum_{x_t^{\bar{n}}} p(x_t^{\bar{n}} | x_{t-1}) \frac{1}{p(x_t^{\bar{n}} | x_{t-1})^2} (p(x_t^{\bar{n}} | x_{t-1}) - p(x_t^{\bar{n}} | \bar{x}_{t-1}))^2 \right] \\ & \quad + \frac{1}{3} \left[ \sum_{x_t^{\bar{n}}} p(x_t^{\bar{n}} | x_{t-1}) \frac{1}{p(x_t^{\bar{n}} | \bar{x}_{t-1})^3} |p(x_t^{\bar{n}} | x_{t-1}) - p(x_t^{\bar{n}} | \bar{x}_{t-1})|^3 \right]. \end{aligned}$$



We can then bound the differences between the kernels with our Assumption 5:

$$\begin{aligned}
& \mathbf{KL}(p(\mathbf{y}_{[T]}^K) \parallel \tilde{p}(\mathbf{y}_{[T]}^K)) \\
& \leq \sum_{t \in [T]} \sum_{x_{[0:t-1]}} \sum_{\bar{x}_{t-1}^K} p(\bar{x}_{t-1}^K | x_{[0:t-1]}^K) p(x_{[0:t-1]}) \\
& \quad \sum_{\bar{n} \in [N] \setminus K} \frac{1}{2} \left[ \sum_{x_t^{\bar{n}}} p(x_t^{\bar{n}} | x_{t-1}) \frac{1}{p(x_t^{\bar{n}} | x_{t-1})^2} \frac{s_{\bar{n}}^2}{N^2} |d_{K, \bar{n}}(x_{t-1}^K) - d_{K, \bar{n}}(\bar{x}_{t-1}^K)|^2 \right] \\
& \quad + \frac{1}{3} \left[ \sum_{x_t^{\bar{n}}} p(x_t^{\bar{n}} | x_{t-1}) \frac{1}{p(x_t^{\bar{n}} | \bar{x}_{t-1})^3} \frac{s_{\bar{n}}^3}{N^3} |d_{K, \bar{n}}(x_{t-1}^K) - d_{K, \bar{n}}(\bar{x}_{t-1}^K)|^3 \right],
\end{aligned}$$

and Assumption 6:

$$\begin{aligned}
& \mathbf{KL}(p(\mathbf{y}_{[T]}^K) \parallel \tilde{p}(\mathbf{y}_{[T]}^K)) \\
& \leq \sum_{t \in [T]} \sum_{x_{[0:t-1]}} \sum_{\bar{x}_{t-1}^K} p(\bar{x}_{t-1}^K | x_{[0:t-1]}^K) p(x_{[0:t-1]}) \\
& \quad \sum_{\bar{n} \in [N] \setminus K} \frac{1}{2} \frac{s_{\bar{n}}^2}{\epsilon^2 N^2} |d_{K, \bar{n}}(x_{t-1}^K) - d_{K, \bar{n}}(\bar{x}_{t-1}^K)|^2 + \frac{1}{3} \frac{s_{\bar{n}}^3}{\epsilon^3 N^3} |d_{K, \bar{n}}(x_{t-1}^K) - d_{K, \bar{n}}(\bar{x}_{t-1}^K)|^3 \\
& \leq \sum_{t \in [T]} \sum_{x_{[0:t-1]}} \sum_{\bar{x}_{t-1}^K} p(\bar{x}_{t-1}^K | x_{[0:t-1]}^K) p(x_{[0:t-1]}) \\
& \quad \sum_{\bar{n} \in [N] \setminus K} \left[ \frac{1}{2} \frac{s_{\bar{n}}^2}{\epsilon^2 N} + \frac{1}{3} \frac{s_{\bar{n}}^3}{\epsilon^3 N} \right] \frac{1}{N} |d_{K, \bar{n}}(x_{t-1}^K) - d_{K, \bar{n}}(\bar{x}_{t-1}^K)|^2
\end{aligned}$$

where in the last step we used  $|d_{K, \bar{n}}(x_{t-1}^K) - d_{K, \bar{n}}(\bar{x}_{t-1}^K)| < N$ . Similarly to the proof of Theorem 1 we can reformulate in terms of expected variance but this time we will work on

$d_{K,\bar{n}}(\mathbf{x}_{t-1}^K)$  and so:

$$\begin{aligned}
& \mathbf{KL}(p(\mathbf{y}_{[T]}^K) \parallel \tilde{p}(\mathbf{y}_{[T]}^K)) \\
& \leq \left[ \frac{1}{2\epsilon^2 N} + \frac{1}{3\epsilon^3 N} \right] \\
& \quad \sum_{t \in [T]} \sum_{\bar{n} \in [N] \setminus K} \frac{s_{\bar{n}}^{MAX}}{N} \sum_{x_{[0:t-1]}} \sum_{\bar{x}_{t-1}^K} p(\bar{x}_{t-1}^K | x_{[0:t-1]}^{\setminus K}) p(x_{[0:t-1]}) |d_{K,\bar{n}}(x_{t-1}^K) - d_{K,\bar{n}}(\bar{x}_{t-1}^K)|^2 \\
& \leq \left[ \frac{1}{2\epsilon^2 N} + \frac{1}{3\epsilon^3 N} \right] \\
& \quad \sum_{t \in [T]} \sum_{\bar{n} \in [N] \setminus K} \frac{s_{\bar{n}}^{MAX}}{N} \left[ 2\mathbb{E} \left\{ \mathbb{E} \left[ d_{K,\bar{n}}(\mathbf{x}_{t-1}^K)^2 \mid \mathbf{x}_{[0:t-1]}^{\setminus K} \right] \right\} - 2\mathbb{E} \left\{ \mathbb{E} \left[ d_{K,\bar{n}}(\mathbf{x}_{t-1}^K) \mid \mathbf{x}_{[0:t-1]}^{\setminus K} \right]^2 \right\} \right] \\
& \leq 2 \left[ \frac{1}{2\epsilon^2 N} + \frac{1}{3\epsilon^3 N} \right] \sum_{\bar{n} \in [N] \setminus K} \frac{s_{\bar{n}}^{MAX}}{N} \left[ \sum_{t \in [T]} \mathbb{E} \left\{ \text{Var} \left[ d_{K,\bar{n}}(\mathbf{x}_{t-1}^K) \mid \mathbf{x}_{[0:t-1]}^{\setminus K} \right] \right\} \right] \\
& \leq 2 \left[ \frac{1}{2\epsilon^2 N} + \frac{1}{3\epsilon^3 N} \right] \sum_{t \in [T]} \mathbb{E} \left\{ \frac{1}{N} \sum_{\bar{n} \in [N] \setminus K} s_{\bar{n}}^{MAX} \text{Var} \left[ d_{K,\bar{n}}(\mathbf{x}_{t-1}^K) \mid \mathbf{x}_{[0:t-1]}^{\setminus K} \right] \right\},
\end{aligned}$$

where  $s_{\bar{n}}^{MAX}$  has the same definition as in the previous proof. □

## B SimBa-CL as composite likelihood

Here we discuss further on SimBa-CL as composite likelihood method, with a particular focus on the estimation of the sensitivity matrix and variability matrix and the observed information.

### B.1 Observed information

In the main paper we reported  $S(\theta)$  and  $V(\theta)$  as our sensitivity matrix and variability matrix, which we defined as:

$$S(\theta) = \mathbb{E}_{\theta} \left\{ -\text{Hess}_{\theta} \left[ \log \tilde{p}_{\mathcal{K}}(y_{[T]}^K | \theta) \right] \right\} \quad \text{and} \quad V(\theta) = \text{Var}_{\theta} \left\{ \nabla_{\theta} \left[ \log \tilde{p}_{\mathcal{K}}(y_{[T]}^K | \theta) \right] \right\}.$$

This formulations suggests a bootstrap approach where the expectations are estimated by simulating from the model and computing hessian and gradient of the composite likelihood in the simulated data accordingly. However, it is often common to use an observed information approach, where the observed data are plug-in our instead of simulated data. It is worth noting that for the above formulation of variability and specificity matrix this is not ideal as

the observed data are not independent and identically distributed, meaning that we do not really have a way to estimate the mean and the variance in the equations above.

In the main paper we also reported another formulation of the sensitivity matrix and variability matrix, where approximate Barlett identities are used:

$$S(\theta) \approx \sum_{K \in \mathcal{K}} \mathbb{E}_\theta \left\{ \nabla_\theta [\log \tilde{p}_K(\mathbf{y}_{[T]}^K | \theta)] \nabla_\theta [\log \tilde{p}_K(\mathbf{y}_{[T]}^K | \theta)]^\top \right\},$$

$$V(\theta) \approx \sum_{K, \tilde{K} \in \mathcal{K}} \mathbb{E}_\theta \left\{ \nabla_\theta [\log \tilde{p}_K(\mathbf{y}_{[T]}^K | \theta)] \nabla_\theta [\log \tilde{p}_{\tilde{K}}(\mathbf{y}_{[T]}^{\tilde{K}} | \theta)]^\top \right\}.$$

These alternative formulations are more suited to the observed information approach as we could assume independence across blocks and identical distribution of the blocks and get:

$$S(\theta) \approx \sum_{K \in \mathcal{K}} \left\{ \nabla_\theta [\log \tilde{p}_K(y_{[T]}^K | \theta)] \nabla_\theta [\log \tilde{p}_K(y_{[T]}^K | \theta)]^\top \right\},$$

$$V(\theta) \approx \sum_{K, \tilde{K} \in \mathcal{K}} \left\{ \nabla_\theta [\log \tilde{p}_K(y_{[T]}^K | \theta)] \nabla_\theta [\log \tilde{p}_{\tilde{K}}(y_{[T]}^{\tilde{K}} | \theta)]^\top \right\}.$$

It is surely not surprising that this approach will not perform well when the blocks are highly correlated and different in distribution.

For completeness we report the experiment table from the main paper where empirical coverage when learning the full model is measured. Here we add an extra row showing the resulting coverage across parameters when using the observed information. As clear from the bad coverage, the observed information might lead to overconfident sets, this is probably due to the challenge of identifying the parameters and so the optimizer getting stuck in local maxima of the likelihood.

Parameter	$\beta_0$	$\beta_\lambda$	$\beta_\gamma$	$q$	$\iota$
Without Barlett	0.17 and 0.05	0.61 and 0.87	0.8 and 1.	0.87 and 0.5	0.02
With Barlett	0.98 and 0.89	0.99 and 0.75	0.97 and 0.97	1. and 0.98	0.92
With Barlett OI	0.48 and 0.30	0.51 and 0.31	0.01 and 0.06	0.62 and 0.02	0.03

Table 6: Empirical coverage per each parameter when computing the Godambe information matrix with and without the approximate Barlett identities and when using the observed information. Whenever the parameter is bi-dimensional the coverage per each component is reported in the same cell separated by “and”. “OI” refers to observed information.

## B.2 Estimating the sensitivity and variability matrix

Bootstrap sampling seems like a good strategy to compute estimate of the variability and sensitivity matrix, precisely given  $P$  samples from the model:

$$y_{[T]}^i \sim p(y_{[T]} | \hat{\theta}_{CL}) \text{ for } i \in [P],$$

where  $\hat{\theta}_{CL}$  is our maximum SimBa-CL estimator, can be used to get:

$$S(\hat{\theta}_{CL}) \approx \frac{1}{P} \sum_{i \in [P]} \left\{ -\text{Hess}_{\theta} \left[ \log \tilde{p}_{\mathcal{K}} \left( y_{[T]}^K | \hat{\theta}_{CL} \right) \right] \right\} \text{ and}$$

$$V(\hat{\theta}_{CL}) \approx \frac{1}{P-1} \sum_{i \in [P]} \left[ \nabla_{\theta} \left[ \log \tilde{p}_{\mathcal{K}} \left( y_{[T]}^K | \hat{\theta}_{CL} \right) \right] - \frac{1}{P} \sum_{i \in [P]} \left\{ \nabla_{\theta} \left[ \log \tilde{p}_{\mathcal{K}} \left( y_{[T]}^K | \hat{\theta}_{CL} \right) \right] \right\} \right]^2.$$

Similarly when invoking the approximate first and second Barlett identities we have:

$$S(\hat{\theta}_{CL}) \approx \sum_{K \in \mathcal{K}} \frac{1}{P} \sum_{i \in [P]} \left\{ \nabla_{\theta} \left[ \log \tilde{p}_{\mathcal{K}} \left( y_{[T]}^K | \hat{\theta}_{CL} \right) \right] \nabla_{\theta} \left[ \log \tilde{p}_{\mathcal{K}} \left( y_{[T]}^K | \hat{\theta}_{CL} \right) \right]^{\top} \right\},$$

$$V(\hat{\theta}_{CL}) \approx \sum_{K, \tilde{K} \in \mathcal{K}} \frac{1}{P} \sum_{i \in [P]} \left\{ \nabla_{\theta} \left[ \log \tilde{p}_{\mathcal{K}} \left( y_{[T]}^K | \hat{\theta}_{CL} \right) \right] \nabla_{\theta} \left[ \log \tilde{p}_{\mathcal{K}} \left( y_{[T]}^{\tilde{K}} | \hat{\theta}_{CL} \right) \right]^{\top} \right\}.$$

Note that all the differentiation operations can be run in parallel on  $P$ , making the bootstrap approach relatively cheap when consistent computational resources are available.

### B.3 Approximate first and second Barlett identities

In this section, we motivate the use of the Barlett identities in our computations. The first Barlett identity states:

$$\mathbb{E}_{\theta} \left[ \nabla_{\theta} \log (p(\mathbf{y}_{[T]} | \theta)) \right] = 0,$$

which we want to discuss for the SimBa-CL case.

For SimBa-CL we have:

$$\begin{aligned} \mathbb{E}_{\theta} \left[ \nabla_{\theta} \log (\tilde{p}_{\mathcal{K}}(\mathbf{y}_{[T]} | \theta)) \right] &= \sum_{K \in \mathcal{K}} \mathbb{E}_{\theta} \left[ \nabla_{\theta} \log (\tilde{p}_{\mathcal{K}}(y_{[T]}^K | \theta)) \right] = \sum_{K \in \mathcal{K}} \mathbb{E}_{\theta} \left[ \frac{\nabla_{\theta} (\tilde{p}_{\mathcal{K}}(y_{[T]}^K | \theta))}{\tilde{p}_{\mathcal{K}}(y_{[T]}^K | \theta)} \right] \\ &= \sum_{K \in \mathcal{K}} \sum_{y_{[T]}^K} \left[ \nabla_{\theta} (\tilde{p}_{\mathcal{K}}(y_{[T]}^K | \theta)) \frac{p(y_{[T]}^K | \theta)}{\tilde{p}_{\mathcal{K}}(y_{[T]}^K | \theta)} \right] \\ &\approx \sum_{K \in \mathcal{K}} \sum_{y_{[T]}^K} \left[ \nabla_{\theta} (\tilde{p}_{\mathcal{K}}(y_{[T]}^K | \theta)) \right] = 0, \end{aligned}$$

where we use the  $\tilde{p}_{\mathcal{K}}(y_{[T]}^K | \theta) \approx p(y_{[T]}^K | \theta)$ , i.e. a simulation feedback close to 1, and the fact that  $\tilde{p}_{\mathcal{K}}$  is still a proper probability distribution and so sum up to 1. Obviously, if we consider SimBa-CL with feedback the first Barlett identity holds exactly cause we are targeting the true marginals.

We now discuss the second Barlett identity:

$$\mathbb{E}_\theta [\text{Hess}_\theta \log (p(\mathbf{y}_{[T]}|\theta))] = -\mathbb{E}_\theta \left\{ \nabla_\theta [\log p(\mathbf{y}_{[T]}|\theta)] \nabla_\theta [\log p(\mathbf{y}_{[T]}|\theta)]^\top \right\}.$$

Note that for SimBa-CL we have:

$$\begin{aligned} \mathbb{E}_\theta [\text{Hess}_\theta \log (\tilde{p}_\mathcal{K}(\mathbf{y}_{[T]}|\theta))] &= \sum_{K \in \mathcal{K}} \mathbb{E}_\theta [\text{Hess}_\theta \log (\tilde{p}_\mathcal{K}(\mathbf{y}_{[T]}^K|\theta))] \\ &= \sum_{K \in \mathcal{K}} \mathbb{E}_\theta [\nabla_\theta \nabla_\theta \log (\tilde{p}_\mathcal{K}(\mathbf{y}_{[T]}^K|\theta))] = \sum_{K \in \mathcal{K}} \mathbb{E}_\theta \left[ \nabla_\theta \left( \frac{\nabla_\theta \tilde{p}_\mathcal{K}(\mathbf{y}_{[T]}^K|\theta)}{\tilde{p}_\mathcal{K}(\mathbf{y}_{[T]}^K|\theta)} \right) \right] = \\ &= \sum_{K \in \mathcal{K}} \mathbb{E}_\theta \left[ \left( \frac{\text{Hess}_\theta \tilde{p}_\mathcal{K}(\mathbf{y}_{[T]}^K|\theta)}{\tilde{p}_\mathcal{K}(\mathbf{y}_{[T]}^K|\theta)} \right) - \left( \frac{\nabla_\theta \tilde{p}_\mathcal{K}(\mathbf{y}_{[T]}^K|\theta) \nabla_\theta \tilde{p}_\mathcal{K}(\mathbf{y}_{[T]}^K|\theta)^\top}{\tilde{p}_\mathcal{K}(\mathbf{y}_{[T]}^K|\theta)^2} \right) \right] \\ &= \sum_{K \in \mathcal{K}} \sum_{y_{[T]}^K} \left[ \left( \frac{\text{Hess}_\theta \tilde{p}_\mathcal{K}(y_{[T]}^K|\theta)}{\tilde{p}_\mathcal{K}(y_{[T]}^K|\theta)} \right) - \left( \nabla_\theta \log \tilde{p}_\mathcal{K}(y_{[T]}^K|\theta) \nabla_\theta \log \tilde{p}_\mathcal{K}(y_{[T]}^K|\theta)^\top \right) \right] p(y_{[T]}^K|\theta) \\ &\approx - \sum_{K \in \mathcal{K}} \sum_{y_{[T]}^K} \nabla_\theta [\log \tilde{p}_\mathcal{K}(y_{[T]}^K|\theta)] \nabla_\theta [\log \tilde{p}_\mathcal{K}(y_{[T]}^K|\theta)]^\top p(y_{[T]}^K|\theta) \\ &= - \sum_{K \in \mathcal{K}} \mathbb{E}_\theta \left\{ \nabla_\theta [\log \tilde{p}_\mathcal{K}(y_{[T]}^K|\theta)] \nabla_\theta [\log \tilde{p}_\mathcal{K}(y_{[T]}^K|\theta)]^\top \right\}, \end{aligned}$$

where again we used our simulation feedback being approximatively 1.

Combining the definitions of mean and variance with these approximate Barlett identities leads to our proposed estimates of the sensitivity and variability matrix.

## C Experiments

### C.1 Empirical evaluation of the KL-divergence

In this section we expand more on the empirical KL-divergence, which is used as an evaluation metric to measure the similarities between different SimBa-CL.

It is essential to recognise that any distribution  $q(x)$  can be approximated empirically as  $q(x) \approx \sum_{z \in [E]} q(z) \delta_z(x)$ , where  $E$  corresponds to the number of evaluations of  $x$ . While this approximation provides a sparse representation of  $p(x)$ , it nonetheless offers a means to estimate the KL-divergence as follows:

$$\mathbf{KL} [p(\mathbf{x}) || q(\mathbf{x})] \approx \sum_{e \in [E]} p(x^e) \log \left( \frac{p(x^e)}{q(x^e)} \right).$$

We can then simulate multiple times from the model to have some approximate evaluation of the chosen SimBa-CL, and we can then compare different SimBa-CL using the above evaluation metric.

Note that after simulating multiple times from the model we have a sample per each SimBa-CL and we can create multiple samples by leaving one simulation out at the time. This will allow us to produce a sample of KL-divergences from which we can compute mean and variance. The table with mean and variance for our experiments is reported in the main paper. However, as we are comparing distributions another valid comparison is to graphically look at the boxplots of the log SimBa-CL, which we report here.

Figure 6 depicts a comparison between the logarithm of the fully factorise SimBa-CL with and without feedback. The distribution of the two log-likelihoods appears similar, indicating that excluding the feedback does not result in a significant loss of precision. Figure 7 compares the logarithm of the fully factorise SimBa-CL without feedback with the logarithm of the coupled SimBa-CL without feedback. Again we can observe that the two distributions become more and more similar when we increase  $N$  and reduce the variance in the system.

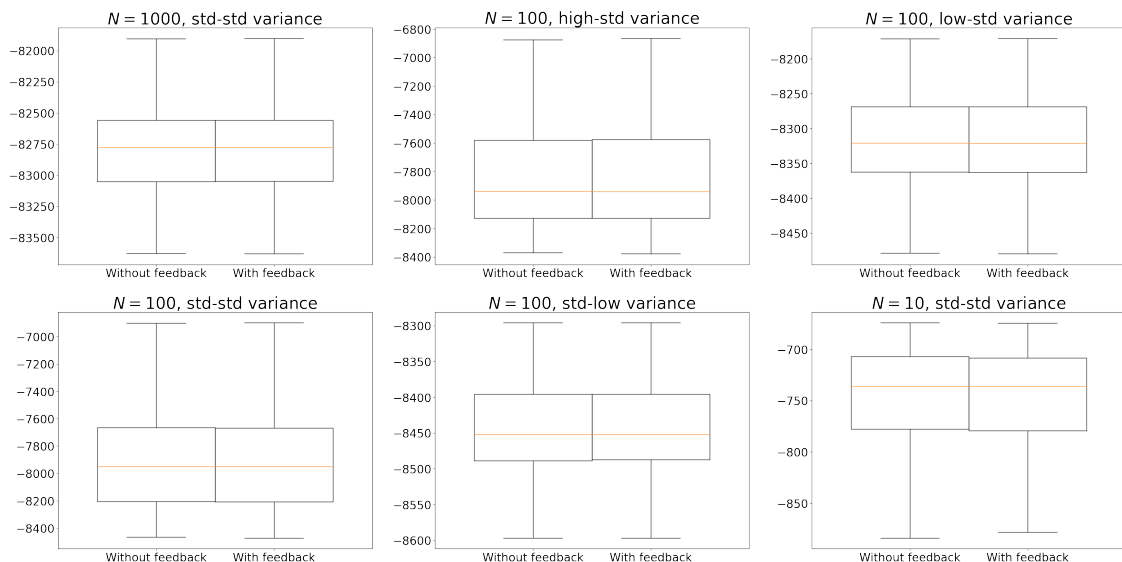


Figure 6: Comparing empirical KL between fully factorised SimBa-CL with feedback and fully factorised SimBa-CL without feedback under different scenarios.

## C.2 Optimization of the parameters

To optimize the parameters of our models and so compute the maximum SimBa-CL estimator we generally used Adam optimizer [Kingma and Ba, 2014]. Precisely, we provide gradient via automatic differentiation in TensorFlow and used the build-in optimizer. As a loss function we used  $-\sum_{n \in [N]} \log(\tilde{p}(y_{[T]}^n | \theta)) / (NT)$  with initial learning rate for Adam given by 0.1. We

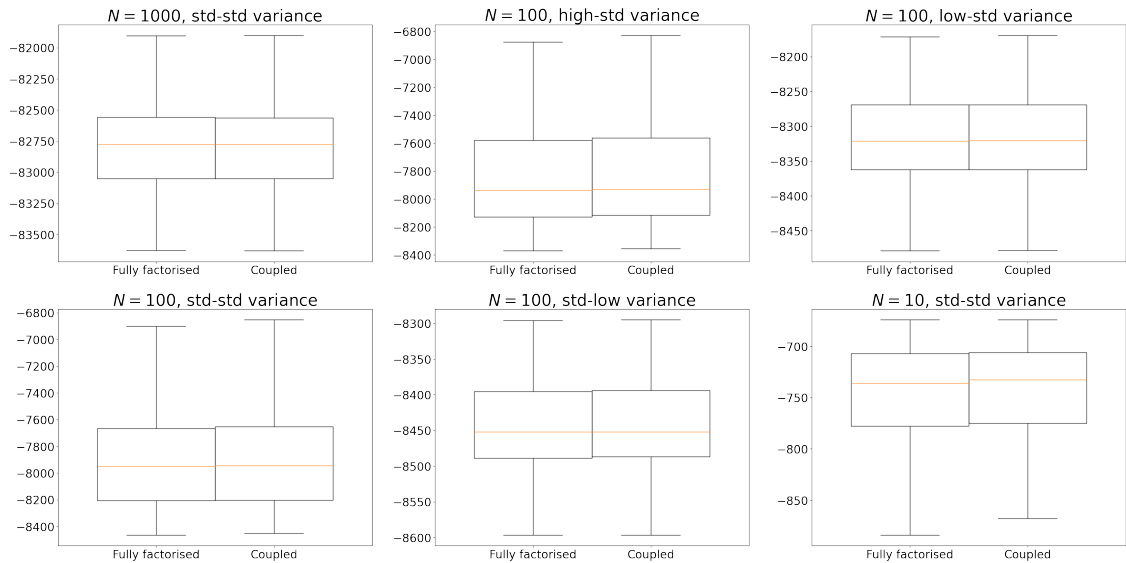


Figure 7: Comparing empirical KL between fully factorised SimBa-CL without feedback and coupled SimBa-CL without feedback under different scenarios.

run 500 optimization steps for the 9-dimensional synthetic data scenario and 3000 for the FM data. We check convergence via stability of the loss function. We also evaluate SimBa-CL using 500 simulations, but just 100 for the FM data to meet the memory constraints. For the 2-dimensional synthetic data scenario, we use vanilla gradient descent with learning rate 100 and 200 optimization steps, again we check convergence via stability of the loss function.

Convergence plots are reported below for the different scenarios. We can always notice that the optimization process is able to find a local minima of the loss function and that we stop our optimization after convergence is reached.

It is important to comment on the optimization for the FM experiment. In the figure we can spot multiple drop while performing the optimization, these drops refer to failure of the optimization procedure where the gradient has pushed the parameters in regions with zero likelihood. To solve this issue we reset the optimization by sampling a new random initial condition and restart the optimization from there, resulting in the vertical drops in Figure 8. Even though this might lead to some optimizations to not converge, remark that we run 100 optimization procedure in parallel and choose the best one in terms of SimBa-CL score.

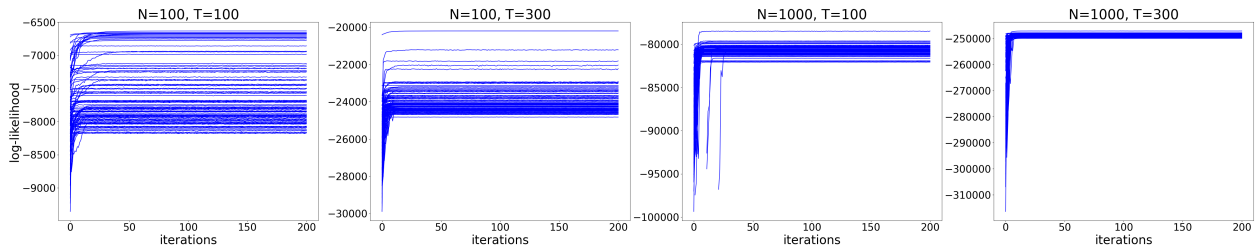


Figure 8: Log-likelihood convergence during the optimization of  $\beta_\lambda$ , when studying the asymptotic properties of SimBa-CL.

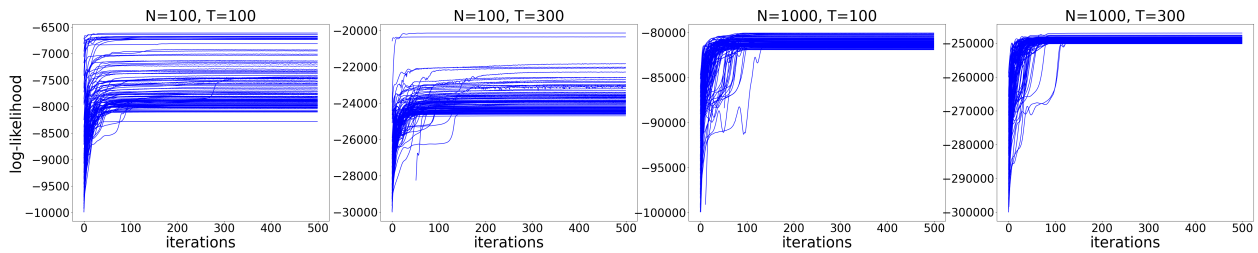


Figure 9: Log-likelihood convergence during the optimization of all the nine parameters, when studying the asymptotic properties of SimBa-CL.

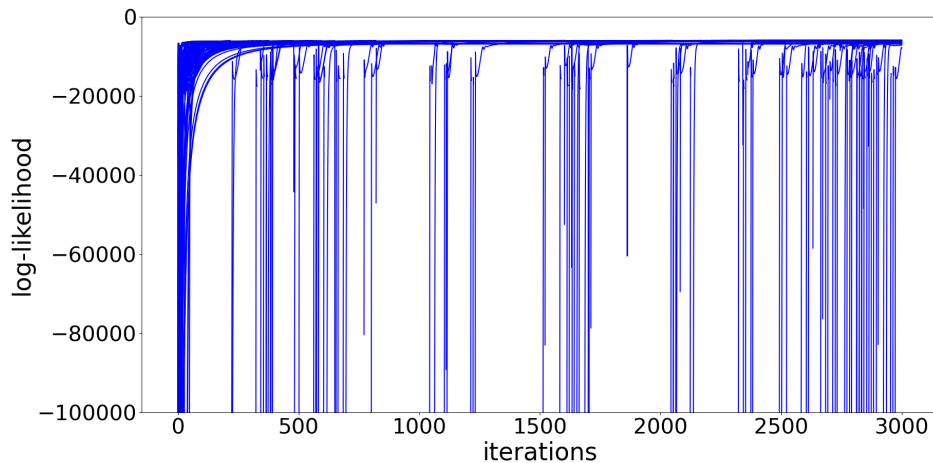


Figure 10: Log-likelihood convergence during the optimization for the FM experiment.

### C.3 Asymptotic properties of SimBa-CL

In this section we provide some additional details on the asymptotic properties of SimBa-CL. Specifically, we provide a graphical representation of the empirical coverage for both the 2 dimensional and 9 dimensional case. For the 2 dimensional case we also provide graphical representation of the confidence sets, which are ellipsoids.



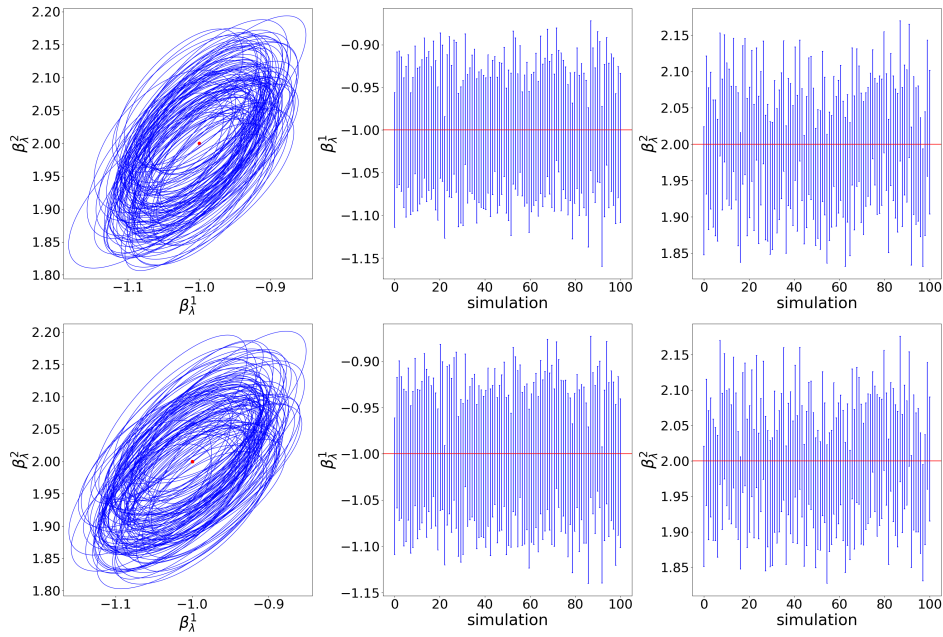


Figure 11: Coverage of the confidence sets with and without Bartlett identities. First row for the latter and second row for the former. From left to right, graphical coverage of  $\beta_\lambda$ ,  $\beta_\lambda^1$  (marginally) and  $\beta_\lambda^2$  (marginally). Color red (for dots or solid lines) is used for the true parameter.

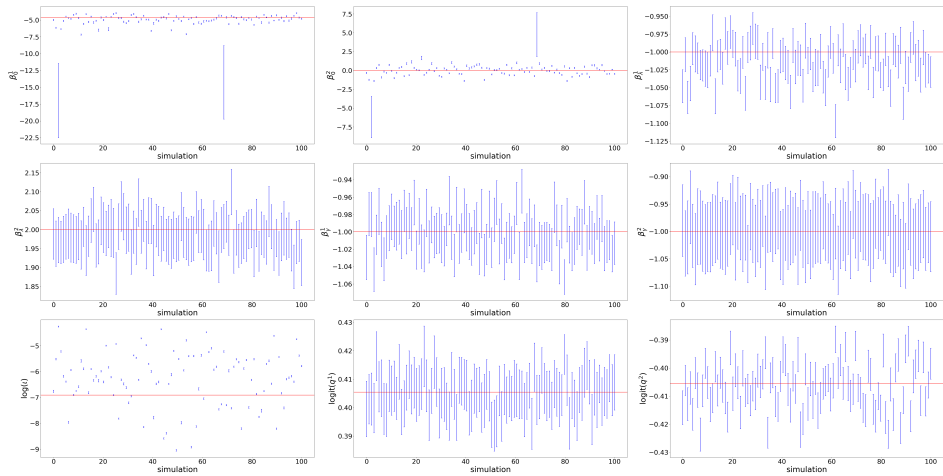


Figure 12: Coverage of the confidence intervals from the diagonal of the Godambe information matrix estimated without the approximate Bartlett identities. Parameters labels are displayed on the x-axes. Red solid lines are used for the true parameters.

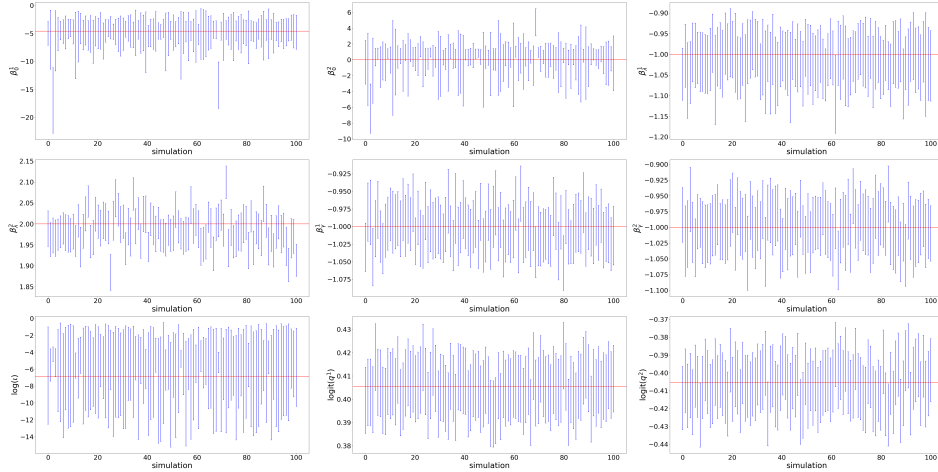


Figure 13: Coverage of the confidence intervals from the diagonal of the Godambe information matrix estimated with the approximate Bartlett identities. Parameters labels are displayed on the x-axes. Red solid lines are used for the true parameters.

## C.4 Spatial SIS

Consider an individual-based susceptible-infected-susceptible (SIS) model as the one from previous experiments. Suppose however that the spatial interaction is not homogeneous, and that a spatial kernel is measuring the infection pressure from one individual to the other. We then have:

$$p_{n,0}(\theta) = \left[ \frac{1 - \frac{1}{1 + \exp(-\beta_0^\top w_n)}}{1 + \exp(-\beta_0^\top w_n)} \right];$$

$$K_{n,x_{t-1}}(\theta) = \left[ \begin{array}{c} e^{-\lambda_n \left( \frac{\sum_{\bar{n} \in [N]} s(n, \bar{n}, \psi) \mathbb{I}(x_{t-1}^{\bar{n}} = 2)}{N} + \iota \right)} \\ 1 - e^{-\gamma_n} \end{array} \quad \begin{array}{c} 1 - e^{-\lambda_n \left( \frac{\sum_{\bar{n} \in [N]} s(n, \bar{n}, \psi) \mathbb{I}(x_{t-1}^{\bar{n}} = 2)}{N} + \iota \right)} \\ e^{-\gamma_n} \end{array} \right];$$

$$q_{n,t}(\theta) = q,$$

where  $\lambda_n = 1/1 + \exp(-\beta_\lambda^\top w_n)$  and  $\gamma_n = 1/1 + \exp(-\beta_\gamma^\top w_n)$  and  $s(n, \bar{n}, \psi) := \exp(-E_{n, \bar{n}}^2 / (2\psi^2))$  with  $E_{n, \bar{n}}$  euclidean distance between  $n$  and  $\bar{n}$  and  $\psi$  positive parameters. For this model we set our baseline to  $N = 1000$ ,  $T = 100$ ,  $w_n$  to be such that  $w_n^1 = 1$  and  $w_n^2 \sim \mathbf{Normal}(0, 1)$ , and the data generating parameters  $\beta_0 = [0.1, 0]^\top$ ,  $\beta_\lambda = [-1, 2]^\top$ ,  $\beta_\gamma = [-1, -1]^\top$ ,  $q = [0.6, 0.4]^\top$ ,  $\iota = 0.01$  and  $\psi = 1$ .

Given the above model we can repeat a similar experiment to the one from the main paper and learn the parameters on a grid to study the shape of the SimBa-CL surfaces. In this study we consider only fully factorised SimBa-CL with and without feedback and we have excluded the general partition case.

The comments on  $\beta_0, \beta_\lambda, \beta_\gamma, q$  are the same as for the homogeneous scenario.  $\iota$  and  $\psi$  needs some additional attention. Firstly notice that the more we increase  $\psi$  the more the

spatial effect is strong and we highly penalise infected that are far away. This automatically tells us that over a certain threshold it will be useless to increase  $\psi$  as the penalisation is already very strong. Secondly, there is an obvious identifiability issue when looking at  $\iota$  and  $\psi$  together. Indeed, increasing  $\psi$  and decreasing  $\iota$  will lead to similar epidemics, where the difference is that most of the infection are either coming from the spatial interaction or the environment. This “banana” shape makes these two parameter hard to learned and we have to be careful when reporting uncertainty around them to avoid being overconfident on a local maxima.

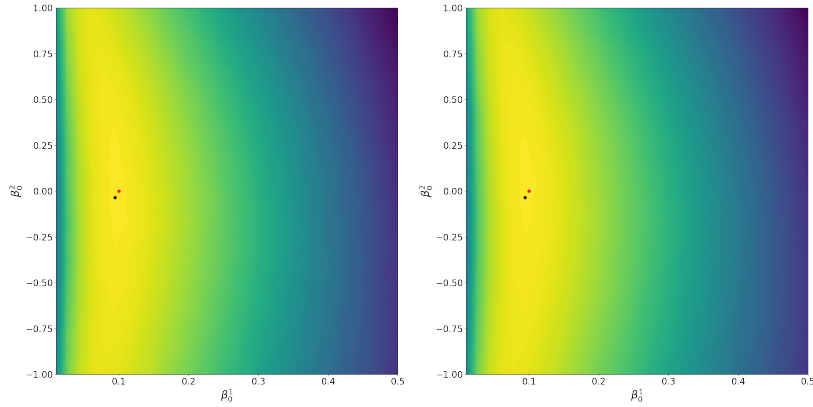


Figure 14: Profile likelihood for  $\beta_0$  in spatial SIS.

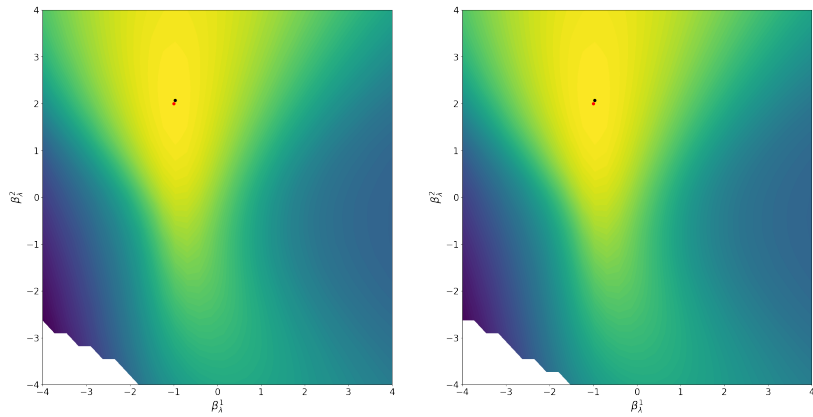


Figure 15: Profile likelihood for  $\beta_\lambda$  in spatial SIS.

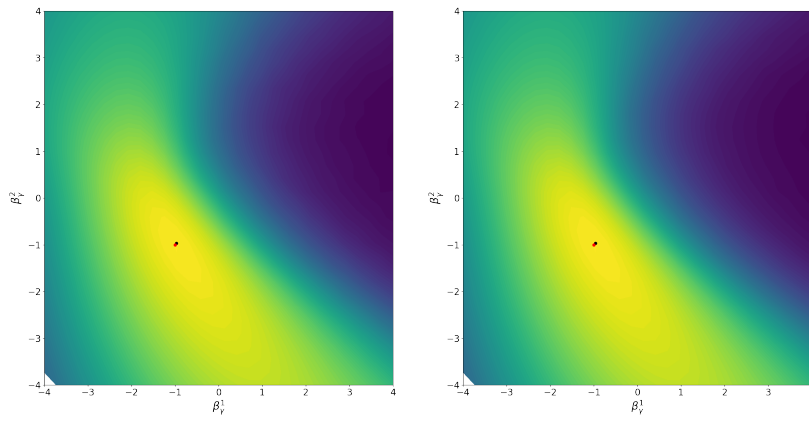


Figure 16: Profile likelihood for  $\beta_\gamma$  in spatial SIS.

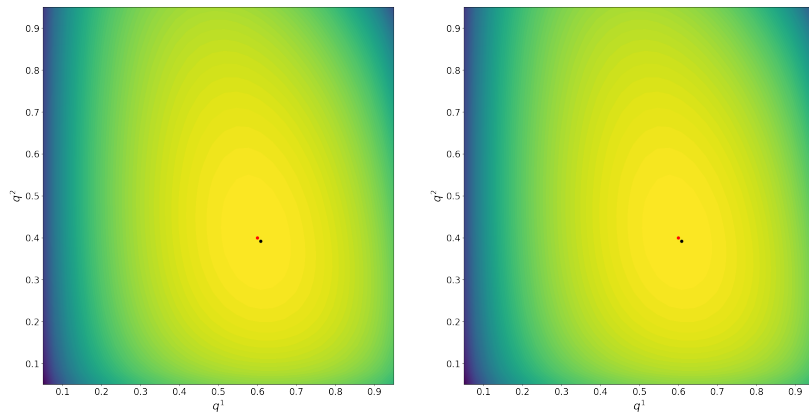


Figure 17: Profile likelihood for  $q$  in spatial SIS.

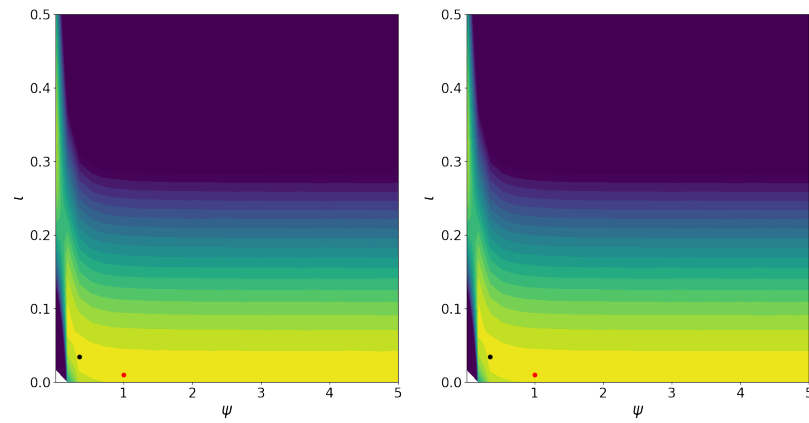


Figure 18: Profile likelihood for  $\nu$  and  $\psi$  in spatial SIS.

## C.5 FM modelling choices

When working with the foot and mouth data we can have different modelling choices. One option is to learn the initial probability of infection as a common parameter across infected farms:

$$p(x_0^n|\theta) = \begin{bmatrix} 1 - p_0\mathbb{I}(n \in F_I) \\ p_0\mathbb{I}(n \in F_I) \\ 0 \\ 0 \end{bmatrix},$$

where  $F_I$  is the set of infected farms over time and so  $n$  belongs to  $F_I$  if it will be observed infected at some time  $t$ . This leads to satisfying likelihood scores, but to unreal epidemics, as it sets  $p_0 \approx 1$  meaning that all the epidemics observed in the future are already infected at time 0 and no spatial interaction is learned.

Another option is to reverse engineer the infection process and use a geometric distribution for the infection time:

$$p(x_0^n|\theta) = \begin{bmatrix} 1 - (1 - e^{-\gamma}) e^{-\gamma\tau_n} \\ (1 - e^{-\gamma}) e^{-\gamma\tau_n} \\ 0 \\ 0 \end{bmatrix},$$

where  $\tau_n$  is the infection time of individual  $n$ . This again leads to satisfying likelihood scores, but it is susceptible to critic given that we are informing the initial distribution with future observation.

More discussion can follow regarding the choices of the spatial kernel and covariates. We decided to not normalise the covariates and follow the approach of [Jewell et al. \[2009\]](#), even though normalisation of the covariates might lead to better results as explained in [Jewell et al. \[2013\]](#). In terms of spatial kernel an obvious alternative choice is the use of a Gaussian spatial kernel, where the decay is modelled through a Gaussian function.

Even though optimal modelling choices for the FM data is an interesting problem, this is beyond the scope of this experiment, which is included as a pure real data application.